Network: Comput. Neural Syst. **10** (1999) R1–R66. Printed in the UK PII: S0954-898X(99)07250-4

TOPICAL REVIEW

Temporal aspects of neural coding in the retina and lateral geniculate

Jonathan D Victor

Department of Neurology and Neuroscience, Weill Medical College of Cornell University, 1300 York Avenue, New York, NY 10021, USA

E-mail: jdvicto@med.cornell.edu

Received 7 June 1999

Abstract. The early stages of visual processing provide excellent models for the study of how information is represented in, and processed by, the activity of neurons. The fact that the retina contains both non-spiking and spiking neurons leads us to frame questions about neural coding in a general fashion, rather than in a manner specific either to point processes or continuous signals. In particular, we ask about the role of the statistical structure of the response, the extent to which the neural representation is 'literal', and how information content can be estimated from laboratory data. The broad theme that emerges from a review of experimental data is that each stage of visual processing is accompanied by new features, including adaptive filtering, feedback, rectification and spike generation. These dynamical elements allow an increasingly rich set of strategies for the representation and processing of visual information at retinal and thalamic levels.

> Time is that great gift of nature which keeps everything from happening at once.
> C J Overbeck [283].

1. Introduction and scope

Informally speaking, 'temporal coding' refers to the notion that the detailed temporal structure of a spike train, and not simply the mean firing rate, contributes to the information that it carries. Especially in recent years, there has been an accumulation of experimental evidence that the temporal patterns of activity of neurons and neural populations are indeed important for signalling and processing information—in a range of sensory systems ([65] and references therein) as well as in motor systems [297, 313]. The idea that neural systems make use of temporal structure is also attractive on theoretical grounds, since it would allow an impulse train to carry much more information than if only its average firing rate were significant. Temporal coding is of particular interest in mammalian vision, given the large processing demands of visual tasks such as scene analysis and object identification. On the other hand, the role of temporal factors in visual processing is often ignored, perhaps in view of the progress that has resulted from analysis of the spatial structure of receptive fields of individual neurons, and the spatial maps that characterize the organization of neural populations.

In section 2 of this review, we attempt to be rigorous about what constitutes temporal coding and how temporal coding may be characterized. In section 3, we discuss some technical matters concerning the analysis of neural responses and their information content, with the aim of describing the conceptual issues, rather than providing a tutorial.

0954-898X/99/040001+66$30.00

In the second half of this review, section 4, we discuss experimental results related to temporal coding in the retina and thalamus. Considering the recent interest in temporal patterns of activity in visual cortex, the emphasis on retinal and thalamic neurons might seem out of place. But there are several reasons for this choice. Firstly, when we attempt to frame a rigorous definition for temporal coding, we find that it necessarily encompasses transformations that occur at the precortical level. Secondly, to describe the kinds of processes that might contribute to temporal coding, we find that we must consider not only aspects of temporal coding that rely on the discrete nature of spike trains, but also issues that are relevant to continuously varying signals as well. In general, there is no guarantee that these two aspects of temporal coding can be considered independently. However, the retina is conveniently organized into a first stage of processing in which only slow potentials are present, and a second stage in which spike trains emerge. Thirdly, many precortical processes are relatively accessible to a detailed understanding, in that a correspondence between anatomy, cellular biophysics, and receptive field dynamics of retinal neurons is often available. This gives the study of precortical sites a critical role in the understanding of temporal aspects of neural coding. Moreover, an understanding of precortical processing is required to appreciate the quantitative and qualitative changes in signal processing at later neural stages.

1.1. Why is temporal coding important?

The challenge facing neuroscience is not just to understand function at the most elementary scales of the nervous system (e.g., channels), but to provide an understanding of how function at larger scales of organization (e.g., neurons, neural circuits and neural systems) is derived from the properties of its constituents [72]. Even if feasible, an immense computational model would not, in and of itself, represent a satisfying account of these relationships, because it would lack insight into the critical features of the constituents. In a sense, the situation is analogous to the relationship between the properties of individual particles of an ideal gas, and that of a macroscopic sample of the gas. In principle, the behaviour of a gas could be deduced from a computational simulation of a large number of particles. But far greater insight is provided by statistical thermodynamics—which indicates that knowledge of only a few state variables suffices to predict behaviour.

There have been some attempts to apply this kind of approach to neural ensembles [359, 435]. The barriers are formidable and obvious: a neuron has far more 'state variables' than a particle of an ideal gas, and neural connectivity plays a fundamental role. Equally important, however, is that it is unclear what are appropriate candidates for the state variables that represent neural activity—an obvious choice is overall firing rate, but details of firing patterns and higher-order statistics may be equally important [57]. That is, the investigation of the role of temporal structure, in broadest terms, is the delineation of the state space for neural activity (e.g., [181, 224]), and is thus a fundamental step in the development of a theory of brain function.

Temporal properties of individual neurons and neural populations have been postulated to underlie key visual processes, including binding of parts of an object into a whole [98, 421], recurrent and feedback interactions among visual sensory areas [56], visuomotor transactions [294], disambiguation of the many attributes that influence a neuron's response [121, 414], and efficient coding of retinal information [252]. Additionally, under pathological conditions, disturbances of normal firing patterns have been postulated to be associated with derangements of visual processing and perception, including loss of visual awareness [294], dyslexia [222], and amblyopia [317]. While these ideas cannot be considered to be proven, they must be taken very seriously: neurons and their components indeed have complex

dynamics, and measurements of overall firing rate will not necessarily suffice to describe their behaviour [340, 387].

1.2. Other reviews

Several related reviews deserve the reader's attention. Cariani's review [65] considers temporal coding in sensory physiology without restriction to vision, and provides an interesting scheme for a taxonomy of neural codes encompassing both temporal and spatial considerations. The recent book by Rieke, Bialek and co-workers [312] is an excellent introduction to the concepts of information theory and how they can be applied to neurophysiology, with particular emphasis on sensory processing in insect sensory systems and the 'stimulus reconstruction' method. The reviews of Hertz [156], Richmond and Optican [311] and Gawne [120] provide an in-depth review of temporal coding at several levels of the primate's visual system, as revealed through a different set of analytical tools. Meister and Berry's review [251] considers retinal coding in detail, with particular emphasis on what has been learned from multichannel recordings. Funke and Wörgötter's review [118] focuses on temporal coding in the lateral geniculate nucleus. Reid and Alonso [304] review coding in visual cortex from the traditional viewpoint of receptive field structure and its relation to properties of individual cortical neurons. Eckhorn [97] and Singer and Gray [357] review the role of temporal patterns in visual cortex, with an emphasis on the role of synchronization and oscillations. Usrey and Reid [404] review the role of synchrony at retinal, thalamic, and cortical levels, across a range of mammalian species. Finally, for the reader with an interest in a more general introduction to visual neurophysiology and psychophysics, the recent textbook by Wandell [422] is highly recommended.

2. What is temporal coding?

Neural circuits use sequences of action potentials ('spikes') to extract, represent, and process visual information. Spikes are stereotyped all-or-none electrical events triggered by the interplay of inputs from other neurons in the form of graded synaptic potentials. Generally, 'temporal coding' is the notion that the temporal structure of spike trains—the arrangement of spikes in time—plays a significant role in these processes. It is often placed in contrast to 'spike count coding', the notion that the only aspect of a neural response that is significant is the number of spikes it contains. Yet one immediately recognizes that this contrast is more quantitative than qualitative. On the one hand, characterization of a response by the number of spikes it contains necessitates a temporal window in which the spikes are counted—a crude but essential dependence on temporal arrangement. On the other hand, any ensemble of neural responses can be characterized by the statistics of spike counts within a set of 'bins' (or adjacent temporal windows), provided that one is free to consider not only statistics within individual windows, but also correlations across windows. Consequently, any 'temporal code' can be re-interpreted as a sequence of spike count codes, at a sufficiently high degree of resolution. Thus, our goal is not to review the evidence for one or the other kind of coding strategy—attempts at rigorous definition will necessarily blur the distinction.

The retina is unusual in that the neurons involved in the earliest stages of retinal processing (photoreceptors, horizontal cells, and bipolar cells) do not generate action potentials but communicate solely through graded signals. This requires us to take a broader view of temporal coding, and in particular to ask whether the event-like nature of spike trains plays a fundamental role. Spike trains and the slow potentials that drive them are intrinsically temporal structures, and our focus is on what aspects of these structures (i.e., what kinds of statistics, and what scales of temporal resolution) convey visual information.

We recognize at the outset that identification and analysis of temporal coding is dependent on experimental methods for reliable recording of single neurons' responses, and on analytical methods for the characterization of these responses. While the analytical methods have attracted much active research, they cannot be regarded as settled. As we shall see from our discussion of these methods below, there is no universal strategy that is most appropriate to all kinds of data. Assumptions that are overly specific prevent identification of unexpected aspects of neural coding, while assumptions that are overly broad may make it impossible to obtain reliable characterizations of spike train statistics or reliable estimates of information from finite data. Rather, in a practical sense, progress is likely to be made by approaches that test a series of interrelated hypotheses concerning what aspects of a stimulus are likely to be represented in the neural response, and what aspects of the neural response are likely to carry information.

2.1. Qualitative characterizations of coding and representation

It is helpful to consider two qualitative axes along which neural representation and coding might be characterized. For simplicity, we consider only the response of a single neuron to each member of a finite set of stimuli with a definite time of onset (see below). We furthermore assume that we have at our disposal a limitless supply of trials for each member of the stimulus set, and we ignore real-world complications such as habituation, learning, and memory which might result in non-stationarities.

Are the statistics of individual responses important? In the above idealized setting, we can ask whether the responses to individual trials of a stimulus contain temporal structure that is not anticipated from the overall response to that stimulus (i.e., the average response across all trials). This leads to an important relationship between the statistics of a set of spike trains, and whether these spike trains have the potential to represent something other than a continuous graded signal. The average response of a spiking neuron to multiple repeats of the same stimulus is characterized by the peri- or post-stimulus time histogram (PSTH), the probability that a spike will occur at each time following stimulus onset. With the luxury of a limitless supply of trials, we can construct this PSTH with arbitrarily narrow time bins, and determine the probability of firing in each of these bins with arbitrarily high accuracy. That is, the PSTH can be considered to be a firing rate function $R(t)$, where $R(t)\Delta t$ indicates the probability that, on any single trial, a spike occurs within a window of width Δt around the time t. The hypothesis that the PSTH (and therefore $R(t)$) fully characterizes the responses to a stimulus places very strong constraints on the statistics of the individual responses. It requires that the probability of a spike's occurrence at any given time within a trial does not depend on the occurrence of any other spikes in that trial. It follows that the distribution of the number of spikes in any time bin conform to Poisson statistics, with a mean determined by the area under the corresponding interval of the PSTH. That is, the response to a particular stimulus j is represented by a Poisson process whose mean rate is given by a time (and stimulus)-dependent quantity $R_j(t)$. Under the assumption that a set of neural responses has this property, then the analysis of representation and coding is greatly simplified: the PSTHs serve as estimates of the time-dependent rate functions $R_j(t)$, and all aspects of coding and representation can be derived from these functions, either analytically, or via simulated spike trains whose Poisson firing statistics are determined by $R_j(t)$. The rate function $R_j(t)$ fully characterizes the statistics of the responses, and the PSTH is the best estimator of this rate function. If the Poisson hypothesis holds, then the analysis of temporal coding in spike trains reduces to the analysis of the underlying continuous rate functions $R_j(t)$. That is, validation of the Poisson hypothesis

allows us to ignore the dynamics of spike generation. Characterization of temporal coding is then reduced to understanding the origin and timescales of the continuously varying rate functions $R_j(t)$.

However, the reduction of the analysis of temporal coding of spike trains to a study of rate functions may overlook important kinds of behaviour if there is any statistical aspect of the individual responses that deviates in a systematic way from time-varying Poisson processes of matching rate functions. Such deviations from a Poisson process can take many forms, and may have their origin in the intrinsic properties of neurons or in the properties of the network in which they are embedded. Real neurons have an absolute refractory period following a spike, during which a second spike cannot occur. Consequently, firing probabilities within a single trial cannot be independent at the timescale of milliseconds. The presence of a relative refractory period might lead to more subtle deviations from Poisson statistics over a wider timescale. In retinal ganglion cells recorded *in vivo*, firing patterns are much more regular than would be expected from a Poisson process [107, 398], and can be modelled by an integrate-and-fire [187, 301, 302] or a random walk [125] process; under other experimental conditions, retinal ganglion cells fire in a strikingly bursty fashion [32]. At the cortical level, there are several independent pieces of evidence that spike train statistics deviate substantially from Poisson statistics, including bursts [211, 363] and oscillations [97]. The PSTH is insufficient to demonstrate any of these behaviours, since any PSTH can be generated by a Poisson process with a time-varying firing probability. A PSTH with sharp or periodic peaks might suggest the presence of bursts or oscillations, but only if these features are phase-locked to the stimulus cycle.

Figures 1(A)–(C) show examples of different response statistics that are consistent with the same PSTH. In these examples, the scatter in the number of spikes per trial is less than Poisson (A), equal to Poisson (B), and greater than Poisson (C). As this figure suggests, the statistics of the number of spikes per trial is an important index of deviation from Poisson statistics; this is also true in real recordings in the retina [301] and visual cortex [88, 124, 389, 414, 416]—the former typically characterized by less-than-Poisson variance, while the latter is typically characterized by greater-than-Poisson variance. One can determine whether this is the only deviation from Poisson statistics by the exchange resampling procedure [414], in which surrogate datasets are generated by randomly exchanging pairs of spikes among trials. Surrogate datasets generated in this fashion match the original dataset both in terms of the number of spikes in each trial and in the overall PSTH, but have temporal features that are readily distinguishable from those of the original data, as has been shown in the retina [301], lateral geniculate [301], and visual cortex [414].

Identification of deviations from Poisson statistics is logically distinct from demonstration that these deviations play a role in coding. Indeed, to the extent that these deviations represent intrinsic properties of how a neuron transforms a slowly varying membrane potential into a spike train at the point of spike generation, they would result in firing statistics that are more complex, but no more informative, than a Poisson process. However, if departures from Poisson statistics reflect intrinsic membrane behaviour that is selectively activated by particular patterns of synaptic input, then such departures may play an important role in neural coding.

These considerations apply to the analysis of the spatial aspects of coding, as well as to its temporal aspects. In the temporal domain, conformance to Poisson statistics formalizes the notion that it does not matter which examples of a sequence of trials contain which spikes. The same concept can be applied to the analysis of activity within a population of putatively equivalent neurons on a single trial. If firing statistics conformed to Poisson expectations across neurons as well as across trials, then correlations between individual neurons' responses (which might include phenomena such as concerted signalling [250] and neural synchronization

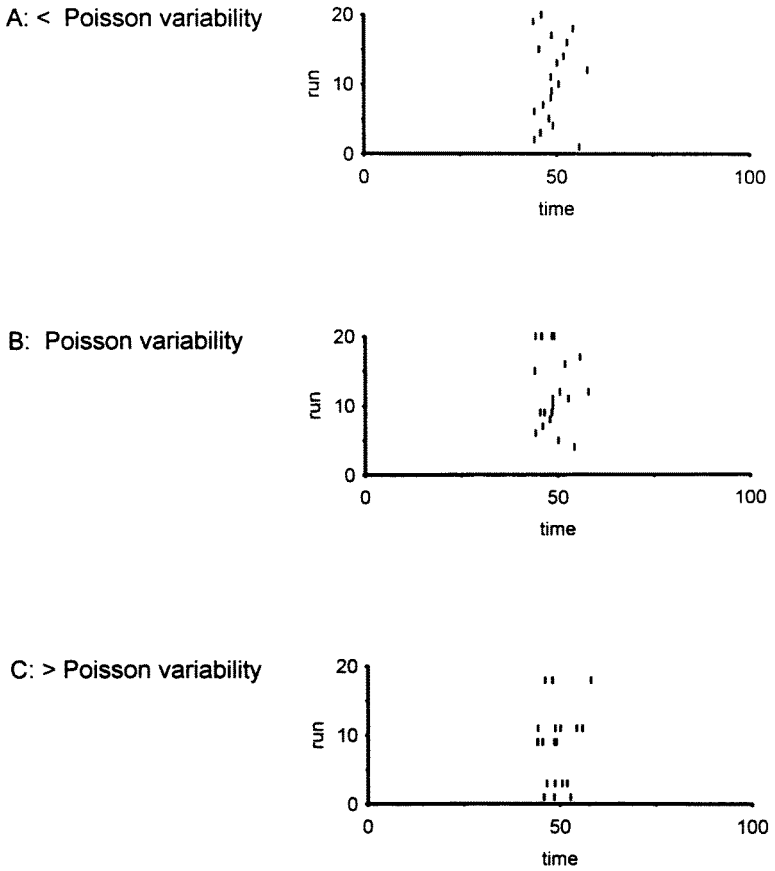

Figure 1. The PSTH does not determine the temporal structure of spike trains. Each set of rasters diagrams a collection of hypothetical neural responses to repeated presentations of the same stimulus. (A) The rasters are generated by a neuron that fires exactly once per trial, in a relatively narrow time window. (B) The rasters are generated by a Poisson process whose event probability varies in time during each trial, and has an average of one spike per trial. (C) The rasters are generated by a neuron that has a 'bursty' firing pattern, but also with an average firing rate of one spike per trial. The PSTHs in all three examples are identical.

[97, 357, 404]) are no different than would be expected from the average activity of the population. Conversely, deviations from Poisson statistics allows neural processing to depend on the specific distribution of spikes across neurons and trials, and requires the investigator to determine whether such dependence is important. From a practical point of view, in order to completely characterize a neuron's responses, the investigator is compelled to examine the statistics of individual trials (and not merely the PSTH), unless there is assurance that the firing patterns obey Poisson statistics.

In summary, the extent to which statistics of individual trials is determined by the PSTH is a conceptual axis that corresponds in a loose sense to a partitioning of temporal coding into the role of an underlying continuous rate function and the role of the dynamics of spike generation. In the retina, this partitioning is made vivid by the presence of an initial processing stage in which neural processing relies solely on manipulation of continuous signals, and a later stage in which neurons turn these signals into spike trains. Neural responses characterized

by Poisson statistics are one extreme: the statistics of spikes on individual trials are completely predictable from the PSTH, and thus, from the rate function; there is no additional information in the details of how spikes are distributed among trials. At the other extreme are response sets that contain structures such as bursts or oscillations occurring at random times. Here, the PSTH is flat and gives no clue to the presence of temporal structure. Intermediate between these extremes are deviations from Poisson behaviour that are time-locked to the stimulus. This category includes bursts time-locked to the stimulus or the response of an integrate-and-fire neuron. For such neurons, the PSTH does reflect the input signal, but decoding schemes beyond simple PSTH estimation provide more efficient ways to recover the input [51].

Is the coding literal? Temporal coding may also be characterized according to whether or not the spike train is a 'literal' representation of the input—a criterion that has been used to distinguish 'encoding' from 'coding' [385]. Conceptually, this is a distinction between situations in which the temporal structure in the response is a direct consequence of temporal structure in the input, and situations in which temporal structure in the response is generated by an interaction of the input signal with the dynamics of individual neurons or the network.

In the most extreme form of a literal code, the temporal structure of a neuron's response replicates the temporal structure present in the input. For example, a neuron which has a maintained discharge might provide a direct literal representation of the time-varying intensity $I(t)$ of a spot in the centre of the receptive field, provided that the timescale of fluctuation of the spot's intensity is substantially slower than the typical firing rate. In this pure form of a literal code, the average firing rate $R(t)$ (determined by a smoothing procedure applied to individual responses or by averaging across many replicate trials) is proportional to $I(t)$. A stage of linear filtering interposed between $I(t)$ and $R(t)$ is in keeping with the notion of a literal code, in that the temporal structure of the response remains a direct consequence of the temporal structure in the input. The essence of the notion of a literal code is preserved even when the intervening transformation is nonlinear or not invertible, even though in the latter case, $I(t)$ cannot always be recovered from $R(t)$.

In non-literal coding, the relationship of the temporal structure of the response to the stimulus is an abstract, and in principle more arbitrary, one. That is, response dynamics is determined primarily by the dynamics of the neural hardware, rather than the stimulus itself. A clear-cut (but hypothetical) example of non-literal coding would be a neuron whose response to a red spot is a tonic elevation of its mean rate, and whose response to a green spot is oscillatory activity.

It would appear that this distinction is straightforward, albeit perhaps difficult to formalize—literal coding is in some sense 'trivial', while non-literal coding is 'interesting'. However, further consideration indicates that this is not the case. As formulated above, the distinction between literal and non-literal coding is just as applicable to non-spiking neurons as it is to spiking neurons, and thus must be applicable to situations in which the spike response contains no information beyond that available in a stimulus-dependent rate function. We consider the response of a generic and grossly oversimplified retinal neuron to transient presentation of a spot of light. Following observations in many types of neurons and across many species, we caricature the neuron's behaviour as a linear combination of an excitatory centre and an inhibitory surround, each with their separate timecourses ([298] and below) . For non-spiking neurons, this combination produces a continuously varying membrane potential $R(t)$ that constitutes the neuron's output; for spiking neurons, $R(t)$ is then transformed into a firing rate according to Poisson statistics. In either case, the timecourse of $R(t)$ depends on the size of the spot, since larger spots will be associated with a greater contribution of the surround dynamics. This coding cannot be classified as literal, because the temporal structure

of the input (its transient onset) is the same in both cases. In sum, a highly simplified classical model demonstrates non-literal temporal coding of spot size. (A recent, far more elaborate, analysis of this kind has been carried out for model lateral geniculate nucleus neurons [132], with the same overall conclusion.) Note that we cannot avoid this problem by insisting that non-literal coding can only be sought with stimuli without an 'onset'. Had we imposed such a requirement, experimental tests for such coding would be nearly impossible, since it would be necessary for stimuli to be present for an indefinitely long period of time.

This example shows that our initial definition of non-literal coding (designed to distinguish 'interesting' from 'trivial' coding) encompasses a phenomenon as simple as centre–surround organization. If the spatiotemporal aspects of centre–surround organization were not a well known phenomenon [298], then the discovery that the timecourse of a response can signal the size of the stimulus would be likely to attract considerable interest and attention. Once the mechanism is known (and in this case the mechanism was known long before the current surge of interest in temporal coding), the phenomenon becomes less interesting. Non-literal coding of stimulus size is merely literal coding of an internal signal (the combined response of centre and surround). This distinction fades further once we recognize that the continuous functions, and not just spike trains, may serve as neural outputs.

It should not be surprising if many examples of non-literal temporal coding turn out to be literal coding of an internal signal, once the underlying mechanism(s) are understood. From a theoretical point of view, a more fundamental distinction than that of 'literal' versus 'non-literal' coding is whether or not the coding manifest in a spike train relies in an intrinsic manner on the dynamics of spike generation. That is, does the presence of spikes *per se* represent a new dynamical feature or, alternatively, is it safe to restrict consideration to firing rate? We have already cited the integrate-and-fire model of spike generation [187] as a simple example of dynamics introduced by spike generation; a more elaborate example is that of 'chattering' cortical neurons [133], whose burst rate can be modulated by a slowly varying input signal. These processes produce non-literal coding, in that they introduce dynamical features not present in their input, whether we consider the 'input' to be the sensory signal itself or an internally generated one. Finally, it is far from clear that an encoding process can always be factored into a signal-processing stage consisting of simple functional elements that act on the input to produce an internal (temporal) signal, followed by a spike-generating stage (which may or may not be a literal encoder). Indeed, it may well be that the most important distinction along the lines of 'interesting' versus 'less interesting' temporal coding is whether the coding process can be factored in this fashion or, alternatively, whether network properties that rely on the repeated interconversion of spike trains and continuous signals play an essential role.

The two characterizations we have considered—the importance of individual trials, and the literal versus non-literal distinction—are fully independent. As discussed above, non-literal coding may be present in a manner that is fully manifest in the PSTH (i.e., if an internally generated temporal signal drives a Poisson neuron) or in a manner that requires inspection of individual responses. The same is true of literal coding. A Poisson neuron driven by a replica of a temporal signal present in the input is an example of literal coding in which individual trials provide no information beyond that of the PSTH. If the same temporal signal drives an integrate-and-fire neuron (or the effective rate of any renewal process [187]), then coding remains literal but the PSTH no longer predicts the statistics of the individual responses, and decoding schemes beyond simple PSTH estimation may provide a more efficient way of recovering the original input [51].

Precise timing need not imply temporal coding. One aspect of the complexity of the relationship between the precision of individual spike times and the notion of temporal coding

is illustrated by the results obtained in two invertebrate visual systems. Bialek and co-workers [33, 34, 312] examined spike train output of H1, a motion-sensitive neuron in the fly's visual system. A literal code was assumed: namely, that the velocity signal was 'decoded' from H1's output by convolution with a linear kernel (in essence, an effective impulse response), and the form of the kernel was optimized to provide the closest match to the timecourse of the stimulus velocity. Addition of nonlinear terms did not improve the representation [34]. Importantly, it was shown that this 'stimulus reconstruction' approach did not miss a substantial amount of the information present in the response [312], in that it was reasonably close to the theoretical limits imposed by noise at the receptor—thus providing strong empirical evidence that the assumed coding strategy was correct. The width of the optimal temporal kernel was narrow in comparison with the timecourse of velocity fluctuations and the mean interspike interval. Correspondingly, the spike train was irregular, and the precise timing of individual spikes (up to the ca 30 ms width of the kernel) conveyed considerable information.

An interesting contrast is presented by the recent studies of the lateral eye of the horseshoe crab *Limulus*, carried out by Passaglia *et al* [286]. Here, the response of the population of optic nerve fibres was determined by a combination of neurophysiological and computational techniques, based on an accurate linear model of the *Limulus* lateral eye [51, 52]. As originally noted by Hartline and Graham [150], spike discharges occurred at a rate of 5–40 impulses per second and were highly regular. But rather than being driven by the input, the timing of a spike was determined primarily by the time of the previous spike and the dynamics of the spike-generating mechanism [187]. Thus [286], stimulus-specific information was present only in the average firing rate over prolonged periods (250–500 ms), in keeping with the temporal integration properties of central neurons that receive the inputs from the optic nerve.

In both sets of experiments, stimulus information is encoded in a literal (and linear) manner, and spike times are highly precise (with variability demonstrably non-Poisson in the case of *Limulus*)—but the fly H1 neuron manifests temporal coding, while the *Limulus* lateral eye provides a clear-cut example of rate coding. Conversely, the absence of precise timing does not rule out the possibility of a temporal code. Oscillations or bursts that are induced by specific stimuli are prime examples of temporal codes, even if their frequency is sufficiently low such that spike timing is imprecise or if they are not phase-locked to the onset of the stimulus. These phenomena have been reported in spiking [9] and non-spiking neurons of the retina [108, 323], as reviewed in [275].

3. Technical matters

Our notion of temporal coding relies on relating the temporal structure of a response to the information that it carries. To identify and characterize temporal coding, it follows that we must have tools for the characterization of temporal structure and the quantification of information. We now discuss these two issues. Our aim is not to provide a set of tutorials, but rather to highlight the relationships between the various approaches that have been used, and to consider some of their advantages and potential pitfalls.

3.1. Characterization of temporal structure

Methods applicable to continuous signals and to spike trains. Many methods for the characterization of temporal structure of spike trains apply equally well to (or were originally developed for) the characterization of continuous signals. The average response to a stimulus may be characterized in the time domain by the post-stimulus histogram, or, equivalently, in the frequency domain by Fourier analysis. Both of these characterizations are 'first-order

statistics' and are thus linear in the data. The usual method used to characterize the spontaneous (background) activity consists of calculation of second-order statistics—in the time domain, the autocorrelation function [287], or in the frequency domain, the power spectrum [48]. Second-order statistics provide a complete description of filtered Gaussian processes but cannot reveal deviations from Gaussian statistics. Higher-order statistics, such as the bispectrum [58], a third-order statistic, can reveal and characterize such deviations, but reliable calculation of these statistics often requires more data than are typically available from a neurophysiologic experiment, and is typically applied to field potentials and rather than spike trains. Gaussian (and non-Gaussian) statistics of low order are consistent both with a *bona fide* stochastic process and also with deterministic chaos. This distinction cannot readily be made with an order-by-order analysis, but can, in principle, be made via calculation of the topological dimension of a time series [14]. A low dimension implies deterministic chaos, while a high dimension implies a stochastic process. However, while such non-parametric methods are theoretically attractive, they suffer from the need for large quantities of experimental data and other practical difficulties [384].

As discussed above, it is important to examine not only the average response to a stimulus, but also how individual responses differ from this average. One possibility is that the variation among individual responses merely represents the additive superposition of stimulus-independent background activity. However, the simple hypothesis that a stimulus-locked 'driven' response and a constant background 'noise' add without interacting is often falsified [57, 240, 382, 383]. For example, one portion of a response may be more variable than another. Or, a stimulus may result in the appearance of oscillations with a relatively constant envelope but a phase that varies from presentation to presentation [383].

An extension of spectral analysis provides a systematic approach to characterize these (and other) kinds of response variability (or interaction of driven activity and noise). For a periodic stimulus, this leads to the phase-locked spectral analysis (PLSA) procedure [331], in which variability is characterized by a sequence of spectra $P_n(\omega)$. This is a carrier (ω) and envelope (n) decomposition, in which $P_n(\omega)$ indicates the strength of a component of response variability at the frequency ω which waxes and wanes with the nth harmonic of the stimulus cycle. If signal and noise did not interact, then $P_0(\omega)$ would be the power spectrum of the background, and $P_n(\omega)$ ($n \neq 0$) would be zero. For transient stimuli, it is convenient to transform the envelope variable (n) into the time domain. This leads to a characterization of responses in terms of power at a frequency ω that tends to be present at specific times after stimulus onset [154, 383].

The carrier may also be analysed in the time domain, which results in a description of response variability in terms of autocorrelation functions computed locally in time. Whether calculations are performed in the time or frequency domains, the key feature of this family of analytical methods is that response measures are squared before they are averaged, so that response segments that are more variable produce reinforcing contributions, independent of the direction of their variation.

To apply any of the above methods to spike data, it is necessary to transform a spike train (a sequence of events) into a function of time. The usual approach is to 'bin' the data. That is, the sequence of spike times is replaced by a function of time $f(t)$ which is constant on intervals (bins) of length $\Delta\tau$, and the value of the function $f(t)$ on each interval indicates the number of spikes that have occurred in this interval. In some circumstances [312], it is convenient to choose the bin length $\Delta\tau$ to be short enough so that every bin contains at most one spike. Thus, $f(t)$ can be considered to represent the spike train, with resolution $\Delta\tau$. A variation on the theme of binning consists of replacement of spikes by smooth bumps, such as Gaussians of some particular width [153].

It may also be useful to replace the spike train by a sequence of delta functions, one at the time of each spike. This avoids the need to choose an arbitrary finite bin width $\Delta\tau$, provided that the analytical measure has an interpretable limit as the bin width $\Delta\tau \to 0$. For example, with this convention, a Fourier component of the response becomes a sum of exponentials, and any filtering related to the smoothing or binning procedure is eliminated.

Replacement of delta-function spikes by smooth bumps is equivalent to application of a (non-causal) linear filter whose impulse response is the bump shape. Binning spike data is also a form of linear filtering, but the filter is not time-independent because of the special roles played by the bin boundaries. The power spectrum $P(\omega)$ of binned spike data has a high-frequency asymptote proportional to $1/\omega^2$, which is achieved for values of $\omega \gg 1/\Delta\tau$, while the power spectrum of a spike train considered as a sequence of delta functions has a constant high-frequency asymptote, equal to the mean firing rate. However, for non-parametric response characterizations, the relationship between analyses of binned, smoothed, and delta-function representations may be less straightforward (see below).

Binning and smoothing do not require detailed assumptions about spike generation or postsynaptic processing. When a specific model for spike generation is under consideration, it is sensible to attempt to use this model to derive a continuous function of time that approximates some aspect of the continuously varying biophysical state of the neuron. Alternatively, computational models for synaptic behaviour [341] can be used to derive a function $f(t)$ that represents the effect of the spike train on the postsynaptic neuron. These model-dependent functions, which may well be nonlinear transformations of the delta-function spike train, can then be subjected to the above strategies of time-series analysis.

An example of the use of a model of spike generation is the analysis of the integrate-and-fire model neuron [187]. In this model, the transmembrane voltage is assumed to represent an integral of synaptic inputs. When this voltage reaches a threshold, a spike occurs and the voltage is reset to a base level. For such a neuron, the derivative of the transmembrane voltage represents the key model state variable $f(t)$. Although the timecourse $f(t)$ cannot be inferred from an observed sequence of spike events, one can at least restrict consideration to timecourses $f(t)$ that are consistent with the observed sequence. Such timecourses cannot be derived by binning or smoothing the spike train. However, a natural choice [189] for $f(t)$ is a piecewise-constant function whose value on the interval between any two spikes is proportional to the reciprocal of the interspike interval.

Methods based on a spike train as a sequence of events. We now consider strategies for the characterization of temporal structure that explicitly consider the 'point process', or event-like, nature of the spike train [287]. We consider primarily situations in which no stimulus is present, or in which the stimulus is constant in time, but many of the methods we discuss can be extended to situations in which there is a time-varying stimulus.

A key qualitative aspect of a spike train is whether it is a 'renewal process'. In a renewal process, by definition, the distribution of possible values for the nth interspike interval In is independent of the preceding interspike intervals $I_{n-1}, I_{n-2}, \ldots$, and each interspike interval is identically distributed. Examples of renewal processes include Poisson processes (with or without refractory period), iterated Poisson processes (every kth event of a hidden Poisson process corresponds to a spike), random-walk models, and integrate-and-fire models (with or without forgetting, with or without a stochastic threshold). In a renewal process, all statistical aspects (including all of the measures described above) are completely determined by the statistics of the interspike interval distribution.

If lengths of successive intervals are not statistically independent, then a first step to characterizing this dependence is the calculation of correlation coefficients between

neighbouring intervals I_n and I_{n-1}, and more generally, between two interspike intervals I_n and I_{n-j} separated by a fixed number of intervening intervals. These quantities, the 'serial correlation coefficients', are analogous to the autocorrelation function. Indeed, in the limit that the interspike intervals of a spike train scatter only infinitesimally from their mean value I_{mean}, the jth serial correlation coefficient is given by the autocorrelation of the smoothed spike train, evaluated at the time jI_{mean}. For spike trains that have large variations in interspike intervals, this approximation does not hold, for two reasons: the effects of the binning or smoothing process need to be considered, and there is no longer a close relationship between the number of intervening interspike intervals and their total duration. In principle, the idea of pairwise serial correlation can also be extended to examine correlations at higher orders, but, just as in the calculation of higher-order analogues of the autocorrelation and the power spectrum, availability of sufficient data is likely to be limiting.

There are approaches to spike train analysis that look beyond pairwise interval statistics, but not in the framework of an order-by-order approach. One approach is to choose a criterion for what constitutes a 'burst' (a minimum number of spikes within some predefined interval), and analyse their statistics and stimulus dependence [32, 363]. A more general approach is to ask whether there are sets of spikes of defined interspike intervals that occur with an unexpectedly high frequency [86, 87, 213]. Highly efficient methods for this purpose have been developed [86]. Such sequences of spikes, which need not be contiguous within the spike train, are known as patterns or motifs, were originally identified in auditory cortex and have been proposed to be an important aspect of cortical function in general [1].

Additional methods take their inspiration from nonlinear dynamics. Rapp *et al* [297] have developed a technique for quantifying the 'algorithmic complexity' of a sequence of spikes. Algorithmic complexity and serial correlation structure are independent attributes of spike train structure, just as the topological dimension and spectral attributes are independent attributes of continuous-time series. When a periodic stimulus is present, then an additional set of tools, based on the 'circle map', can be used [187] to identify and characterize dynamical features of the spike train such as phase locking.

Extensions to multichannel data. In general, all of these methods can be extended to the analysis of datasets that contain simultaneous records of activity in two or more neurons. For example, spectra and autocorrelations generalize in a natural way to cross-spectra and cross-correlations [288], and strategies for identification of 'motifs' of spike intervals in the activity of individual neurons are readily extended to the identification of stereotyped patterns across neurons [2, 313]. Moreover, just as a 'burst' can be taken as a unitary event, a coincidence of activity across neurons can be taken as a unitary event and subjected to further time-series analysis, as if this coincidence represented the activity of a virtual neuron.

There are some issues unique to multichannel data that deserve special mention. From N channels of data, one can compute not only N autocorrelation functions, but also $N(N-1)/2$ cross-correlations, cross-spectra and covariances, and, more generally, $N!(N-r)!/r!$ joint rth-order correlations among r channels. The challenge is not so much knowing how to do the computations but, rather, knowing how to interpret mass of statistical information that emerges.

When a time-varying stimulus is present, it is important to distinguish between correlations induced by common driving by the stimulus, and 'intrinsic' correlations. Here, the usual approach [126, 127] is to calculate a 'shift predictor' or 'shuffled correlogram', by cross-correlating responses on one channel with randomly selected responses on the second channel, rather than with the simultaneously recorded responses on the second channel. The difference between the unshuffled cross-correlation and the shuffled cross-correlation is thus a measure of

correlated activity which cannot be accounted for merely by joint activation of the two neurons by the stimulus. Cross-correlations can be interpreted in terms of functional connectivity [126, 127, 288], but there are important caveats [53].

The shuffle-corrected cross-correlogram is sensitive to correlations of activity among neurons that are present throughout the stimulus cycle, but cannot resolve whether or not these correlations vary with time. The joint PSTH [4, 127] is a refinement of the cross-correlogram, which is able to resolve dynamically changing cross-correlations. Similar information in the frequency domain can be provided by extending phase-locked spectral analysis to multichannel data [331].

3.2. Quantification of information

Shannon's groundbreaking ideas [344] provide the basis for most approaches to the quantification of information in the nervous system. We briefly review some of the elements of information theory, and then consider its application to experimental data.

Consider a set $\{s_a\}$ of abstract symbols ('stimuli'). For a stimulus set which consists of 2^M equally-probable elements, it is necessary to know the answer to M yes–no questions to determine which item is present. That is, M bits of information are required to change the state of knowledge about which item is present from the *a priori* state (2^M equally probable elements) to certainty. Non-integer quantities of information make perfectly good sense, too. For example, suppose a stimulus set contains ten equally probable items, e.g., the digits $\{0, \ldots, 9\}$. Answers to three yes–no questions are only guaranteed to disambiguate one digit out of eight, while four yes–no questions would occasionally be more than sufficient, so the information required is between three and four bits. However, now assume that the digits are presented in a stream, and that stimuli are lumped into triples prior to identification. There are $10^3 = 1000$ equally likely triples. Since 1000 is between $2^9 = 512$ and $2^{10} = 1024$, the total information required for three judgements is between nine and ten bits. That is, the information required to specify one decimal digit can be said to lie between $\frac{9}{3}$ and $\frac{10}{3}$ bits. By extending this kind of argument, one can show that if the items in a stimulus set occur with probability $p(s_a)$, then the amount of information required to specify which item is present is given by

$$H = -\sum_a p(s_a) \log_2 p(s_a), \tag{1}$$

with the convention that if $p(s_a)$ is zero, then its term is considered to have no contribution to this sum. For a stimulus set with C elements, the maximal value for the information (equation (1)) is $\log_2 C$, which is achieved by equation (1) when the probability assigned to each of the symbols is equal to $1/C$.

In order to quantify the information in a spike train, we proceed as follows. Assume that an ideal observer is attempting to use a neural response to determine which stimulus (from within the class $\{s_a\}$) is present. The probabilities $p(s_a)$, the *a priori* probabilities of these stimuli, represent the observer's state of knowledge prior to the neural response. We further assume that the observed neural response falls into one of a discrete category of responses, $\{r_b\}$, and that the observer knows the conditional probabilities $p(r_b|s_a)$ that a response in category b is elicited by a stimulus in category a. Thus, once a response (say, in category b) is recorded, the observer will revise the probability estimates for each of the stimuli s_a from $p(s_a)$ to the *a posteriori* probabilities $p(s_a|r_b)$. By Bayes' theorem, the conditional probabilities $p(r_b|s_a)$ and $p(s_a|r_b)$ are related to the joint probability $p(s_a, r_b)$ that s_a and r_b occur together by

$$p(s_a)p(r_b|s_a) = p(r_b)p(s_a|r_b) = p(s_a, r_b). \tag{2}$$

Thus, the amount of information provided by registry of a response in category b is difference in the uncertainty associated with the *a priori* probability distribution $p(s_a)$ and the *a posteriori* probability distribution $p(s_a|r_b)$, each calculated according to equation (1). Across all possible response categories b, the expected information is the sum of the information provided by a response in each of the categories b weighted by the probability $p(r_b)$ of such a response. This leads to the following expression for the 'transinformation' (in bits) associated with this neuron and this set of stimuli and response categories:

$$H = -\sum_a p(s_a)\log_2 p(s_a) - \sum_b p(r_b)\log_2 p(r_b) + \sum_{a,b} p(s_a, r_b)\log_2 p(s_a, r_b). \tag{3}$$

Note that this equation is symmetric under interchange of stimulus and response, even though stimulus and response sets were not treated equivalently in our derivation. The equation is a combination of three terms similar to equation (1): the first two terms are the sum of the informations associated with the stimulus set alone and the response set alone, and the final term subtracts the information associated with the set of stimulus–response pairs $\{(s_a, r_b)\}$. With this in mind, it can be shown that the transinformation must be non-negative, and can only be zero if stimulus and response are independent: $p(s_a, r_b) = p(s_a)p(r_b)$. On the other hand, consider the situation where each stimulus a reliably elicits responses in only one class $b = \sigma(a)$. In this case, it follows that the transinformation is maximal, and equal to the information associated with the stimulus set (because, after a response is registered, then stimulus uncertainty is reduced to zero). Thus, transinformation quantifies the *non-independence* of stimulus and response. It is noteworthy that there is no assumption about the nature of the association between stimuli and responses: in a one-to-one association, the maximal value of the transinformation is achieved for any permutation σ.

Even under ideal circumstances of a limitless dataset and complete knowledge of the neural coding scheme, the transinformation depends on the choice of the stimulus set and the probabilities assigned to individual stimuli. For this reason, it is often useful [312, 320, 434] to consider the channel capacity of a neuron: the maximum transinformation that can be achieved for any choice of stimulus set. The channel capacity is the limiting signalling capacity of a neuron.

Overcoming bias in information estimates. There is a major issue that must be confronted prior to implementation of the transinformation formalism. The estimate of equation (3) is a *biased* estimate of the 'true' value of the transinformation that would be obtained from an infinitely large sample of data. The source of this bias is straightforward—even if stimuli and responses are uncorrelated, the right-hand-side of equation (3) cannot be negative, and any deviation (due to finite sample size) of empirically estimated probabilities from $p(s_a, r_b) = p(s_a)p(r_b)$ will lead to a positive value for H. Less formally, since no assumption concerning the nature of the stimulus–response linkage is made, any apparent deviation from independence is seen as evidence of a possible linkage.

There are several ways to deal with this bias. One method is to calculate the transinformation from 'shuffled' datasets, in which the stimuli and observed responses are randomly associated [69, 415]. This leads to a distribution of values for the transinformation H_0 that would be expected merely from the bias of the estimator, given the available sample size. Values of H calculated from the unshuffled data that lie outside this range necessarily indicate a linkage between stimulus and response classes that is more than expected by chance. It is reasonable to consider the difference $H - H_0$ as an estimate of the transinformation after correction for the bias. However, this is not rigorously justified. Indeed, in situations that have been analysed analytically [285] or computationally [281], H_0 is an overly large correction to

the bias of datasets that contain strong stimulus–response linkages. Another strategy [131, 186] is to reduce the bias of the estimator of equation (3) by ensuring that the classification scheme for assignment of responses into categories does not overfit the data. In this approach (typically employed when a neural network is used to classify responses), the network is trained on one subset of the data, and then the classification scheme is applied to a non-overlapping dataset.

An elegant way to deal with the estimator-bias problem was recently developed by Treves and Panzeri [285, 396]. Provided that the rule for categorizing responses acts independently on each response, the asymptotic estimate for the bias of equation (3) is given by [255, 285, 396]

$$H_{bias} = \frac{1}{2N \log_e 2}(C_{SR} - C_S - C_R + 1). \tag{4}$$

Here, C_S indicates the number of stimulus categories, C_R indicates the number of response categories, and C_{SR} indicates the number of possible pairings of stimulus and response categories. It is most conservative to take $C_{SR} = C_S C_R$, but other choices may be justified under circumstances in which it can be argued that certain stimulus–response pairings are impossible [285]. Higher-order correction terms (i.e., involving N^{-2}, N^{-3}, ...) in equation (4) are not typically useful, in that for small N they can make the estimate worse, indicating that there is insufficient data for a sensible calculation, while for large N they decrease so rapidly that they are negligible [285]. Equation (4) can be derived from the observation that naive estimates of the information associated with a single set of C symbols (equation (1)) are biased downward by [66]

$$H_{bias} = -\frac{C - 1}{2N \log_e 2}. \tag{5}$$

It is also possible to arrive at an upper bound for the transinformation by consideration of the maximum possible number of distinguishable responses that a neuron can generate (independent of any particular set of stimuli). It is convenient to bin the spike train into intervals of width $\Delta\tau$, where $\Delta\tau$ is assumed to be the firing precision of the neuron, and is sufficiently short so that no bin can contain more than one spike. It is further assumed that each bin's occupancy is independent. With these assumptions, the upper limit for the transinformation is given by [225, 312]

$$H_{\max} \approx RT \frac{1 - \log_e R\Delta\tau}{\log_e 2}, \tag{6}$$

where R is the mean firing rate. This bound is the 'entropy' of a set of Poisson spike trains of length T, rate R and timing precision $\Delta\tau$. The transinformation can only achieve this bound in the absence of 'noise' (so that each stimulus will elicit only one response), and for a stimulus set which leads to the Poisson response statistics presupposed in the derivation of equation (6). Constraints on the statistics of possible responses (e.g., non-independence of bin occupancies) decrease the entropy of the spike train, and thus decrease this upper bound. This approach is particularly powerful when combined with 'stimulus reconstruction' methods to provide a lower bound for transmitted information [34, 312]. The approach can also be refined by replacing equation (6) with empirical estimates of the number of distinguishable responses based on a vector-space embedding (see below)—an approach known as the 'direct method' [321].

Categorization rules. The information-theoretic framework is quite general, and does not make assumptions about which features of a response are significant. But implicit in this approach (i.e., direct calculation of information via equation (3)) is the need for a rule to categorize individual neural responses into response classes. This is ultimately a matter of

biology, not mathematics, in that the rule for categorization can be viewed as a means to formalize a hypothesis for what aspects of the spike train are important. If one intends to interpret the transinformation as the information which is *used* by the visual system, then this categorization rule must somehow be a match for the decoding process.

The transinformation can also be used as a means to characterize the extent to which various aspects of temporal structure are *available for* signalling. In this approach, the transinformation is calculated for each of a set of candidate categorization rules [414, 415]. Each classification rule formalizes a particular aspect of temporal structure; if a classification rule leads to a large value of transinformation, then one can conclude that the temporal structure that it embodies has high stimulus specificity. The lack of any assumptions concerning the nature of the stimulus–response linkage carries the liability of downwardly biased estimators, but in this context it has the benefit that a variety of categorization rules can be compared on an equal footing.

Discretization and the structure of the response space. Equation (4) would suggest that bias is minimized by minimizing the number of stimulus and response categories. But reduction of the number of stimulus or response categories is a source of *downward* bias in the estimation of transinformation. Grouping distinct stimuli together makes systematic dependence of responses on their distinguishing features appear to be chance variability of responses to stimuli within the same category, and this lowers the transinformation. An overly coarse response categorization may cause distinct responses, associated with somewhat different *a posteriori* probabilities, to be treated together. Ignoring the distinction between these *a posteriori* probabilities also lowers the apparent amount of information contained in the responses. In both cases, the apparent information is reduced as a direct result of the discretization of the stimulus or response space. This reduction in apparent information due to categorization is more critical for the estimation of information capacity or transinformation in an absolute sense, than for comparing categorization rules that each lead to the same number of categories. Indeed, under circumstances in which the stimuli are under the experimenter's control, the bias in estimation of transinformation due to stimulus discretization can be eliminated simply by choosing an explicitly discrete set of stimuli.

However, the need to categorize the responses cannot be dealt with in this fashion. One class of approaches is to make assumptions concerning the structure of the response space itself, and to use these assumptions to compensate in some fashion for the need to discretize. If one is willing to make substantial assumptions concerning the nature of the relationship between stimulus and response, then one can make use of powerful analytic tools. For example, assuming (i) that spike trains can be considered as approximations to continuous signals, (ii) that the stimulus–response relationship is a linear one, (iii) that noise is Gaussian, additive, and stimulus-independent, and (iv) that the stimulus set consists of time series drawn from a Gaussian ensemble, then one can use classical results from the Shannon theory [344] to derive the exact transinformation [320, 312] for a response of duration T:

$$H = \frac{T}{4\pi \log_e 2} \int_{-\infty}^{\infty} \log_e[1 + Z(\omega)]\, d\omega, \tag{7}$$

where $Z(\omega)$ is the signal-to-noise ratio at the frequency ω.

However, it may not be practical or reasonable to make all of these assumptions. Representation of spike trains as a sequence of bins naturally leads to consideration of these responses within a vector space, but does not require an assumption that input and output are linearly related. For a reasonable discretization (e.g., 5 ms) and response length (e.g., 100 ms), the number of bins, and thus the dimension of this vector space, is very large. Most of the vector space is sparsely occupied or unoccupied by data, and thus, an attempt to use volume

elements that fill the entire vector space to classify responses can lead to intolerably large biases. Rather than deal with the entire vector space, one can examine projections onto a relatively small number of principal components [246, 281, 282]. Alternatively, one can perform the clustering only in heavily occupied regions of the vector space, and 'regularize' the data by a smoothing process [69]. These approaches reduce the effects of discretization, but they require assumptions concerning the nature of response variability and implicitly assume that responses can be clustered by a Euclidean metric based on the binned spike trains. Another approach [434] makes use of a statistical model of the stimulus–response relationship (an empirical truncated-normal distribution for spike counts), whose mean and variance are estimated from the data) and then uses this model as the basis for information calculations. These approaches work well for situations in which most of the temporal structure of a spike train is described by its envelope; their applicability to the more structured spike trains seen at in the retina and lateral geniculate are as yet unclear.

When only two stimulus categories are present, it is possible to dispense with assumptions concerning the nature of response variability through the use of the receiver operating characteristic (ROC) [134]. A univariate response measure is postulated, and the categorization rule is essentially a threshold value of this measure for assignment of responses to either of two classes. The ROC analysis then examines the performance of this categorization rule, parametric in all values of the threshold. Essentially, this is like having a continuum of response classes, parametrized by the value of the response measure. This approach has been used primarily in the study of discrimination of direction of visual motion [16, 276, 342] and with spike counts (rather than other aspects of temporal structure) as a response measure, but these are not intrinsic limitations of the approach.

Neural network classifiers [131, 254] and clustering schemes based on metric spaces [413–415] readily deal with multiple stimulus categories and make the fewest assumptions concerning the nature of response variability. Neural network classifiers implicitly postulate some form of response measure, while metric space methods merely postulate a way of judging the similarity of two responses. Both of these approaches are more general than classification of responses based on spike counts or spike rates, considered as vectors in a space with a Euclidean distance. However, the penalty for generality is that these approaches necessarily suffer from downward biases in the estimation of information due to discretization [414].

4. Temporal aspects of visual signals

4.1. Retina

Anatomical overview. A schematic overview of retinal anatomy is presented in figure 2. Quanta of light are transformed into graded neurophysiological signals by photoreceptors [19]. Retinal ganglion cells, which form the output of the vertebrate retina, generate action potentials [149], the all-or-none spike discharges that propagate along the optic nerve to the brain. The most direct path from the photoreceptor to the ganglion cell consists of two synapses: from photoreceptor to bipolar cell, in the outer plexiform layer, and from bipolar cell to retinal ganglion cell, in the inner plexiform layer. This 'radial' pathway is complemented by networks of lateral interactions at each plexiform layer: horizontal cells at the outer plexiform layer and amacrine cells at the inner plexiform layer [93]. Many synaptic connections within the plexiform layers are reciprocal and have a unique synaptic structure known as a 'ribbon', whose function is unknown but the subject of intensive study (e.g., [407]). With the exception of some amacrine cells [113, 264, 371, 392], retinal interneurons, like photoreceptors, do not fire action potentials, but communicate entirely by graded signals

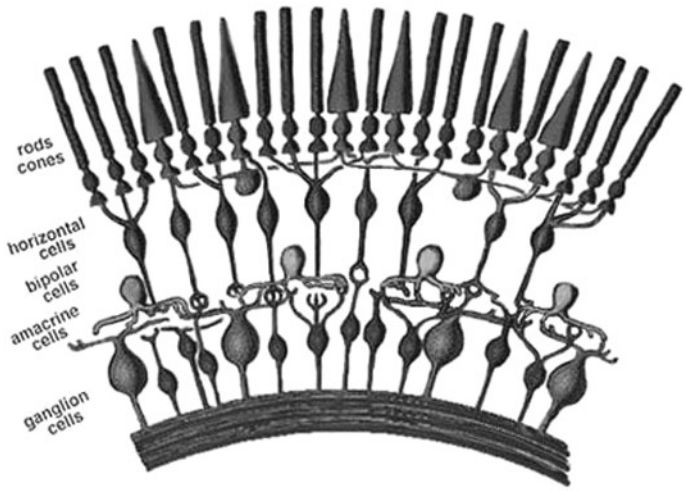

Figure 2. A schematic overview of retinal anatomy, from H Kolb (http://insight.med.utah.edu/Webvision/imageswv/schem.jpeg), with permission.

[433]. The major categories of retinal neurons are also subdivided into many subtypes, based on morphological, physiological, and neurochemical features [43, 44, 103, 119, 238, 425, 427]. Both plexiform layers are subdivided into multiple sublaminae, and connections within these sublaminae are, in general, subtype specific. These important and interesting details vary substantially across species. The interested reader is referred to one of the many reviews [45, 93, 190, 376, 425] of retinal anatomy and functional correlation.

Photoreceptors. The remarkable ability of the retina to operate over at least a 10^9-fold range of light intensities [346] is primarily due to the properties of the photoreceptors. In the lower half of the intensity range, signalling is accomplished primarily by rods, while in the upper half of the intensity range, signalling is accomplished primarily by cones. However, rather than forming the initial stages of independent and non-overlapping functional streams, rod and cone signals intermix, within the cone itself [270], within horizontal cells [270], and within certain amacrine cells [428]. Rod saturation is gradual. Consequently, at intensities encountered in the typical daylight environment, both classes of photoreceptors contribute to signalling. Furthermore, even at light levels for which the foveal response can be considered to be cone-driven, the overwhelming numerical predominance of rods in the periphery means that their contributions to non-foveal vision cannot be neglected.

To a first approximation, photoreceptor responses depend in a linear way on their photon catch [332], see figure 3. The behaviour is very close to linear for dim flashes whose intensity does not fluctuate over more than a decade (figures 3(A) and (B)). But the gamut of useful vision (even with the subdivision of photoreceptor labour into two classes) requires that receptors provide useful signals over a 10^5-fold range. Over most of the operating range of the retina, contrast changes of one part in 100 are readily detected. This wide dynamic range is incompatible with strict linearity. Were this to be accomplished by strictly linear photoreceptors, their outputs would need to be precise to within one part in 10^7. Instead, the sensitivity of rods and cones decrease with increasing illumination, in a manner in which the size of the response to a fixed change in contrast remains approximately constant [278], a relationship known as Weber's law [422]. Adaptation consistent with Weber's law can

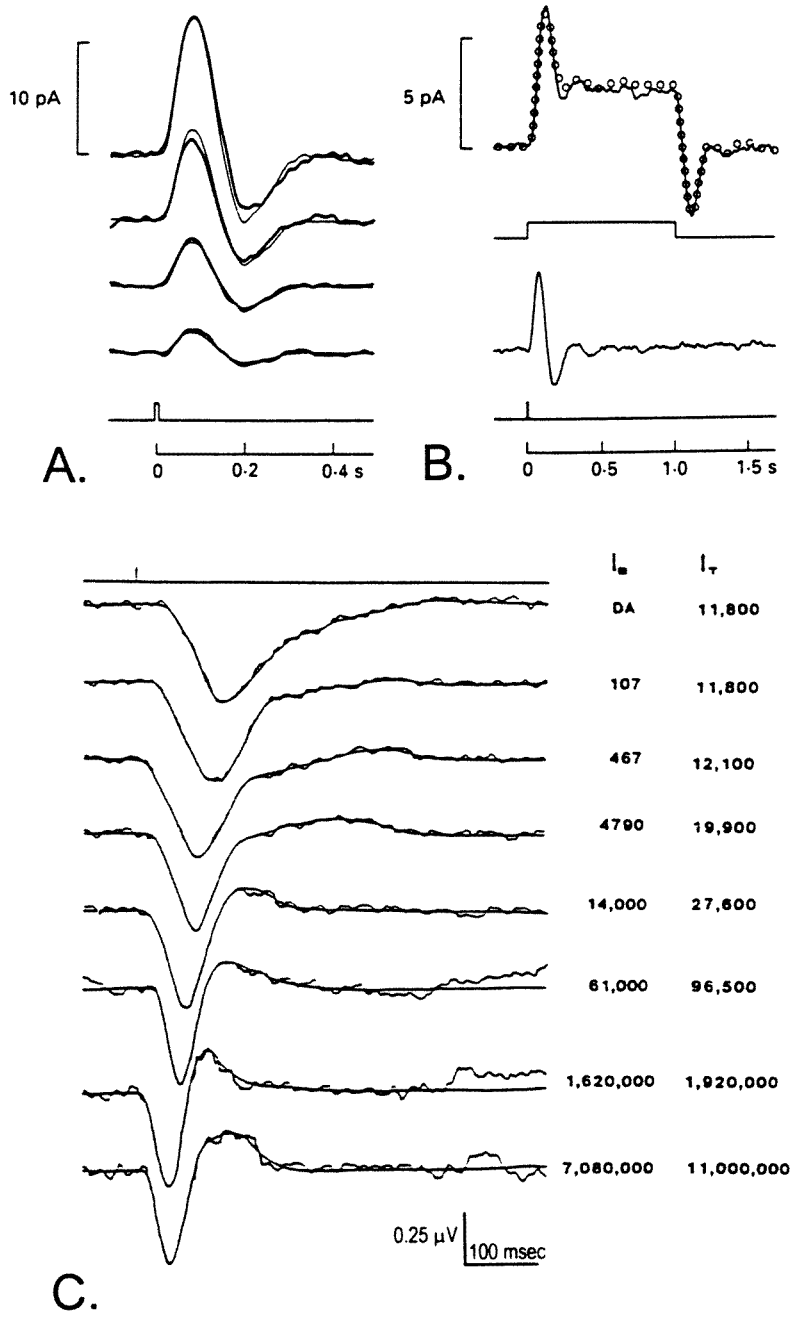

Figure 3. (A) For dim flashes, photoreceptor responses are very nearly proportional to intensity. Bold traces are measured responses to flashes of four intensities separated approximately by factors of two; thin traces are the prediction based on exact proportionality. (B) For dim flashes, responses obey superposition in time. The upper trace compares a measured step response (solid curve) with prediction based on superposition of responses to a brief flash (open circles); the lower trace is the measured flash response. (C) With large changes in intensity, the step response changes dramatically in overall timecourse. (A) and (B) show macaque cone responses, from Schnapf *et al* [332]. (C) shows turtle cone responses, from Daly and Normann [82]. All figures are reproduced with the consent of the original publishers.

be thought of not only as an efficient signalling strategy, but also as the removal of factors irrelevant to object identification (mean illumination) while leaving critical factors (relative contrast) invariant. That is, the disadvantages of nonlinear distortion at the earliest stage of sensory processing are outweighed by an advantage related to the nature of natural visual scenes. Ethologically significant objects in the natural world are distinguished and identified by differences in their reflectance, but they are not self-luminous; thus, it is important to signal relative intensity (contrast) rather than absolute intensity.

With increasing light intensity, photoreceptor responses show a dramatic change not only in gain but also in dynamics [21, 22, 82, 267, 277, 332]. In turtle rods [91], a 20-fold increase in intensity at the low end of the operating range is associated not only with a 5-fold decrease in sensitivity (i.e. membrane voltage response per photoisomerization), but also with a 2.5-fold shortening of the latency-to-peak response. Across the range of intensities, the impulse response remains monophasic, corresponding to a transfer function that is purely lowpass. A similar change in response timescale is seen across the operating range of the turtle cone [82], but the impulse response becomes diphasic at high intensities, corresponding to a bandpass transfer function (figure 3(C)). In primate cones, the change in shape of the impulse response is even more dramatic [332]—from a monophasic waveform to a nearly balanced diphasic waveform. The nearly balanced diphasic impulse response indicates that at high light levels there is only a minimal response to DC changes in light intensities, while the response to flicker remains large.

The change in photoreceptor dynamics from lowpass to bandpass, and the shortening of the integration time with increasing light intensity, cannot be regarded as extraction of a kind of perceptually useful invariance similar to the light-induced changes in overall sensitivity. However, these changes do have advantages for signalling economy [290]. At low light intensities, the quantal nature of light represents an external noise source, which reduces the informativeness of high-frequency signals. As light intensities increase, reliable photon counts can be achieved with progressively shorter pooling times. Application of Wiener's theory of optimal filters to these intuitive ideas suggests that photoreceptors can be considered to be adaptive filters that shift their dynamics to optimize coding of scene information in the setting of photon noise [290]. Similar considerations apply in the spatial domain as well, in that spatial pooling is useful to limit photon noise under low-intensity conditions, but when photon arrival is sufficiently rapid, higher spatial resolution is attainable with acceptable signal-to-noise. As would be predicted from the optimal-filtering viewpoint [290], spatial pooling in the retina also decreases as illumination increases. However, much of the change in spatial pooling is not intrinsic to individual photoreceptors but rather is a combination of changes in photoreceptor coupling and, more prominently, post-receptoral mechanisms.

Under high light levels, many primates (including man) have trichromatic colour vision: the appearance of any given light can be matched by linear combinations of three arbitrarily chosen 'primaries' [46, 422, 441]. It is well established that the differential wavelength sensitivities of the cones form the basis of this trichromacy and account for performance on colour-matching and colour-discrimination tasks [23, 332, 333, 362]. However, photoreceptor properties alone do not account for the major temporal features of chromatic vision. Luminance flicker can be discriminated from steady illumination up to frequencies of approximately 60 Hz [182], but purely chromatic flicker becomes indistinguishable from steady illumination in the 20–30 Hz range [184]. Chromatic signals requiring the short-wavelength ('blue') cone are processed with still lower temporal resolution [49]. These psychophysical differences in the processing of luminance and chromatic signals are parallelled by electrophysiologic differences, as measured in individual retinal ganglion cells in the monkey [207], and in visual evoked potentials [262, 295, 299] and magnetic fields [300] in man. However, the dynamics of individual cones from each of the three classes are strikingly similar [332], and

appropriate psychophysical studies [377] indeed reveal that even the short-wavelength cone has rapid intrinsic dynamics. Thus, the difference in temporal sensitivity to luminance and colour changes must be due to differences in post-receptoral processing [184, 328], rather than intrinsic differences in the photoreceptor dynamics [377].

In summary, photoreceptors may be characterized as adaptive filters, whose gain decreases and response speed accelerates with increasing average illumination. Compared with rods, cones have a lower absolute sensitivity, a shorter response latency, and more bandpass behaviour, but response dynamics across cone classes are similar.

Horizontal cells. Horizontal cells constitute the first neural stage of lateral interaction within the retina. Two broad anatomical classes of horizontal cells have been recognized [119]: the 'inner' horizontal cell typical of primate retinae, which has a well-defined dendritic tree with cone inputs and a well-defined axonal arbor that provides outputs to rods [191], and the 'outer' horizontal cell typical of fish retinae, that lacks a well-defined axon but rather forms a syncytium [322]. Horizontal cells also receive indirect inputs from both photoreceptor classes, by virtue of gap junctions between the photoreceptors and feedback to photoreceptors from other horizontal cells [270, 289].

Physiologically, horizontal cells are classified as 'L-type' (luminance) if they hyperpolarize in response to light of all wavelengths, or 'C-type' (chromatic) if they hyperpolarize in response to some wavelengths but depolarize in response to other wavelengths. In the cat [274, 374] and monkey [81, 426], it appears that only L-type horizontal cells are present. Catfish retina, which contains only one cone type [67], also contains only L-type horizontal cells. C-type horizontal cells are prominent in other fish [60, 324, 442] and amphibia [380]. Primate retinae appear to have a subtype ('HIII') of horizontal cell which receives input from only the two long-wavelength (L and M) cones; HI and HII horizontal cells differ in their dendritic morphology but contact all cone classes [192, 195].

For a relatively wide range of contrasts (up to ca 0.6), turtle [393] and cat [258] horizontal cells can be regarded as linear. Based on their transfer properties, either measured with sinusoidal [108] or white-noise [234] modulation [258] of large fields, cat horizontal cells can be classified into three groups based on their frequency cutoffs and latencies: H_{n} ('narrow')-type, with a latency of 45–55 ms and a frequency cutoff of 25–40 Hz, H_{m} ('medium')-type, with a latency of 20–30 ms and a frequency cutoff of 55–70 Hz, and H_{w} ('wide')-type, with a frequency cutoff of 95–110 Hz (figure 4). The frequency-response curves of the two faster subtypes contain peaks or prominent shoulders at high temporal frequencies [108], consistent with observed oscillatory responses and suggesting a model of parallel bandpass inputs from the photoreceptors [108, 135]. For small stimuli (1.5 deg or less), responses are restricted to a lower frequency range, and the narrow peaks at high temporal frequencies are lost [109]. This suggests that these resonances reflect a network property of the outer plexiform layer, rather than intrinsic characteristics of transmission from photoreceptors. For contrasts in the 0.7–0.9 range [109], response nonlinearities become apparent. Distortion is more prominent for stimuli that produced a large response (i.e., low temporal frequencies and large area), suggesting the presence of a compressive nonlinearity following linear temporal filtering. For L-type horizontal cells in the turtle [68, 394], high-frequency resonances are not present, and there is less dependence of response dynamics on the spatial characteristics of the stimulus. In catfish, the entire horizontal cell layer is well described by a syncytium of cells (the 'S-space'), both anatomically and physiologically [146, 235, 265, 322, 436]. The shift of the horizontal cell response to higher temporal frequencies with increased stimulus area [67, 236] is well described by a linear model [200] incorporating linear, passive spread within the S-space and subtractive feedback to the photoreceptors [20, 325].

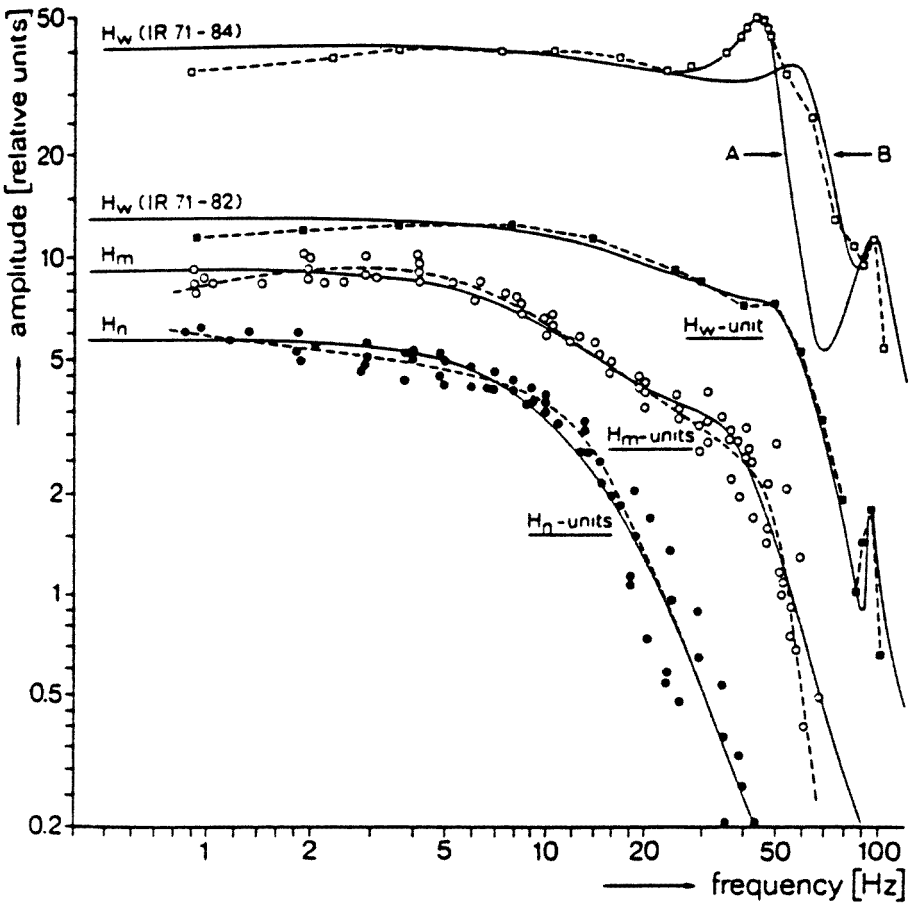

Figure 4. Transfer functions of the three kinds of horizontal cells in the cat (two examples of H_w cells are shown). Symbols are measurements based on sinusoidally varying luminance stimuli; continuous curves are model predictions based on parallel and serial combination of simple filter elements. From Foerster *et al* [108]. Figure reproduced with the consent of the original publishers.

For lights that modulate only a single cone class, C-type horizontal cells respond in an approximately linear manner [324, 380]. However, the dynamics of the response depends strongly on which cone class is stimulated [442], even at frequencies as low as 5 Hz [380]. Moreover, for stimuli that drive two cone classes, the combination of the cone signals is typically non-additive [60, 442]. Since these phenomena are not present in L-type horizontal cells of the same retina which also receive cone input, they probably reflect properties of the C-type horizontal cells and/or the cone-to-horizontal cell transmission process, rather than the cones themselves.

Detailed dynamical measurements in the turtle [395] suggest a feedback model of light adaptation, in order to account simultaneously for Weber law behaviour at low temporal frequencies and a common asymptote at high temporal frequencies. The phenomenological feedback reflects, in part, the intrinsic properties of the phototransduction mechanism [21, 22], but the spatial properties of light adaptation indicate that the horizontal cell itself plays an important role [203].

In summary, distinct classes of horizontal cells have different dynamics, and some have high-frequency resonances. Like photoreceptors, they are approximately linear for small to moderate signals. The dynamics of signal transfer between photoreceptor and horizontal cell depend on photoreceptor type, and inputs from different photoreceptor types may interact nonlinearly. Horizontal cells participate in the dynamics of light adaptation, both via their intrinsic properties and feedback to the photoreceptors.

Bipolar cells: overview. Bipolar cells receive light signals from photoreceptors at the outer plexiform layer, and contact the retinal output, the ganglion cells, at the inner plexiform layer. They represent the first neural processing stage in which antagonistic centre–surround organization is apparent [93], the initial subdivision of retinal information into ON and OFF pathways [334], and, in the primate, the initial subdivision of retinal information into chromatic and achromatic pathways.

The centre–surround organization of the bipolar cell receptive field [93, 146] is generated by combining the direct input from photoreceptor signals from a small region of space with antagonistic signals pooled over a wider region of space by the horizontal cell. In the tiger salamander, pharmacologic dissection [146] of this combination demonstrates that it is approximately linear. The extent of surround inhibition increases with increasing light intensity, and under dark-adapted conditions, it may be entirely absent [37].

Bipolar cells: origin of the ON and OFF dichotomy. As reviewed by Wässle *et al* [427], multiple morphological subtypes of bipolar cells have been recognized in primates, each with presumptive functional correlates. Some bipolar cells, known as 'diffuse' bipolars [44, 291], appear to contact all cones within their dendritic field and, thus, they are unlikely to carry chromatic signals. Other bipolar cells, known as 'midget' bipolars, contact only a single cone pedicle [291]. Midget bipolar cells make two kinds of synaptic contacts with cone pedicles, 'flat' and 'invaginating' [191, 193], and terminate respectively in the outer and inner portions of the inner plexiform layer. These two kinds of midget bipolars generate opposite responses to light in the receptive field centre and represent the initial division of retinal signals into an OFF pathway (flat bipolars) and an ON pathway (invaginating bipolars) [103, 274]. The microcircuitry of the midget bipolar pathway is strikingly precise: contacting every foveal cone pedicle are two bipolar cells [61], presumably one ON and one OFF. The bipolar cells that contact the 'blue' (short-wavelength) cones are morphologically distinct [198, 232]. In contrast to midget bipolar cells serving the medium- and long-wavelength cones, it appears that only invaginating (ON) S-cone bipolars are present [80, 427], although there is one report of candidate OFF S-cone bipolars [195]. Finally, there is a separate class of bipolar cells that contact the rods. Anatomy, immunoreactivity [137], and physiology [85, 429] of these rod bipolars provide converging evidence that they all depolarize in response to light. That is, in the rod system, the separation of ON and OFF pathways is deferred to the inner plexiform layer.

Quantitative analysis of ON and OFF neurons reveals significant departures from the symmetrical 'push–pull' behaviour that their name might suggest, beginning with the bipolar cell. In order for ON and OFF signals to be generated in the outer plexiform layer, the same neurotransmitter, glutamate, must depolarize OFF-centre bipolar cells, and must hyperpolarize ON-centre bipolar cells [353]. ON- and OFF-centre bipolar cells have distinct immunocytochemical characteristics [427]. Since photoreceptors hyperpolarize in response to light, synaptic transmission to OFF bipolar cells must be sign-preserving (i.e. excitatory), as it is in the overwhelming majority of glutamatergic synapses elsewhere in the nervous

system. In contrast, glutamatergic synaptic transmission to ON bipolar cells is sign-inverting (i.e. inhibitory) and appears to rely on a second-messenger system. This arrangement incurs an extra delay, estimated at 10 ms by Shiells and Falk [353]. The distinctive signal transduction pathway in ON bipolar cells underlies its selective dysfunction in muscular dystrophy [106] and perhaps other disease states [447].

The difference in transmission mechanism appears to be the source of substantial differences in the dynamics of ON and OFF pathways [75]. In snapping turtle [10], hyperpolarizing bipolar cells show a decrease in membrane voltage noise with light (consistent with closing of channels), and the noise spectrum is consistent with synaptic events of halfwidth 15 ms, while depolarizing bipolar cells show an increase in membrane voltage noise with light, and have a noise spectrum consistent with synaptic events of halfwidth 49 ms. Spatial asymmetries between ON and OFF pathways have been demonstrated, including a twofold difference in receptive field sizes in tiger salamander (ON bipolar receptive fields smaller) [146] and psychophysical [400] and electrophysiological [447] differences in man.

Generation of ON and OFF signals may be somewhat different in the catfish. There are no clear differences in dynamics between ON and OFF catfish bipolar cells [322], and all bipolar cells are of the invaginating type [322]. ON and OFF catfish bipolar cells of each class have a linear antagonistic centre–surround organization [325], with the surround response delayed by approximately 10–20 ms, consistent with a transport delay in the S-space [67].

There is indirect physiological evidence for an asymmetry of dynamics of ON and OFF pathways at the bipolar cell level in the cat. The nonlinear pathway of the Y ganglion cell (see below) can be modelled as an array of initial linear elements identified with the bipolar cells, followed by rectification, followed by a stage of spatial pooling [410]. The implicit time within the initial linear stage is approximately 9 ms longer for ON Y cells than for OFF Y cells. This difference is in good agreement with the estimate of the added delay due to the second-messenger pathway required by the on bipolar cell's sign-inverting response to glutamate [353]. This dynamical asymmetry is not seen in X ganglion cells [409], suggesting that bipolar-to-ganglion cell transmission is associated with a greater delay in OFF cells than in ON cells, thus providing for a similar total transmission delay (photoreceptor to bipolar to ganglion cell) in the ON and OFF pathways.

In mammals, ON and OFF signals are not recombined until the primary visual cortex [334]. The evolutionary advantages of dual transmission of ON and OFF signals are not entirely clear [38, 354]. One possibility is that the dual pathways could enable efficient and linear transmission of luminance information by push–pull combination of neurons, each of which can only signal unidirectional quantities effectively because of a low maintained discharge. After pharmacologic blockade of retinal ON pathways with the glutamate analogue 2-amino-4-phosphonobutyrate [337, 334], there is a selective deficit in detection of luminance increments and contrast sensitivity, but colour, motion, and shape perception are relatively unimpaired. On the other hand, ON and OFF pathways can be isolated psychophysically, via adaptation to sawtooth waveforms [199] and masking paradigms [38]. The distinct spatial and temporal characteristics of the isolated pathways [39, 40, 447] suggest that their role is more subtle than that of simple push–pull combination—that is, not limited to working in concert to form a single luminance signal. One possibility recently proposed by Bowen [38] is that the distinct properties of the ON and OFF pathways can disambiguate the effects of contrast and contrast adaptation.

Nonlinearities at the bipolar cell stage. Although intrinsic processes within the photoreceptors account for much of light adaptation, additional adaptive processes must take place at later stages. Bipolar cells' membrane potentials do not vary by more than

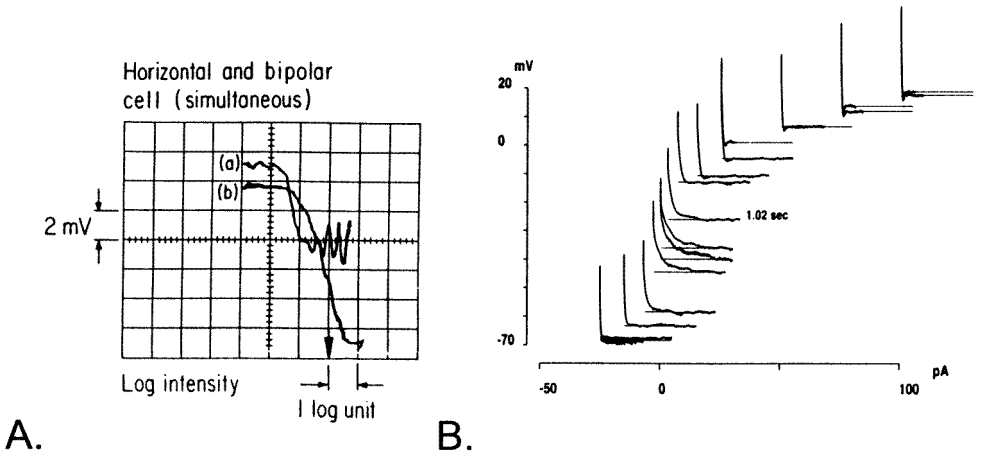

Figure 5. (A) Comparison of operating ranges in bipolar cells and horizontal cells. Simultaneous intracellular recordings were made as light intensity was swept from low to high. The horizontal cell (b) shows a much broader response range than the bipolar cell response (a), but the bipolar cell continued to respond to luminance steps beyond the point at which its steady-state response saturated (oscillations on the right end of curve a), from Werblin [430]. (B) Dependence of dynamics of isolated bipolar cells of the tiger salamander on mean current inputs. Impulses responses are measured under current-clamp conditions by cross-correlating the voltage response with a white noise input currents. For a mean current input near zero, the impulse response is approximately a descending exponential. With depolarizing mean currents, the response quickens and an undershoot develops. From Mao *et al* [230]. All figures are reproduced with the consent of the original publishers.

approximately 30 mV [205, 433]. Near their resting potential, with current considered as input, isolated bipolar cells [230] have a very high gain, equivalent to an input resistance of approximately $5 \times 10^9\ \Omega$. As a consequence, an input current of only a few pA, perhaps the result of opening of only 45 synaptic channels [388], would result in saturation of the bipolar cell's voltage response. Thus, bipolar cells are faced with the same problem as cones—the need to retain high sensitivity, yet also to signal responses over a wide dynamic range. Moreover, as was shown by Werblin [430], bipolar cells have a steeper intensity-response curve, and thus, at any given adaptation level, a narrower operating range, than do photoreceptors or horizontal cells (figure 5(A)).

Transmission from photoreceptors to bipolar cells indeed is marked by a response saturation, or 'clipping' [13, 24, 440]. While some of this clipping is likely to be due to processes intrinsic to the photoreceptors [13, 15, 267], postsynaptic mechanisms must play a role, since the bipolar cell voltage response shows saturation at light intensities 1–2 orders of magnitude lower than light intensities which saturate the synaptic input, as gauged from the current response [204]. Studies in the isolated bipolar cell of the tiger salamander have provided evidence of adaptive filtering [230]. With depolarization, bipolar cell characteristics change from high gain and lowpass behaviour, to low gain and bandpass behaviour (figure 5(B)). Transfer functions at all levels of depolarization share a common high-frequency asymptote, similar to the adaptive behaviour observed in the horizontal cell [395]. The ionic mechanism underlying this behaviour appears to be the activation of a tetraethylammonium (TEA)-sensitive potassium channel [229], which corresponds to the observation that clipping of photoreceptor signals is also blocked by TEA [204]. As in photoreceptors, this adaptive behaviour, though strongly dependent on the mean level of the input, allows for approximate linear behaviour

for small signals that fluctuate around this mean. In the intact retina, mutual coupling of bipolar cells under dark-adapted conditions [37] is an independent source of adaptive changes in spatiotemporal properties. Overall, the changes in rod to bipolar transfer dynamics with dark adaptation [33] can be understood to implement a kind of optimal filtering in the face of photon noise [290].

In summary, the centre–surround receptive field of bipolar cells represent the initial site of high-pass spatial filtering of visual information, and the many morphologically distinct classes of bipolar cells represent the subdivision of visual signals along ON versus OFF, and chromatic versus achromatic pathways. Little is known about intrinsic bipolar cell dynamics in mammals because of the technical difficulties associated with recording from these tiny neurons. However, evidence from fish and amphibia, as well as indirect evidence in mammals, indicates that bipolar cells behave as adaptive quasilinear filters, with significant changes in response gain and dynamics for relatively small changes in input signal size. ON bipolar responses are likely to be delayed by approximately 10 ms with respect to OFF bipolar responses, and surround responses are delayed compared with centre responses.

Amacrine cells: overview. Amacrine cells occupy the inner plexiform layer and provide the anatomical pathway for interactions among bipolar cell outputs and modulation of transmission between bipolar cells and ganglion cells. Anatomically, the inner plexiform layer is subdivided into an outer sublamina ('a'), consisting of two substrata, which is the site of termination of OFF bipolar cells, and an inner sublamina ('b'), consisting of three substrata, which is the termination site of ON bipolar cells [103, 272] There are over 25 morphologically distinct subtypes of amacrine cells [119, 195, 233, 238], and they make use of at least eight neurotransmitters [376]. High-resolution histochemical methods demonstrate that within each substratum, only specific subtypes of bipolar, amacrine, and ganglion cells form synapses [47, 253]. Reciprocal [136, 448] and serial [71, 138, 448] synapses among all cellular components of the inner plexiform layer are commonplace. This anatomy brings with it the expectation of a correspondingly complex and intricate physiology.

Amacrine cells: new dynamical elements. Amacrine cell light responses are generally more transient than the responses encountered in the more distal retinal neurons [264, 271, 273, 391, 392, 431, 432, 433, 448]. Most amacrine cells are interconnected via an extensive serial inhibitory network [71, 138, 448] whose overall output to the ganglion cells is inhibitory [115, 145]. Additionally, some amacrine cells have qualitatively nonlinear response properties [113, 172, 173, 264, 326, 327, 391, 392, 433] even for small inputs, including depolarizing responses to change in illumination, independent of the direction of this change (the 'ON–OFF' response, figure 6(A)).

The increased transience seen in amacrine cells is partly due to their network properties [115, 145]. In mudpuppy and tiger salamander, amacrine cells provide an inhibitory ($GABA_C$-ergic) feedback input to bipolar cells, which is in turn inhibited by mutual inhibitory ($GABA_A$-ergic) synapses among amacrine cells. But response dynamics also depend on the intrinsic properties of the postsynaptic receptor in isolation. For example, the glycinergic amacrine cell input to ganglion cells generates both tonic and phasic inhibitory currents, depending on the subunit composition of the postsynaptic receptor [145].

The origin of the highly nonlinear ON–OFF response has been a matter of great interest. Since many ganglion cells are relatively linear (see below), the ON–OFF behaviour must be a property of the amacrine cells themselves, and not the bipolar cell output. Some amacrine cells [113, 264, 371, 392] fire action potentials, indicating that they have strong

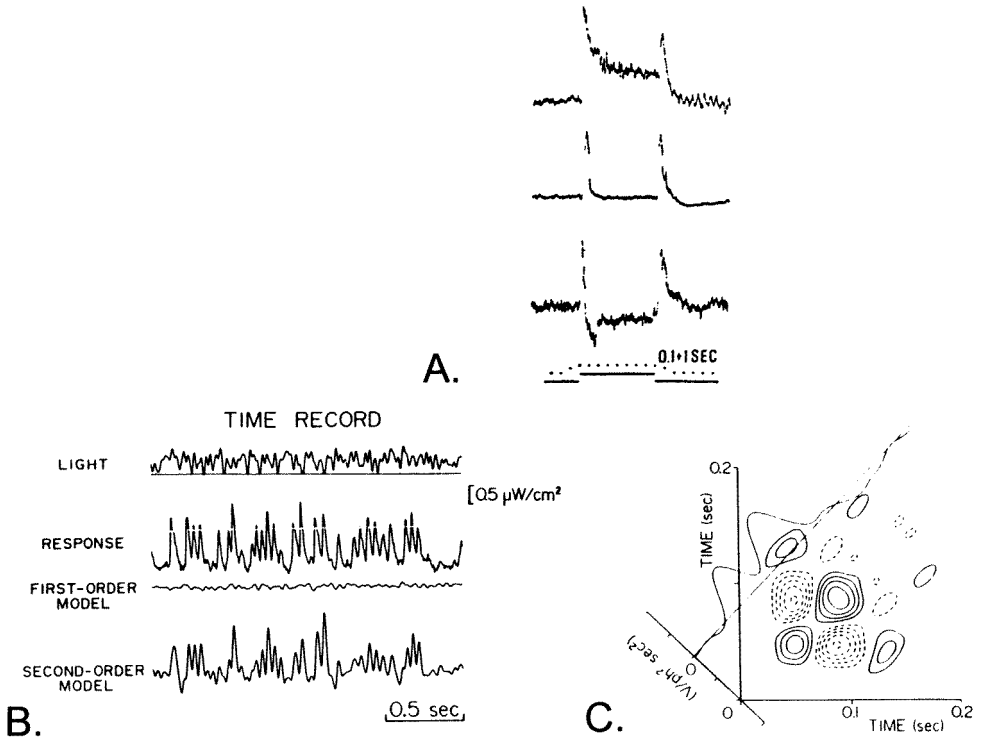

Figure 6. (A) ON–OFF behaviour recorded intracellularly in three carp amacrine cells. From Toyoda *et al* [392]. (B), (C) The nonlinear dynamics of the catfish C-type amacrine cell as revealed by cross-correlation of the voltage response and a white noise input. (B) The best-fitting linear filter ('first-order model') accounts for almost none of the response; the best-fitting model with a quadratic nonlinearity ('second-order model') accounts for most of the response. (C) The Wiener kernel associated with the second-order model of (B). From Sakuranaga and Naka [327]. All figures are reproduced with the consent of the original publishers.

intrinsic nonlinearities. However, spikes *per se* are not the source of the ON–OFF response nor the amacrine cells' transience, since neither of these phenomena are restricted to spiking amacrine cells. Rather, the spike response appears to represent simple rate encoding of a graded depolarization that already manifests transience and ON–OFF responses [197].

The basis of the ON–OFF amacrine's depolarizing responses following both increases and decreases of illumination is most directly investigated in the turtle, in which it is feasible to inject current into a presynaptic bipolar cell while recording an amacrine cell's response [231]. One proposed mechanism is that the depolarizing response is generated by incomplete cancellation of signals from ON and OFF bipolar cells [231, 392] of differing dynamics. Studies in the turtle [231] do not support this possibility: in response to transiently increasing illumination, the response of the hyperpolarizing (OFF) bipolars leads the depolarizing response from the ON bipolars. The sum of these opposing signals has a transient timecourse similar to that of the amacrine light-on response, but it is of the wrong polarity (since the hyperpolarizing component has a shorter latency). This difficulty cannot readily be fixed by assuming that the bipolar cells inhibit the amacrines, since both light-on and light-off depolarization of the amacrine cell is mediated by excitatory post-synaptic potentials [113, 231]. Furthermore, the amacrine cell's depolarizing response to transiently decreasing illumination bears little resemblance to the

difference in ON and OFF bipolar cells' response to light off. In cat, bipolar cell connections to ON–OFF amacrine cells are primarily within a single sublamina (either ON or OFF but not both) of the inner plexiform layer [113], providing further evidence that direct combination of ON and OFF bipolar signals by the ON–OFF amacrine cell is unlikely.

Most probably, a full account of each phase of the ON–OFF amacrine's response requires a combination of a direct bipolar input with an input whose sign has been inverted via an inhibitory interneuron. Since the outer retina is qualitatively linear, ON and OFF bipolar signals need to be rectified prior to this combination. Otherwise, whatever mechanisms account for the amacrine response to increasing illumination would lead to a response of the wrong polarity to decreasing illumination. Light-on and light-off responses scale similarly across a wide range of illumination [231], which implies that the sensitivities and dynamics of these responses must be tightly matched. Finally, in turtle, amacrine cell ON–OFF responses to central and peripheral illumination have different reversal potentials, implying distinct neurotransmitters or receptor systems [231].

In carp [392], cat [113], and monkey [371], ON–OFF amacrine cells have spatially homogeneous receptive fields. Other amacrine cells in these species have prominent centre–surround spatial antagonism [392]. In contrast to behaviour in the outer plexiform layer, combination of centre and surround signals in spatially inhomogeneous amacrine cells deviates from simple additive combination. That is, it is likely that the intrinsic nonlinearities that are qualitatively manifest in the ON–OFF amacrine cells are also present in amacrine cells with centre–surround organization. In ON–OFF amacrine cells, they are responsible for the bulk of the response, since the linear contributions of spatially coincident ON and OFF signals effectively cancel. In amacrine cells with centre–surround organization, ON and OFF signals do not cancel, but their combination is modified by the amacrine cells' intrinsic nonlinearities. This may be the basis of the amacrine cells' 'antagonistic response to change' [431].

In the catfish, amacrine cells may be classified into two types, C and N, on the basis of their dynamics [326, 327]. Both subtypes produce transient on-off responses to light and to current injection into horizontal cells. Analysis with white noise inputs [234] can be used to characterize their dynamics in terms of a series of models, consisting of the best-fitting linear model, the best fitting second-order model, etc. For the type C amacrine cell [327], the best-fitting linear model accounts for almost none of the cell's response, while the main features of the response are captured by the best-fitting second-order model (figure 6(B)). This second-order model is described by a kernel function $K_2(\tau_1, \tau_2)$, essentially the cross-correlation of the response $r(t)$ with the product of the inputs at times $t - \tau_1$ and $t - \tau_2$. In type C amacrine cells, the measured values of this kernel (figure 6(C)) approximate a product form, $K_2(\tau_1, \tau_2) = L(\tau_1)L(\tau_2)$. This means [234] that the neuron's behaviour is consistent with that of a linear filter whose impulse response is $L(\tau_1)$, followed by a static nonlinearity. The computed impulse response of the initial linear stage has an initial peak at 30–60 ms, and then an undershoot which effectively removes the DC component of the response [327]. The nonlinearity is often assumed [266, 327] to be a squaring operation, but it is more appropriate to consider it to be a sharp, symmetric rectification: a quadratic model leads to substantial deviation between data and model [266] when a wide range of input intensities are considered.

N-type amacrine cells are distinguished both by a sustained component of the response to light delivered while dark-adapted [266], and by high-frequency membrane fluctuations which follow, but far outlast, transient increases and decreases in illumination [326]. These membrane fluctuations occur in the frequency range of 15–25 Hz. To a first approximation, the even-order dynamics of the N-type cell can be accounted for by bandpass filtering the C-type response, consistent with known inner plexiform layer connectivity [266]. However, this does not account for their oscillatory transients. Models based on Wiener kernels beyond

second order provide only a modest improvement [326]. This suggests that the rapid membrane transients are best regarded as a manifestation of spontaneous oscillatory activity [161] that is entrained by the stimulus, rather than as the output of a gently nonlinear filter.

Amacrine cells and rod signals. Since there is only one kind of rod bipolar, the ON–OFF dichotomy awaits the inner plexiform layer under scotopic conditions. The AII cell, a narrow-field amacrine cell, plays a crucial role in this regard [271, 273, 428]. It depolarizes to light, and its major input is via glutamatergic synapses from rod bipolars [271, 428]. The AII cell provides rod input to the ON system via gap junctions with ON cone bipolars [256]. In macaque, AII amacrine cells form reciprocal chemical synapses with midget OFF bipolars [136, 139]. The AII synapses are glycinergic [139], presumably inhibitory, and thus enable rod-origin ON signals from the AII cell to drive OFF-pathway cone bipolars. Thus, under scotopic conditions, ON signals likely lead OFF signals, since the former are relayed at the inner plexiform layer by gap junctions, while the latter require a sign-inverting chemical synapse.

The AII amacrines form an extensive network of gap junctions with each other and with bipolar cells. The permeabilities of these two sets of gap junctions are independently regulated [256], with nitric oxide and cGMP reducing amacrine-to-bipolar coupling and dopamine and cyclic AMP agonists reducing AII–AII coupling. Modulation of this coupling may underlie the transition between rod-dominated and cone-dominated responses [256]. Coupling within the AII network increases the effective summing area of subsequent retinal receptive fields, with the joint effects of improving signal-to-noise ratio at the expense of spatial resolution, and increasing correlated activity among ganglion cells [406]. Because of the divergent pattern of connectivity from outer to inner retina, the quantal signal from one rod appears in at least five neighbouring AII amacrine cells. It has been postulated that the active membrane properties of AII cells, along with appropriate gap-junction conductances, leads to selective detection of the synchronous occurrence of such signals in the face of membrane noise [360].

Amacrine cells and direction selectivity. Computation of a directionally selective motion signal is an important part of visual processing [268]. Neurons with directionally selective motion responses are found in invertebrates [33, 34, 303, 312] and vertebrates, both in the central nervous system [16, 276, 342] and in the retina [7, 315] of many species, including rat [47], rabbit [238, 239], and cat [315, 379]. A common denominator of computational schemes of motion extraction [3, 152, 268, 303, 405] is an interaction between inputs that are offset both in time and in space. Because of the relative ease of access, retinal circuitry provides a good model system to study basic mechanisms of directional selectivity.

Anatomical and neurochemical evidence indicate that amacrine cells play a crucial role in the genesis of directional selectivity in the retina. The morphologically distinctive 'starburst' cholinergic amacrine cells form overlapping arrays of dendritic fields within the inner plexiform layer and provide inputs to directionally selective ganglion cells [8, 47, 238, 239]. These amacrine cells express a $GABA_A$ receptor whose unusual subunit composition (α_2, β_1, β_2/β_3, γ_2, and δ) [47] is likely to be associated with a slow conductance response [424], by virtue of the δ subunit. Additionally, these cholinergic amacrine cells receive direct (and presumably more rapid) glutamatergic bipolar cell input [47]. Thus, the inputs to cholinergic amacrine cells have the necessary spatiotemporal characteristics for generation of a motion signal. However, selective laser ablation of the starburst amacrine cells markedly reduces responses to moving stimuli, but direction selectivity is intact [151]. This suggests that starburst cells nonspecifically enhance responses to moving stimuli, but do not confer direction selectivity. An alternative possibility for the origin of the spatiotemporal offsets necessary for direction selectivity [424]

is dynamical differences among the GABA receptors on different amacrine cells: $GABA_A$ receptors that lack the δ subunit (and have α_1 or α_3 subunits rather than α_2) are also present in the inner plexiform layer, but are specifically absent in the cholinergic amacrine cells [424].

Directional selectivity is highly precise [141]. Given the large dendritic spread of amacrine and ganglion cells, it appears necessary to postulate that the spatiotemporal interactions are local processes within the dendritic tree [239]. However, the mode of interaction of the spatiotemporally offset inputs remains unclear. Both shunting inhibition [6, 390] and linear combination followed by a threshold [142] could provide for the necessary nonlinear interaction, but it is unclear [140, 142] how (or whether) either of these processes produce an interaction that is the computational equivalent of multiplication [3, 303, 405].

Ganglion cells: overview. Retinal ganglion cells are the output neurons of the retina, and their axons form the optic nerve. In intraretinal processing, graded voltage signals play a primary role. But because of the long distance between the ganglion cell body and their central targets, the target neurons have access only to the sequence of actively propagated spike trains. Additionally, ganglion cells represent an information bottleneck between eye and brain. Thus, they provide crucial insights into strategies for the efficient transmission of information, and the ways in which sensory information is transformed into spike trains.

In most physiological investigations of ganglion cells, their output is considered to be their 'firing rate' as a function of time, i.e. the average number of spikes in a sequence of relatively narrow time bins, as estimated from multiple trials of the same stimulus. (Other approaches have been taken recently, and these will be discussed below.) In the absence of a patterned or time-varying visual stimulation, retinal ganglion cells generally have maintained firing rates. Thus, despite the point-process nature of their output, the analysis of ganglion cells' receptive field properties can be considered as an attempt to define a relationship between a continuous spatiotemporal input and a continuous temporal output. The formal input is spatiotemporal contrast, the pattern of fluctuations of light above and below its mean; the formal output is the variation of the firing rate above and below its mean.

Ganglion cells dynamics: quasilinear aspects. Enroth-Cugell and Robson's landmark study of cat retinal ganglion cells [100] showed that they can be grouped into two classes (X and Y) based on qualitative features of spatial summation: the qualitatively linear X cells, and the qualitatively nonlinear Y cells. In particular, X cells yield opposite responses to introduction and withdrawal of a grating, while Y cells produce an increased firing rate both with introduction and withdrawal of the grating. This linear/nonlinear distinction is independent of the ON versus OFF dichotomy: ON and OFF are present among both X and Y cells. Subsequently, Boycott and Wässle [43] recognized two clearcut classes of dendritic morphologies (α and β). At any given retinal eccentricity, dendritic fields of the α cells are several times larger than those of the β cells. (With increasing retinal eccentricity, all dendritic fields grow, so that a peripheral β cell is larger than a central α cell.) These differences in dendritic field size corresponded well to differences in the physiological receptive fields of X and Y cells. Later anatomical studies demonstrated that retinal inputs to the β cells were bipolar-dominated, while the retinal inputs to the α cells were amacrine-dominated [425]. These lines of evidence indicated that the X and β classes corresponded, as did Y and α, and that the amacrine input is the source of the distinctive Y cell nonlinearity. X and Y cells differ in their central destinations—X cells project only to the lateral geniculate nucleus of the thalamus, while Y cells project both to the lateral geniculate nucleus and to the superior colliculus. X and Y cells also differ in axon diameter and hence conduction

velocity (Y faster than X), although this distinction only amounts to a few ms [379], and accounts for only a portion of the dispersion in retinal signals that arrive at visual cortex [56, 339].

This tidy picture, while providing reassuring suggestions at multiple levels that structure and function are intimately related, is oversimplified in at least two ways. Within the cat retina, there is a heterogeneous population of retinal ganglion cells (perhaps as many as 50% of the total) that are morphologically neither α nor β [43], and have a range of distinctive physiological properties, including direction-selective cells and cells that have highly regular firing patterns [314, 319, 379]. These 'W cells' [379] differ from X and Y cells in their central destinations, generally have a slower conduction velocity [379], and presumably include cells homologous to the direction-selective neurons prominent in other species, such as rabbit [7]. Secondly, there is much debate as to whether (or how) the X and Y classes seen in cat correspond to ganglion cells classifications in other species, especially the primate [315, 335, 336, 348]. Nevertheless, because a wide range of species studied, including goldfish [35], mudpuppy [399], eel [347] and mouse [378], have ganglion cells that are qualitatively linear and also those that are qualitatively nonlinear, much attention has been focused on the receptive field structure of cat X and Y cells.

To a first approximation, the firing rate of X cells (considered as a change from their mean firing rate) is a linear transformation of the spatiotemporal pattern of contrast (considered as the fractional change in illumination about the mean illumination). Because of this approximate linearity, the approximate translation invariance of the retina [358] and the extensive psychophysical data available for comparison [64, 183], this linear transduction is typically analysed and described in the frequency domain, both temporally and spatially. Stimulation with a high spatial frequency isolates the centre mechanism more effectively than the use of a small spot: anatomical considerations indicate that the surround overlaps the centre spatially, but gratings near the resolution limit of the cell would be resolved only by the summing mechanism of finest spatial scale (i.e. the centre). Isolated in this manner [114, 409], centre dynamics of X cells are bandpass. The peak of the temporal transfer function is generally 4–8 Hz, and the slope of the high frequency rolloff is equivalent to 16–20 simple lowpass (RC) stages [409], substantially steeper than that of photoreceptors.

Stimulation with increasingly lower spatial frequencies recruits progressively larger contributions from the surround. Under these conditions, the degree of attenuation at low temporal frequencies increases (by as much as a factor of 100 for diffuse illumination [114]), and the peak temporal frequency of the transfer function increases. This spatiotemporal coupling, a shift in responsiveness to higher temporal frequencies with lower spatial frequencies [101] (see figure 7(A)), is a characteristic feature of early visual processing even in primitive invertebrate systems such as the horseshoe crab *Limulus* [52, 298]. In *Limulus*, this coupling can be explained in a precise and quantitative fashion by linear summation of a centre and an antagonistic, but somewhat slower, surround. The surround contribution, which contributes to the transfer function at low spatial frequencies, is antagonistic to the centre at low temporal frequencies. But at sufficiently high temporal frequencies, the surround's delay brings its contribution into phase with the centre, and thereby reinforces the response. In the vertebrate retina, surround contributions require lateral transmission (presumably within the horizontal cell, but possibly with an amacrine contribution) to reach the ganglion cell, and thus are likely to be delayed in comparison with the centre's response. However, despite the anatomic substrate for spatiotemporal coupling via addition of a delayed surround antagonism, this mechanism fails to account in a quantitative fashion for ganglion cell behaviour in the cat retina [114]: at low spatial frequencies, temporal tuning peaks at frequencies (e.g., 30–60 Hz) where both the centre and surround mechanisms' responses are severely attenuated.

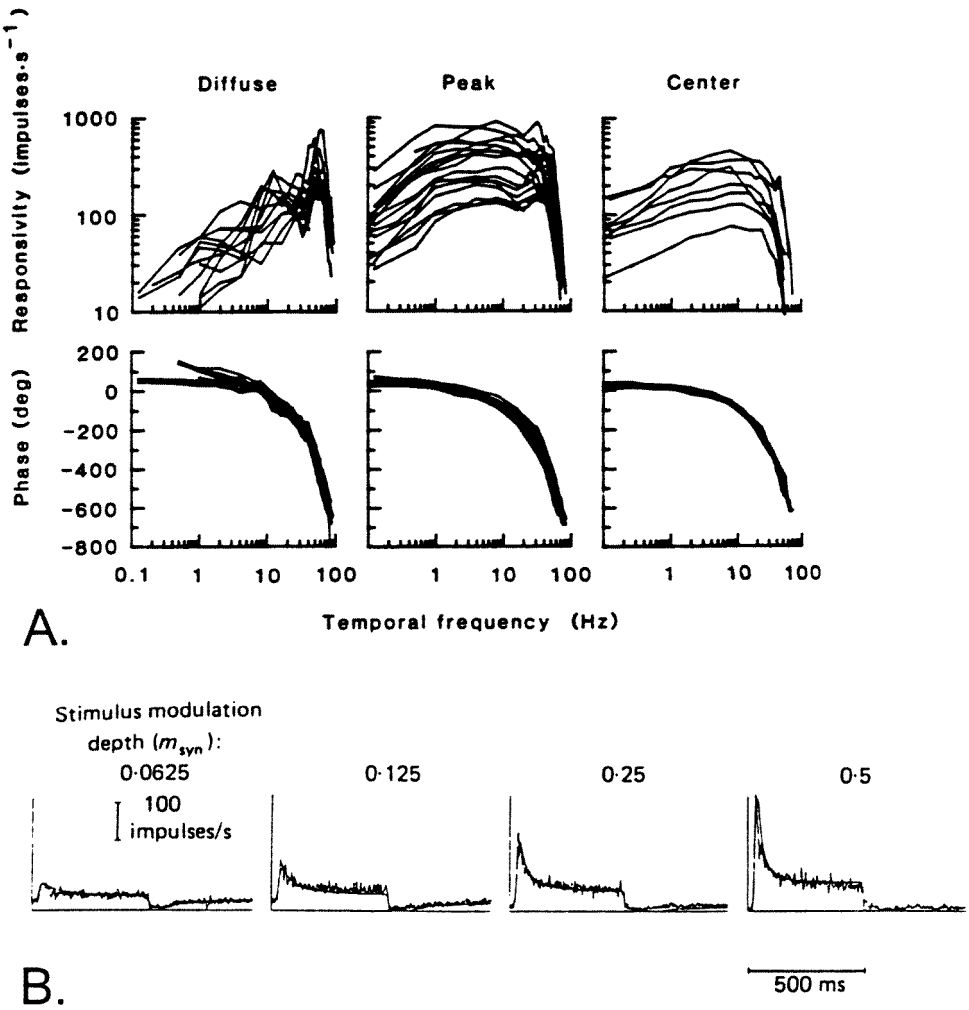

Figure 7. (A) Dependence of the dynamics of 17 cat ON-centre X-type retinal ganglion cells on spatial frequency. For each cell, transfer functions are measured from the spike response elicited by modulated sine gratings at three spatial frequencies: near 0 (left, labelled 'diffuse'), at the cell's peak response (middle), and at a spatial frequency sufficiently high so as to isolate the centre's response (right). From Enroth-Cugell *et al* [101]. (B) The dynamics of the contrast gain control in an ON-centre X-type ganglion cell of the cat. Irregular curves are histograms of extracellularly recorded spike responses elicited by abruptly reversing gratings presented at four contrasts; smooth curves (nearly superimposed) represent predictions of a model with rapid contrast-dependent adjustment of dynamics. From Victor [409]. (C) Dynamics of M and P ganglion cells in the macaque as determined from extracellularly recorded spike responses to luminance grating modulated by a sum of sinusoids at contrasts of 0.02/sinusoid (filled circles), 0.04/sinusoid (open circles), 0.08/sinusoid (filled squares) and 0.16/sinusoid (open squares). M cells show a greater low-frequency attenuation and a contrast-dependent change in dynamics. P cells show no change in gain or dynamics as overall contrast changes. From Benardete *et al* [29]. (D) The emergence of phase-locking behaviour at high contrasts, coexisting with contrast-independent response variability (lowest panel). Extracellular recordings of a cat ON-centre X ganglion cells. From Reich *et al* [301]. All figures are reproduced with the consent of the original publishers.

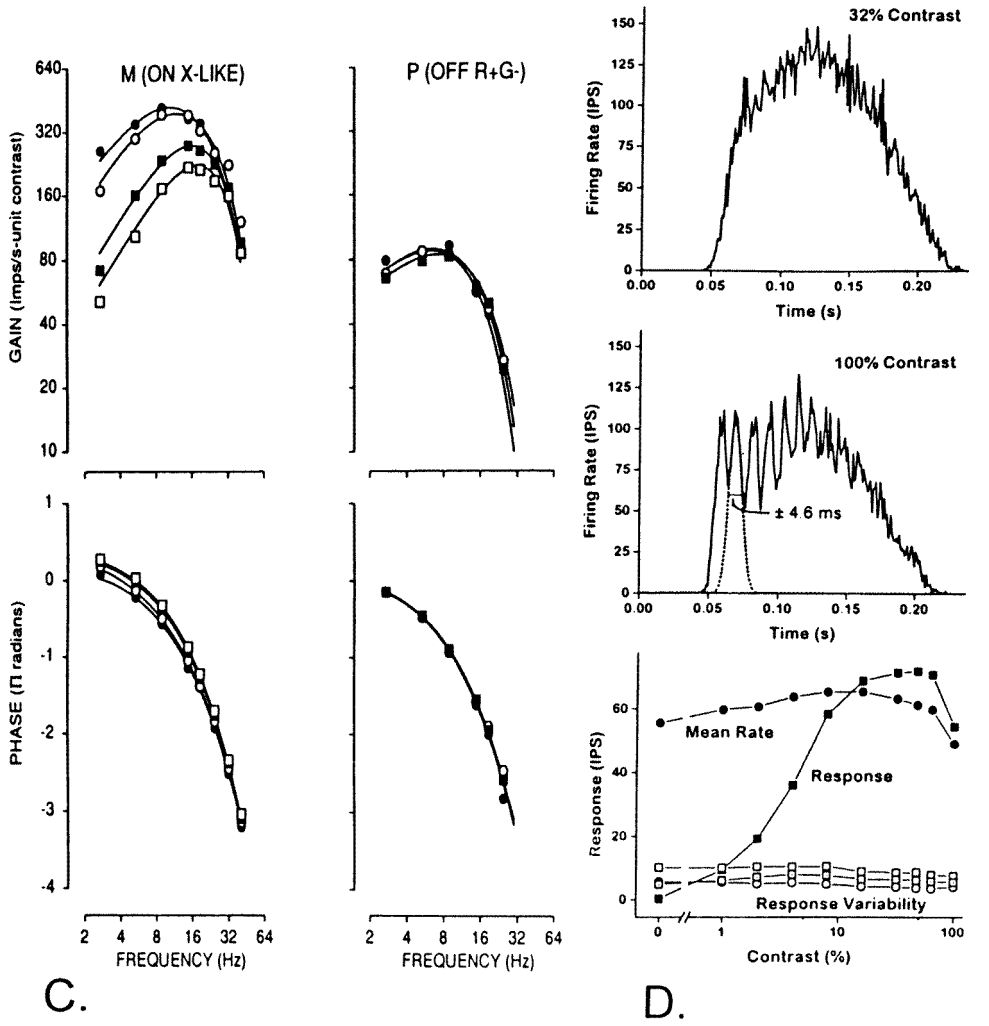

Figure 7. (Continued)

A phenomenological account of the spatiotemporal sensitivity of ganglion cells within the framework of a linear centre–surround model requires that the effective centre and surround sizes increase with increasing temporal frequency [114]. However, no mechanism has been proposed to explain this increase, and the model does not lead to a clear prediction of how ganglion cells would respond to spatially broadband stimuli. Furthermore, annular stimulation of the X cell reveals both a phase lag and a shift to higher temporal frequencies with increasing distances from the centre [411]. This is a clue (see below) that the X cell surround is more than a reflection of spatial antagonism at the bipolar cell level by spatially homogeneous input from horizontal cells.

Ganglion cells dynamics: nonlinear subunits and adaptive temporal filtering. The simultaneous presence of qualitatively linear (X) and nonlinear (Y) responses in the retina implies that the nonlinear dynamics of the Y cell are generated by the retinal circuitry rather

than at the level of the photoreceptor. The failure of a linear model of centre–surround interactions even for X cells is an additional clue to the presence of new dynamical elements and nonlinearities at the level of the retinal ganglion cell.

Many ganglion cells are highly sensitive to contrast (firing rate modulations as high as 3 impulses per second per percent contrast). Maintained firing rates of ON X cells are typically 80 impulses per second or less; maintained firing rates of Y cells are often lower (ca 40 impulses per second), and OFF X cells may have little or no spontaneous activity. Because of this high contrast sensitivity, ganglion cells necessarily show nonlinearities in response to high contrast stimuli—strictly linear behaviour would require a negative firing rate in response to moderate-contrast stimuli of the polarity that reduces the firing rate. This simple analysis identifies one benefit of having ON and OFF varieties of ganglion cells—responses to high contrast patterns can be faithfully conveyed.

This nonlinearity, the impossibility of negative firing rates, cannot account for centre–surround dynamics or the ON–OFF response, but it does complicate the analysis of the receptive field structure of ganglion cells. To analyse such nonlinearities, methods that rely on noise-like inputs [234, 412, 419] have been employed. These approaches have the advantage that they reduce the confounding effects of output nonlinearities [369]—including not only truncation of the response at the lower bound of 0 impulses per second, but also response compression due to an upper limit on firing rates.

We focus on studies based on the sum-of-sinusoids approach [419]. This method, based on Fourier analysis of responses to stimuli consisting of a spatial pattern whose contrast is modulated in time by a sum of sinusoids, is in effect an implementation of the Wiener theory [234] in the frequency domain. A strictly linear system's responses to such stimuli is confined to Fourier components present in the input, and these responses are identical to those that would be recorded in response to individual presentation of the sinusoids. Nonlinear dynamics are revealed both by the presence of responses at frequencies equal to the sums and differences of the input frequencies, and by the dependence of the response at one frequency on the presence or absence of stimulation at another frequency. Stimulus frequencies can be chosen so that their pairwise sums and differences are distinct. With such a choice, the spectrum of the response corresponds to direct experimental estimation of a discrete sample of points on the Fourier transform of the second-order Wiener kernel [412]. For transductions that are smooth in the frequency domain (as anticipated for biological transductions), this discrete sampling provides a useful characterization of the second-order dynamics of the system. Moreover, since the responses are confined to narrow frequencies, this approach preserves much of the benefits of digital filtering that favour sinusoidal analysis of linear transductions [408].

In response to contrast modulation by a sum of sinusoids, ON X ganglion cells' responses are generally confined to the stimulation frequencies, consistent with linear behaviour [417]. OFF X ganglion cells' responses contain Fourier components at the sum and difference frequencies, but these intermodulation components are accounted for by the low maintained firing rate of the cell, and the nonlinearity required by the impossibility of a negative firing rate. Y cells, on the other hand, generate strong responses at frequencies equal to pairwise sums and differences of the input signals [417, 418]. This is the hallmark of a prominent even-order nonlinearity and is consistent with the original observations of Enroth-Cugell and Robson [100] concerning Y cells' qualitatively nonlinear responses to introduction and withdrawal of contrast. At spatial frequencies near the resolution limit of the Y cell, this nonlinear behaviour dominates the response.

However, the nonlinear behaviour, although formally even-order, is not well approximated by a quadratic function. The size of the nonlinear response scales approximately like a power law, with an exponent in the range 0.8–0.9 [410, 418]. This power-law nonlinearity provides a

much better account of Y cell responses than does a Wiener series truncated at order two. The size of the nonlinear response is insensitive to the spatial phase of the grating [159, 418], which suggests [159, 410, 418] that the nonlinear response of the Y cell is generated by a spatial array of subunits. Analysis of the response dynamics indicates [418] that linear temporal filtering both precedes and follows the nonlinearity, although there are details that require elaboration on this linear–static-nonlinear–linear cascade. As a function of spatial frequency, the subunit dynamics show a spatiotemporal coupling analogous to that of the X cell response: a shift to higher temporal frequencies at lower spatial frequencies. This spatiotemporal coupling occurs mainly prior to the nonlinear transformation—i.e. within the nonlinear subunit.

These observations lead to the idea that the Y cell subunit and the X cell centre–surround mechanism both have the bipolar cell as their common substrate. X cells, whose inputs are bipolar-dominated, have qualitatively linear behaviour. For Y cells, the same bipolar cell signal is processed via a network of amacrine cells, which are postulated to generate the nonlinear response and the second stage of temporal filtering. At low spatial frequencies (that presumably recruit receptive field elements of larger summing areas), the Y cell response contains contributions from qualitatively linear mechanisms [158, 418]. Although these responses also show the spatiotemporal coupling characteristic of centre–surround organization, their much lower resolution indicates that they are not generated by the same neural elements that generate the X cell centre and surround, and probably have their origin in the inner plexiform layer. These ideas are reinforced by detailed study of the spatial attributes of X and Y cell responses [364, 368].

In addition to the distinctive Y cell nonlinearity, there is a dynamic nonlinearity that affects both X and Y cells—the contrast gain control [349]. For step responses (figure 7(B)), the gain control is manifest as an increase in the relative prominence of the transient component of the response as contrast increases. In the frequency domain, the contrast gain control is manifest as a contrast-dependent change in the effective transfer function. Responses at low frequencies ($<$1–2 Hz) grow less than proportionately to contrast, while responses at frequencies greater than 4 Hz are proportional to contrast, and have increasing phase advances of up to a quarter of a cycle in the 4–8 Hz range [349]. The gain control is more prominent in Y cells than in X cells; this, along with the contribution of the subunit nonlinearity, accounts for their generally more transient behaviour [349, 351].

The adaptive shift in dynamics can be modelled as increasing the gain of a feedback circuit that results in highpass behaviour. Faithful reproduction of observed responses requires that the strength of the feedback circuit be controlled by a neural measure of contrast whose memory is short (ca 100 ms) [351, 409] but whose area of spatial summation is at least as large as the receptive field [350]. That is, the array of subunits that drives the Y cell nonlinear response also generates the neural measure of contrast that modulates the quasilinear responses of both X and Y cells. The dynamics of the contrast gain control allow approximately sinusoidal responses to single sinusoidal inputs [409] and are consistent with approximately linear spatial summation under some circumstances [102]. Nevertheless, the contrast gain control is a spatial nonlinearity that produces a more transient response to low spatial frequencies, than would be expected from linear centre–surround combination [350]. Its greater prominence in Y cells than in X cells [349] and its effect on the nonlinear response of the Y cell subunit [410] suggest that its anatomical basis is in the network of amacrine cells in the inner plexiform layer.

The contrast gain control may be the phenomenon observed by McIlwain as the ‘shift effect’ [170, 249]. It is also qualitatively similar to the suppressive effect of a windmill stimulus on low-frequency responses, which in the mudpuppy is known to rely on the amacrine cells [386, 432]. Direct evidence linking this mechanism to the amacrine cells has also been obtained from intracellular recordings of amacrine cells in the cat [271].

This analysis of ganglion cell behaviour indicates that centre–surround antagonism, which makes its first appearance in bipolar cells, is modified at the inner plexiform layer, both in its spatial and temporal aspects. Furthermore, there are early, and prominent, dynamic nonlinearities in visual processing. The contrast gain control could be viewed as playing the role of an adaptive adjustment in response range and dynamics, to improve the efficiency of the packaging of retinal information into spike trains—as contrast increases, progressively less temporal integration may be required to overcome outer-retinal noise, and thus, high temporal frequency fluctuations may be more likely to represent useful visual information. This role in the efficient packaging of visual information is analogous to the role played by light adaptation in the outer retina [290, 395].

The subunit nonlinearity is difficult to understand merely on the basis of signal-to-noise considerations, since it fundamentally entails an intermixing of ON and OFF signals. Presumably, rather than contributing to the reconstruction of the visual world, these signals are used in later processing in contexts in which a temporal change *per se*, and not its polarity, is crucial. Such contexts include motion processing and edge extraction.

Ganglion cell dynamics in the primate. In primates, two major morphological categories of ganglion cells that project to the lateral geniculate nucleus have been identified: M cells, which project to the two lowest (magnocellular) layers of the lateral geniculate nucleus, and the P cells, which project to the upper four (parvocellular) layers of the lateral geniculate nucleus. The anatomical and physiological characteristics of these classes have been reviewed extensively [174, 206, 209, 336, 348]; we note only certain major features here. M ganglion cells have a dendritic field with a 'parasol' morphology, consistent with the collection of signals from multiple bipolar and amacrine cell inputs, while (at least in the fovea and parafovea) the much more restricted dendritic field of the P cells indicates that they receive input primarily from a single bipolar cell of the midget variety [194]. One consequence of this wiring difference is that P cells carry chromatic signals, since (at least near the fovea) their inputs are dominated by a single bipolar cell, whose input is in turn dominated by a single cone. This is in contrast to M cells, whose photoreceptor inputs consist of a mixture of cone classes, and thus appear wired to transmit achromatic signals. The difference in dendritic field size probably accounts for the much larger receptive field of M cells, in comparison to P cells. A third difference between the cell classes, which may also have its basis in the number of bipolar cell inputs, is a dramatic difference in the contrast–response function [179]: M cells have high contrast sensitivity but their responses begin to saturate at contrasts in the neighbourhood of 0.30; P cells' contrast sensitivity is approximately tenfold lower but they have a response that is proportional to contrast over the entire contrast range. This difference in the contrast–response functions is enhanced at lower light levels [293], pointing to a greater rod contribution to the M cell response.

P cells are widely considered to have 'sustained'or 'tonic' responses, compared with the more 'transient' or 'phasic' dynamics in M cells [174] (figure 7(C)). However, both kinds of cells typically have bandpass dynamics, with P cell responses maximal in the neighbourhood of 4–8 Hz, and M cell responses maximal at 16 Hz or higher. Both classes of retinal ganglion cells demonstrate a shift to higher temporal frequencies at lower spatial frequencies. As in the cat, the picture is qualitatively but not quantitatively consistent with linear summation of homogeneous centre and surround mechanisms [129, 130, 361]. In contrast to the retinal ganglion cells of the cat, P cells do not adaptively change their dynamics as contrast increases [29]. M cells do show this adaptive shift [28, 29], and the detailed dynamics of this process match those seen in cat X and Y cells [351, 409]. For luminance stimuli, the dynamics of P cells' responses to grating stimuli and to stimuli restricted to centre or surround are approximately

linear [26, 177], while M cells fall into two categories: a qualitatively linear subset, and a minority (ca 25%) that manifests the frequency-doubled responses characteristic of the cat Y cell [177]. These physiological distinctions, as well as supportive anatomical evidence [296] have led to the notion that X and Y categories of the cat correspond to subcategories M_X and M_Y of the primate (with which they share high contrast sensitivity, strong rod input, and analogous central destinations), while the P cells are specific to the primate, with the unique features of the chromatically selective midget bipolar input, the lack of a contrast gain control, and a central target (the parvocellular layers of the lateral geniculate nucleus) that does not have a homologue in the cat [29, 206].

The dynamics of ganglion cell responses depend strongly on the chromatic aspects of their inputs. The 'tonic' description of the P cell response applies to stimuli that vary in luminance; for stimuli that vary in chromaticity, their dynamics become more phasic, with a rolloff at 20 Hz or higher [207]. This chromatic-temporal coupling is more prominent for stimuli that cover the surround. For P cells whose centre mechanism is driven by a long-wavelength (L or M) cone, the change in dynamics can be explained by additive combination of the centre response with an antagonistic surround that is driven by a mixture of cones and has somewhat slower dynamics [207]. These ganglion cells ('+L − M', '+M − L') typically respond with opposite polarities at low temporal frequencies (10 Hz and below) to stimuli whose spectral composition stimulates the L or M cones in isolation [443]. The approximate additive combination of signals from each cone class also applies to P cells whose centre receives input from the short-wavelength cone ('+S − (M + L)'), but these cells have somewhat different dynamics than P cells whose centre is driven by L or M cones. For these cells, the response to stimuli that drive the S cone in isolation response falls off more rapidly above 20 Hz (probably reflecting receptoral differences), and that L and M cone signals are in phase, rather than antiphase [443].

M ganglion cell responses cannot be explained on the basis of linear summation of cone signals. In most M cells, there is a frequency-doubled response that is most prominent at high temporal frequencies and high luminances [208]. The spectral characteristics indicate that it is driven by the two long-wavelength cone signals [208] that combine to form local nonlinear subunits [210]. For M cells in which the combination of cone signals within the subunits is antagonistic [210], the frequency-doubled response is most prominent for chromatic flicker and might well be absent for luminance flicker (thus, accounting for the behaviour of the M_X subtype). For M cells in which the combination of cone signals within subunits is in-phase (i.e. non-antagonistic), M_Y-like behaviour results.

While the P cells appear to have neither the subunit nonlinearity nor the contrast gain control nonlinearity present in M cells, they have other distinctive nonlinearities [27]. Quantitative analysis of surround responses in isolation reveals the presence of linear–nonlinear–linear (LNL) dynamics. Moreover, there is a strong adaptive effect of the level of steady illumination of the surround on the gain and dynamics of the centre. Increased steady illumination of the surround decreases the centre gain in ON cells, increases the centre gain in OFF cells, and accelerates centre dynamics in both subtypes. After changes in overall levels of retinal illumination, responsivity of both M and P cells adapts over a period of approximately 100 ms, but abrupt changes in overall chromaticity induce changes in responsivity that require several seconds to complete (for both M and P cells). This indicates not only the presence of post-receptoral sites for adaptation, but also that there are separate post-receptoral sites driven by sums and differences of cone signals [444].

Anatomical evidence indicates that the centre mechanism of the P cell is driven by a single cone type, as relayed through a midget bipolar cell [41, 42, 62, 94]. As indicated above, to a first approximation [89, 212], the chromatic antagonism characteristic of most P ganglion cells can be accounted for by linear combination of a small centre mechanism whose sensitivity

is determined by a long- or medium-wavelength cone, and a larger, nonselective surround mechanism. A chromatically nonselective surround is consistent with the notion that the receptive field surround is formed by horizontal cells [93, 228, 433], and that primate horizontal cells connect indiscriminately with cones of all classes [81, 426], or at least with the two long-wavelength cones [192, 195]. However, other studies indicate that the surround is at least somewhat chromatically selective [306, 361]. In view of the nonselective anatomical linkages in the outer plexiform layer, a chromatically selective surround requires a contribution to the surround from amacrine cells in the inner plexiform layer. These issues have recently been discussed in greater detail by Lankheet *et al* [202]. The short-wavelength system is organized differently, with blue–yellow chromatic opponency generated in a distinctive bistratified ganglion cell [80], that combines inputs from an ON S-bipolar cell and an OFF bipolar that contacts both long- and medium-wavelength cones [63, 79]. These cells may form the retinal origin of a portion of the koniocellular (intercalated) pathway (see below).

Implications for 'parallel processing'. Physiological features of P and M cells, along with the patterns of connectivity among central visual areas, have suggested that visual processing is organized into parallel streams [105, 446]. In broad terms, these streams are considered to consist of a ventral 'what' pathway, that supports object identification and thus makes use of fine spatial detail and colour, and a dorsal 'where' pathway, that supports processing of motion [402]. In this view, the 'what' pathway is supplied by the parvocellular pathway, while the 'where' pathway, which extracts visual motion, is supplied by the magnocellular pathway. However, there is accumulating evidence that this is an oversimplification [354]. The evidence for discrete processing streams based on connectivity among cortical areas [157] is not as clear-cut as was originally thought. Although there is clearly the anatomical substrate for a predominant parvocellular input to the ventral stream and a predominant magnocellular input to the dorsal stream [221], there is also anatomical [227] and physiological evidence [269] for intermixing of these signals [354]. Psychophysical studies of the perception of moving stimuli with chromatic components implies that both kinds of signals contribute to motion analysis [78, 104, 123]. The dynamical features of chromatic and luminance adaptation [444] are direct evidence of interaction of chromatic and luminance signals at the very origin of the M and P pathways.

Thus, it appears that the intuitively simple strategy of segregated transmission of various aspects of visual information (i.e. form, colour, and motion) is not the one adopted by the visual system, and that this intermixing is present at the retinal output. Perhaps, as discussed in more detail below, this is because the retinal ganglion cell output must serve as an efficient vehicle for the transfer of biologically relevant visual information. A key aspect of this efficiency is redundancy removal [11, 12, 83, 92, 96, 318]. Such redundancy removal necessarily entails entwining spatial, chromatic, and temporal attributes of the visual stimulus [335] and is thus at odds with independent transmission of these separate visual attributes. Because of nonlinearities, differences in quasilinear dynamics, and the manner in which these dynamics are coupled to spatial and chromatic aspects of the stimulus, one cannot regard the partition of retinal output into the P and M pathways simply as a division between slow and fast signals, or chromatic and achromatic signals, or even high-resolution and low-resolution signals [335, 348].

Spike train dynamics. The above discussion considered the retinal ganglion cell output to be a continuous function of time, and ignored the fact that it is a sequence of discrete unitary action potentials. The empirical justification for this simplification is that certain aspects

of the ganglion cell response can be examined without attention to the details of the spike trains. In general, these aspects are captured by 'integral measures' of the response—measures obtained by considering the spike train to be a sequence of delta functions, and integrating against a reference function, such as a sinusoid or a pseudorandom input. These integral measures include mean firing rates, spike counts, Fourier components, Wiener kernels, and their frequency-domain analogues, as described above. The notion that these measures suffice to understand the processing performed by retinal ganglion cells derives direct support from Naka's white noise analysis [197, 234] of intracellular recordings in the catfish. The dynamics obtained from the sequence of spikes (regarded essentially as a train of delta functions) were identical to those obtained from the intracellular slow potentials, with spikes removed.

There are many kinds of transductions for which the integral measures of derived from spiking responses and corresponding continuous inputs will be identical. By definition, in a renewal process, the probability distribution of each spike depends only on the time since the previous spike. Under the hypothesis that this renewal process evolves at a rate that is proportional to the continuous input [107, 128], the integral measures of the spike response will, on average, replicate the continuous input. These 'simply modulated renewal processes' [302] include not only inhomogeneous Poisson processes, but also gamma processes whose rate depends on the stimulus, as well as non-leaky integrate-and-fire neurons [187], which have long been known to enjoy this 'perfect replica' property [187]. This observation has implications for conceptual models of spike generation [125, 187] and for efficient strategies for processing the resulting spike train [34, 51, 373].

Under steady illumination, the spike trains produced by cat ON- and OFF-centre X and Y retinal ganglion cells have an interspike interval distribution similar to that of a gamma process [398] (except for the presence of a refractory period), with a gamma order in the range of 6–10 for ON X cells, and 2–4 for Y cells and OFF X cells. The best-fitting gamma order increases with increasing mean firing rate for X cells but is independent of rate for Y cells. In the absence of modulation, spike train statistics can also be modelled by a random-walk process [125, 217] or an integrate-and-fire process, with leakiness necessary to account for the relative independence of firing rate and variability [218]. However, the spike train does deviate from a strict renewal process, in that there is a consistently negative first serial correlation coefficient in the range of -0.1 to -0.3 in cat [398] and also in invertebrates [345].

The statistics of retinal ganglion cell discharges in the setting of visual stimulation have primarily been studied for periodic stimuli, such as drifting sinusoidal gratings. To a good approximation, response variability, as measured by fluctuations in the Fourier components of the spike train elicited by periodic stimulation, is independent of the stimulus or response amplitude [77]. However, if response variability is measured by the jitter of the timing of spikes, there is a marked reduction of variability as stimulus amplitude increases [301]. At low contrast, the PSTH elicited by drifting gratings is nearly sinusoidal, while at high contrast, the PSTH has narrow peaks and the firing pattern is characterized by spikes at precise firing times (to within a few ms). This behaviour is readily accounted for by a leaky (forgetful) integrate-and-fire model [187]. In essence, the integrate-and-fire transduction process is sufficiently linear (in the time-averaged sense that is relevant to Fourier components) so that signal and noise add. On the other hand, for sufficiently strong depths of modulation, the leakiness allows for a resetting of the spike generating mechanism during the portion of the stimulus cycle in which the input is small. This leads to a marked decrease in the jitter of the initial spikes that occur during the rising phase of the stimulus [302]. These contrast-dependent changes in firing pattern are summarized in figure 7(D). The leaky integrate-and-fire model (with shot noise added to the input) also accurately accounts for the interspike interval distribution produced by ganglion cells in the absence of stimulation, similar to a gamma process of order near four [398].

Recent studies of salamander and rabbit retinal ganglion cells [32] have suggested that the ganglion cell spike train may be better regarded as a set of isolated firing events, with large gaps of time in between events, rather than as a continuous stream of spikes. At moderate contrasts, the inter-event time may be as much as 2 s, but the timing jitter of the firing events (which can contain up to six spikes) is 10 ms or less. Most of the information in the spike train can be extracted from the timing of these events, rather than the number of spikes that they contain [32]. This kind of behaviour can be explained by an elaboration on the idea of an inhomogeneous Poisson process [31], in which it is hypothesized that firing statistics are governed by a combination of a 'free firing rate', the firing probability of an underlying inhomogeneous Poisson process whose rate is determined solely by the stimulus, and a 'recovery function', which depends only on the time since the previous spike and expresses the refractoriness of the neuron. This kind of model can reproduce the precisely timed events (with a variable number of spikes) seen in salamander and rabbit [31]. However, for a reasonable range of parameters, it cannot account for the coupling between firing precision and signal size to the extent seen in cat retinal ganglion cells [302].

Inhomogeneous Poisson processes with refractory period, the 'free firing rate' model [31], and the leaky integrate-and-fire neurons [187, 302] contain a time constant that is stimulus-independent (i.e., the refractory period or the leak constant), as well as a firing rate distribution that is driven by the stimulus. These kinds of spike-generation dynamics thus do not produce firing probabilities that replicate the input and therefore place their own signature on spike trains. For periodic stimuli, the most striking such signature is phase locking to periodic high-amplitude inputs [112, 180, 188, 301, 302].

Although computational models are capable of capturing many of the dynamical features of a ganglion cell's discharge, it is not straightforward to construct a detailed and biophysically realistic model for this process. In salamander, a single-compartment model with five conductances suffices to account for the steady firing behaviour in a qualitative fashion [110]. However, an accurate model of dynamics consistent with voltage-clamp data requires inclusion of five active conductances (Na^+, Ca^{++}, A-type K^+, delayed-rectifier K^+, calcium-gated K^+) and a leakage conductance [111], which are distributed inhomogeneously (dendrites versus soma) in a multicomparment model [112]. The multicompartmental nature of the model is critical, with currents between the dendritic and somatic compartments playing a key role in determining the interspike intervals [112].

Ganglion cells as an information bottleneck. There are far fewer ganglion cells than photoreceptors (in man: approximately 10^6 ganglion cells but 10^8 photoreceptors [422]). The all-or-none nature of ganglion cell spike trains that allows for rapid and long-range propagation of their output is an additional restriction on information capacity. For these reasons, ganglion cells are a model to study neural strategies for the efficient transmission of information. Several themes have emerged. Perhaps the most universal is that of redundancy removal: ganglion cell receptive fields may be considered to be filters that remove the correlation structure intrinsic to 'natural' scenes. To the extent that ganglion cells are quasilinear filters, this view accounts for the spatial and temporal characteristics of their receptive fields [11, 12, 18, 83, 92, 96, 290, 370]. This reasoning also extends to the domain of colour: the chromatic characteristics of primate retinal ganglion cells [12, 96, 318] can also be viewed as an optimal set of filters to represent the chromatic signals present in natural scenes. The notion of redundancy removal does not immediately account for the prominent nonlinearities in some classes of retinal ganglion cells, but one can still speculate that the statistics of the visual world is the evolutionary force that drives the development of adaptive filtering and multiple parallel pathways.

Another strategy that may be used for the efficient representation of information in the retinal output is that of spatial coding via temporally coincident firing [250, 404]. Coincident firing and decorrelation via redundancy removal need not be mutually exclusive, in that the former exploits the fine structure of the individual responses, and the latter may be restricted to integral measures. In the setting of visual stimulation with pseudorandom patterns, high-precision coincidences between firings of neighbouring retinal ganglion cells occur much more often than would be expected by chance alone [252]. Direct coupling between ganglion cells contributes to these coincidences [241], but the fact that these coincidences are correlated with visual input in the overlap of the receptive fields [252] suggests that common input (i.e. a shared interneuron) is the source of the concerted activity. Indeed, cross-correlations between neighbouring ganglion cells in the salamander have three timescales: a brief timescale (<1 ms) that reflects electrical junctions between ganglion cells, an intermediate timescale (10–50 ms) that reflects common input from amacrine cells, mediated by gap junctions, and a broad timescale (40–100 ms) that reflects common input from photoreceptors, transmitted to the ganglion cell layer via chemical synapses [50].

The concerted-firing strategy [250] is thus a combinatorial code that allows a population of retinal neurons to provide a spatial resolution limited not by the size of the ganglion cell receptive fields but by the size of their pairwise, and perhaps higher-order, overlaps. It is a temporal strategy that exploits the sparse, spiking nature of the ganglion cell output to improve the efficiency of spatial coding. In order for the strategy to work, the correlation structure of the visual input must be sufficiently sluggish, so that high-precision coincidences would not often be due to independent activity in the neighbouring ganglion cells [250]. Thus, the concerted-firing strategy is most effective when firing rates are low, so that coincidences due to chance are relatively infrequent. This condition holds in rabbit and salamander ganglion cells, but also may be relevant in many ganglion cells in cat and monkey. Since high-precision correlations (<1 ms) reflect primarily direct coupling between retinal ganglion cells [50], only the correlation structure at a coarser resolution (10 ms or more) has the potential to provide greater spatial resolution. There appears to be little evidence to support a combinatorial code for temporal information [423]. The use of concerted signalling to pass only one type of information (spatial but not temporal) limits the potential ambiguities of this coding strategy.

A third strategy for mitigating the effects of the optic-nerve bottleneck is that of regional specialization of the retina. While quantitative differences in receptive field size are typical across species (increasing size from the centre of the retina to the periphery), this regional specialization is best studied and perhaps most highly developed in primates. In the primate fovea (in man, the central five degrees of the retina [422]) there are more ganglion cells than photoreceptors (3:1), in contrast to the marked excess of receptors in the periphery (1:125). Other anatomical specializations of the fovea, such as morphological alterations of cones, a lack of rods, and a lack of preretinal blood vessels, also facilitate higher acuity. The high ratio of ganglion cells to photoreceptors in the fovea eliminates the need for a spatiotemporal resolution tradeoff (see above paragraph), but it also requires dedicating a disproportionate amount of the optic nerve to the central few degrees of vision. Foveal specialization is continued at the cortical level, with enlargement of the fovea's cortical representation out of proportion to the number of retinal inputs [95, 216]. This arrangement is manifest by enhanced performance on tasks crucial to pattern vision, including vernier acuity [216] and relative phase discrimination [30, 310]. However, effective use of this foveal specialization requires frequent fixational eye movements [420]. These fixational eye movements, that occur up to several times per second, result in a contrast transient that probably functions as a resetting for central pattern processing. Moreover, informative targets for the next eye movement must be chosen rapidly (within a few hundred ms), without conscious attention, and based on information available to non-foveal

vision. Thus, the retinal specialization that provides for high-performance spatial vision has a sweeping consequence for the overall dynamics of primate vision: a cycle of eye movement, contrast transient, pattern analysis, and subsequent target selection [294].

4.2. Lateral geniculate nucleus

The lateral geniculate nucleus (LGN) is a prototypical thalamic 'relay' nucleus, containing a population of neurons that receive sensory input and project to the input laminae of a sensory cortex. The main target of the relay neurons is the input lamina of primary visual cortex (usually designated area 17 in cat, area V1 in macaque, and by either name in man).

Anatomic overview and receptive field properties. Relay neurons of the LGN receive a dominant input from a single retinal ganglion cell [73, 243] and fire only when that retinal ganglion cell produces a synaptic potential, known in this context as an S-potential [178] (figure 8(A)). Thus, the basic spatial and temporal architecture of geniculate relay neurons are similar to those of their retinal inputs—including centre–surround antagonism [73], and spatiotemporal coupling [175, 397], the presence of qualitatively linear and nonlinear cell types [177, 364], and a contrast gain control [280, 338]. On the other hand, most synapses in the LGN (even the synapses onto relay cells) do not come from the retina, but rather from other sources: feedback pathways from visual cortex, ascending inputs from non-visual areas of the brainstem and intrinsic connections, and reciprocal connections with the perigeniculate nucleus [171, 401]. Although the details are far from clear, it is generally considered that the combined effects of the non-retinal inputs and the intrinsic membrane properties provide mechanisms by which the lateral geniculate nucleus can 'gate' retinal signals, as determined by arousal, attention, or behavioural set [356]. Often, both the dominant retinal input (the S-potential) and the relay neuron's spike response can be recorded with a single extracellular electrode. This arrangement allows for a detailed comparison of the LGN response and its retinal input, and makes the relay neuron of the LGN an important model system for the study of regulation of sensory transmission from the periphery to the cortex.

In the cat, the A and A1 laminae of the lateral geniculate nucleus (the 'dorsal LGN') are sites of the terminations of X and Y ganglion cell afferents, with the dorsal-most A lamina receiving input from the contralateral eye, and the more ventral A lamina receiving input from the ipsilateral eye. The typical X LGN cell provides synaptic input to area 17 only, but Y cells project both to areas 17 and 18 [164]. Ventral to the A lamina is the C lamina, which contains terminations of both Y cells and W cells [372] and projects to extrastriate visual areas 18 and 19 [214].

In the primate, the LGN is traditionally considered to have six laminae (but see below), numerically designated from ventral to dorsal. Each of the laminae is driven by ganglion cells from one eye only. Laminae 1, 4, and 6 are driven by the contralateral eye; laminae 2, 3, and 5 by the ipsilateral eye. The two ventral laminae (1 and 2) comprise the magnocellular (M) component of the LGN, with inputs dominated by the M ganglion cells. As anticipated from their retinal inputs, the magnocellular laminae includes neurons with both X-like (approximately 75%) and Y-like (approximately 25%) spatial [177] and temporal [129] properties. Thus, in both lamination and physiology, the two magnocellular laminae of the macaque LGN appear homologous to the dorsal LGN of the cat. The four dorsal laminae of the primate LGN form the parvocellular (P) component, and nearly all of the neurons demonstrate qualitatively linear behaviour for luminance stimuli [177]. Ventral to each of the laminae (in multiple species, including tree shrew [160], *Galago* [167, 279] and the macaque [155]) lies an 'intercalated' lamina of the LGN, containing koniocellular neurons (K cells).

LGN K cells appear to have temporal properties similar to LGN P cells [366]. M and P cells project to primary visual cortex (V1) in a laminar-specific manner [223, 445], although the synaptic anatomy indicates a substrate for an intermingling of M and P cell pathways [445]. Additionally, there are some direct LGN projections to extrastriate cortex, including area V4 [76].

In all primate species examined, receptive field properties vary across the laminae, but there are major differences in the pattern of variation from species to species. In ferret [381] and mink [215], ON and OFF cells occupy distinct sublaminae within the six major laminations. In tree shrew, each lamina contains cells of only one polarity (and one eye of origin): laminae 1 and 2 contain ON cells, laminae 4 and 5 contain OFF cells, lamina 3 contains W-like ON and OFF cells, and lamina 6 contains W-like ON–OFF cells [160]. In primates, the intercalated laminae play a role in carrying chromatic signals, especially those involving S-cone activity. Evidence for this includes a distinctive projection from the intercalated cells associated with lamina 3 to cortical 'puffs' (blobs) [90] associated with chromatic processing; the presence of cone-opponent blue-on cells in the intercalated laminae in marmoset [237]; and the fact that intercalated neurons associated with laminae 3 and 4 (but not those associated with laminae 1, 2, 5, or 6) carry both blue-on and blue-off signals and are driven by bistratified retinal ganglion cells [305]. But the anatomical picture of three kinds of laminae (M, P, and K) is also present in Galago [167], a nocturnal animal with no behaviourally demonstrated colour vision.

Temporal-chromatic interactions. As described above, the receptive-field structure of retinal ganglion cells leads to an interaction of their temporal and chromatic sensitivities. The dependence of response dynamics on chromatic properties of the input, which begins in the retina, has been studied in great detail at the level of the lateral geniculate nucleus [89, 201, 202]. The chromatic tuning of P cells is relatively independent of temporal frequency below 4 Hz, but above 15 Hz much of chromatic opponency is lost. To a first approximation [202], this kind of behaviour can be accounted for by linear combination of antagonistic signals from centre and surround mechanisms with slightly different dynamics, provided that these receptive-field mechanisms have different complements of cone inputs as well. At low temporal frequencies, centre and surround signals are in counterphase. At high temporal frequencies, the effects of the differing dynamics become important, and reduce the centre–surround antagonism or even result in reinforcement. Best-fitting model parameters [202] have effective delays for centre and surround which differ by 3–12 ms. The dynamical modelling [202] is equally successful for hypothetical surround mechanisms consisting of a single cone type, or a mixture, and thus fails to settle the controversy concerning the chromatic composition of the surround. Dynamics have very little dependence on whether the centre is driven by L or M cones but, across cone types, OFF cell centre mechanisms have a delay of approximately 17 ms greater than that of ON cells [201]. This delay cannot be explained by the differences in dynamics between OFF and ON pathways at the bipolar level: for Y-like ganglion cells, the difference is in the wrong direction [410], and for X-like ganglion cells, no ON versus OFF difference is observed [409].

Although the linear model provides a reasonable account of chromatic sensitivity, it fails as a general framework for the P cell receptive field. For uniform fields modulated sinusoidally in time, the spike response is far from sinusoidal, with typical amounts of harmonic distortion (expressed as the ratio of the amplitude of the higher harmonic to the fundamental) of 0.36 (second harmonic), 0.21 (third harmonic) and 0.13 (fourth harmonic) [202]. This cannot be remedied simply by postulating that signals are combined in a fundamentally additive fashion and that there is a nonlinearity at the point of spike generation. In many P cells, even though responses to stimuli that drive individual cone classes in isolation are very nearly linear, responses to the superpositions of such stimuli show qualitative deviations from linearity [25, 27].

At the retinal output and the lateral geniculate, the distinct dynamics of P cell centre and surround, combined with their different cone inputs, implies a dependence of chromatic tuning on temporal aspects of the stimulus. That is, these receptive field features require that the temporal aspects of the response depend on their chromatic properties. However, it is unclear from the available data whether this might result in a robust temporal coding of chromatic information, in that the studies which have explored chromatic tuning in detail have used response measures, such as single Fourier amplitudes, that might overlook dynamical differences.

Transience, the transfer ratio, and the contrast gain control. LGN relay neurons have responses that are more transient than their retinal inputs [219, 356, 365]. One contributing factor to this increased transience is that the surround mechanism of the LGN appears to be stronger than that of its retinal inputs [162]. *A priori*, the stronger surround might have been generated by retinal inputs, following sign inversion by an inhibitory interneuron intrinsic to the LGN. However, dark adaptation, which markedly reduces the strength of the retinal surround, has a comparable effect in the LGN. Thus, most (but not all) of the LGN surround antagonism is a reflection of the surround of its retinal input [74, 175].

In situations in which the S-potential and the relay neuron's response are recorded simultaneously, the 'transfer ratio', the ratio of LGN spikes to S-potential spikes, is a useful index of how the retinal input is modified before being relayed to cortex. A typical value for the transfer ratio is 0.5 [70], but this is affected by many factors. At low contrasts (<0.1), increasing stimulus contrast reduces the transfer ratio. This is in line with the observation that LGN neurons demonstrate a contrast gain control that is more prominent than that of their retinal inputs [176, 280, 338]. However, at higher contrasts, the transfer ratio may stabilize or increase [70, 176]. Transfer ratio is also greater at higher temporal frequencies than at lower temporal frequencies [176]. These observations are also likely related by the effects of the contrast gain control: as contrast increases into midrange and beyond, the retinal response becomes more transient (as a consequence of its contrast gain control [29, 351]), and this shift to high temporal frequencies results in responses that are less attenuated by the contrast gain control of the relay neuron.

The transfer ratio is also influenced by the spatial structure of the stimulus. Most neurons show reduced transfer ratios at lower spatial frequencies [70]. Since responses to low spatial frequency stimuli are more transient than responses to high spatial frequencies, the dynamics of retinogeniculate transmission alone cannot account for this change. Rather, it implies a role for intrageniculate circuitry in regulating the transfer ratio. Level of arousal influences the transfer ratio [439], in that the sustained portion of a relay neuron's response to a transient stimulus is suppressed during drowsiness (as determined by the criterion of EEG synchronization). This alteration in the spatiotemporal properties of LGN neurons necessarily alters the spatiotemporal receptive fields of their cortical targets. The state effect on the LGN activity is believed to be mediated by the perigeniculate nucleus [439], but feedback from visual cortex may also play a role [438]. A direct effect of brainstem inputs on retinogeniculate transmission can also be demonstrated by stimulation of the peribrachial region. This leads to steepening of the contrast–response function of the relay neuron, a higher maximal firing rate, and an increased transfer ratio [148]. Moreover, brainstem inputs also shift the relay neuron between 'burst' and 'tonic' modes (see below)—a change in dynamics that is independent of the transfer ratio.

A class of cells with distinctive firing-rate dynamics. In the lateral geniculate nucleus of the cat, there is a subset of neurons have dynamics that are notably distinct from their retinal inputs,

known as 'lagged' neurons [165, 242, 243]. Lagged neurons are present in both ON and OFF varieties and represent approximately one-third of X-like neurons [165] and approximately 5% of Y-like neurons [244]. In comparison with the response of a corresponding nonlagged cell, the response of a lagged neuron to periodic stimulation has a phase that is delayed by a quarter of a cycle at low temporal frequencies (<4 Hz), and by the equivalent of 40–100 ms at higher temporal frequencies [329] (figure 8(B)). The peak of the temporal frequency tuning curve for a lagged cell is about a factor of two lower than the temporal tuning peak typical of a corresponding nonlagged cell [329]. However, with broadband temporal stimulation, the lagged versus nonlagged distinction appears to represent a continuum of properties, rather than a discrete bimodal classification [437].

The spatial properties of the lagged cells are similar to those of their nonlagged counterparts [165]. Lagged neurons receive direct inputs from the retina, but this input typically produces at most a small transient response, followed by a cessation in firing and then a resumption of activity after 40–80 ms [165, 242]—a timecourse consistent with a $GABA_B$-type IPSP [284] that inhibits firing during the silent period. This, along with a cross-correlation analysis of ganglion cell and lagged cell activity [243], suggests that the 'lag' is due to retinal activation of an intrinsic inhibitory interneuron within the LGN. Indeed, morphologically appropriate intrinsic LGN neurons, whose dynamics are nonlagged, have been identified [166]. Remarkably, lagged neurons can be made to behave in a largely unlagged fashion by stimulation of a brainstem input, the peribrachial region of the pontine reticular formation [163]. Thus, the lagged versus nonlagged distinction is not a hardwired one, but one that can be modulated, presumably via inputs to the inhibitory interneuron described above, or interactions at the level of the lagged neuron itself.

Lagged and nonlagged geniculate neurons converge onto the same cortical neuron, and thus may provide the spatiotemporal offsets required for direction selectivity [330]. Consistent with the properties of lagged cells, cortical direction selectivity is most prominent at 1–2 Hz and tapers off above 8 Hz. Moreover, the impulse responses typical of lagged and nonlagged LGN neurons are a good match for the temporal properties of subregions of receptive fields of directionally selective cortical simple cells, as deduced by detailed modelling of their responses to grating stimuli [196]. However [263], prediction of direction selectivity from linear combination of lagged and nonlagged inputs is much more successful for cortical neurons in the cortical input laminae (especially lamina 4B) than for other cortical neurons (especially lamina 6), indicating that intrinsic cortical circuitry and nonlinear processes [99, 263, 307, 308] play a role in direction selectivity. Lagged LGN neurons have a gentler contrast–response function than the nonlagged cells, suggesting that they may also contribute to signalling contrast over a broad dynamic range [147]. It has also been suggested that the presence of lagged cells in the LGN represents a second stage of efficient coding of information via decorrelation [11]: the spatial structure of retinal and geniculate receptive fields reduces spatial redundancy [83], while nonlagged and lagged cells represent the principal axes of temporal covariance [92].

Concerted signalling. In the cat LGN, there is experimental support for the notion that synchronous firing of nearby neurons can enhance the transmission of spatial information [250]. As shown recently by Dan *et al* [84], high-precision coincident firing accounts for 1–50% of the spikes generated by LGN neurons with overlapping receptive fields. The increase in information that can be extracted by considering coincident firing to be a distinct kind of event ranges from 5–30%. The increase in spatial information is positively correlated with the percentage of synchronized spikes—indicating that the benefit of the combinatorial code overwhelms the potential loss of information due to redundancy. Of particular interest is that the precision of correlation in the LGN is extremely high (<0.3 ms). At lower resolutions

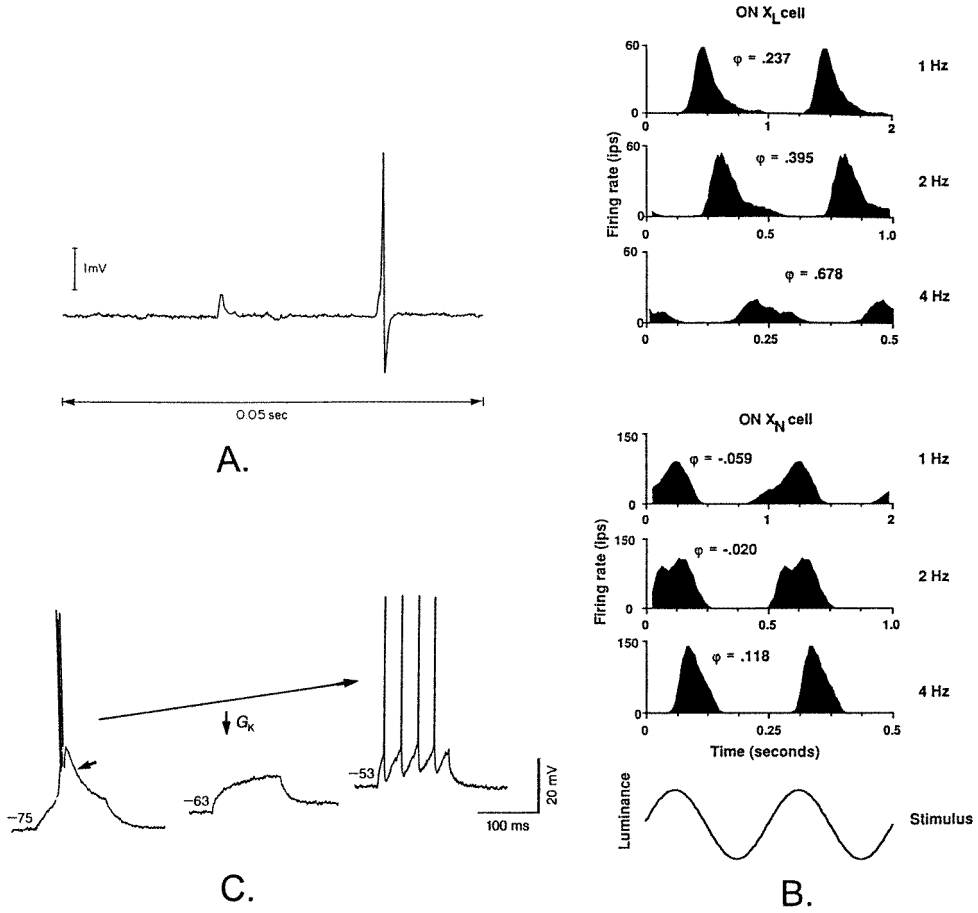

Figure 8. (A) Relationship of the retinal input (S-potential) and relay neuron response as recorded extracellularly in the macaque lateral geniculate nucleus. Some S-potentials fail to elicit a spiking response (initial event), but all spikes are preceded by an S-potential (shoulder on leading edge of second event). From Kaplan and Shapley [178]. (B) Dynamics of lagged (upper panel) and nonlagged (lower panel) X-type relay neurons in the lateral geniculate nucleus of the cat, as demonstrated by histograms of their extracellularly-recorded responses to sinusoidally modulated spots at a range of temporal frequencies. From Saul and Humphrey [329]. (C) Burst and tonic responses of an LGN relay neuron to intracellular current injection. At a holding potential of -75 mV, the voltage-dependent Ca^{++} conductance is activated and a burst response is induced. At a holding potential of -63 mV, the Ca^{++} conductance is inactivated and the depolarizing current is subthreshold for the Na^{+} spike, so there is no response. At a holding potential of -53 mV, the Ca^{++} conductance is inactivated but the depolarizing current is sufficient to reach threshold, and a train of Na^{+} spikes, commensurate with the duration of the depolarizing current, results. From McCormick [247]. All figures are reproduced with the consent of the original publishers.

(5–40 ms), the informational benefit of the combinatorial code would fall off, because of the increase in the number of chance coincidences. The authors suggest that the most likely origin of the high-precision correlation is shared input from single retinal ganglion cells, rather than slower correlations across retinal outputs. Simultaneous spikes in LGN neurons are more effective in activating a shared cortical target neuron than would be expected from the combined efficacy of each spike in isolation [5]. This superadditive interaction, perhaps

conferred by a threshold nonlinearity at the cortical level, may be the basis for decoding a combinatorial temporal representation that enhances the effective spatial resolution of the LGN output. Since cortical neurons receive input from aligned LGN receptive fields, it has also been suggested [5] that the combined effects of synchronized firing by ganglion cells and LGN neurons enhances cortical orientation tuning. This might contribute to the narrowness of cortical orientation tuning, compared with the linear prediction based on their receptive field sensitivity profile [367].

Intrinsic properties and spike train dynamics: two modes of firing. Thalamic relay neurons have intrinsic membrane properties that confer on them distinctive qualitative modes of firing behaviour [168, 169, 185, 247, 352], called 'burst' and 'tonic' (figure 8(C)). In burst mode, depolarization to firing threshold triggers a train of two to seven action potentials in rapid succession (interspike intervals of 5 ms or less). This burst is due to activation of a slow T-type Ca^{++} conductance, which produces a sustained depolarization whose duration is comparable to that of the burst [168, 169, 375]. In 'tonic' mode, the Ca^{++} conductance is inactive, and the LGN neuron fires at most one spike in response to a retinal EPSP.

The transition between these two modes of behaviour is governed by the recent history of the membrane potential of the LGN relay neuron. The Ca^{++} conductance is inactive near the relay neuron's threshold (-52 to -70 mV [53]). Moreover, once inactivated by depolarization, the Ca^{++} conductance requires a period of prolonged (e.g. 100 ms) hyperpolarization (-75 to -82 mV [144, 247] or more [53]) for de-inactivation [144]. Typically [144], bursts are also followed by a long interspike interval, because of inactivation of the Ca^{++} conductance, perhaps along with persistence of the slow inhibitory synaptic inputs that provided the hyperpolarization. This ionic basis confers a distinctive temporal structure on bursts: a long interspike interval before and after a train of impulses with brief (5 ms or less) interspike intervals. The ionic basis for bursts also provides a convincing argument that burst activity does represent a distinct mode: at intermediate membrane potentials (e.g., -60 to -65 mV [168, 169]), the LGN neuron's excitability is at a relative minimum; at more hyperpolarized potentials, the Ca^{++} conductance becomes de-inactivated; and at more depolarized potentials, synaptic inputs are more likely to bring the cell to firing threshold.

Relay neurons can switch back and forth between these distinct modes, not only between episodically presented stimuli [144] but also within a steady-state response [260]. LGN relay neurons have a resting potential typically in the range -52 to -74 mV and are electrotonically compact [36]. This suggests that relatively small, distal synaptic inputs can readily switch a relay neuron between these modes under physiological circumstances. Consequently, non-retinal inputs may be able to activate the T-type Ca^{++} conductance and thereby influence the relay neuron's dynamics, even though they are too small to drive the neuron to spike.

Mukherjee and Kaplan [260] measured transfer characteristics of LGN neurons by simultaneously recording their retinal inputs and their spike outputs under conditions of steady-state sinusoidal stimulation. Transfer characteristics of relay neurons were either bandpass (peak between 2 and 8 Hz) or lowpass, and many neurons shifted between bandpass and lowpass behaviour. This shift was associated with a change in firing pattern between burst (bandpass) and tonic (lowpass) mode. These characteristics could be reproduced by a biophysical model reduced from that of McCormick and Huguenard [248], which consists of the T-type Ca^{++} conductance and a delayed-rectifier K^+ conductance along with the standard Hodgkin–Huxley Na^+, K^+, and leak conductances. However, the model failed to predict the experimental finding of a greater fraction of tonic-mode spikes at higher contrasts, and it also underestimated response variability. These shortcomings were also present in simulations [259] of the full 10-channel McCormick and Huguenard [248] model, and they likely reflect both errors in

modelling the intrinsic dynamics of LGN neurons as well as the omission of non-retinal inputs.

Analysis of firing patterns elicited by simple periodic stimuli shows that in comparison to tonic mode, neurons in burst mode respond at a lower contrast, but information content is lower as well [143]. In qualitative terms, this is because the size of the burst depends more on the internal state of the neuron than on the size of the input. However, since burst firing represents a highly nonlinear phenomenon, the reduced information content seen for sinusoidal stimuli need not necessarily generalize to more complex stimulation patterns. Indeed, analysis of the information content of relay neurons' responses to pseudorandom temporal patterns reveals no substantial difference between tonic mode and burst mode [309]. Spikes fired in tonic mode carried two to three times the information of spikes fired in bursts (considered on a per-spike basis), but bursts carried two to three times the information of tonic spikes (considered on a per-event basis). It is tempting to speculate that the information content of bursts is high because their greater temporal precision [144] mitigates the relative lack of information in firing rate. Analysis via stimulus reconstruction approach [34, 312] suggests that this is not the complete answer, since the filters for an optimal reconstruction of the stimulus from burst or tonic spikes are very similar [309].

Even though both tonic and burst firing represent visually driven activity, speculations concerning the possible physiologic roles of these two modes are inspired in part by the observation that spontaneous bursts are present during deep sleep [247, 375]. These bursts are associated with slow oscillations of the membrane potential (ca 1 Hz) that are synchronized with EEG activity and are dependent not only on the intrinsic properties of LGN neurons but also on their connections with the perigeniculate nucleus [17, 247] and with each other [185, 247]. Thus, the LGN may undergo global shifts from burst to tonic mode, depending on the state of arousal.

Spikes fired within bursts have brief interspike intervals that allow them to be more effective in activating cortical neurons [220, 403], and even make an unreliable synapse behave in a reliable fashion [220]. Along with the qualitatively all-or-none information transfer characteristics of relay neurons during burst mode [143, 352], this suggests that burst mode is more suited for detection, while tonic mode is more suited for discrimination. On the other hand, the non-retinal inputs to the LGN, particularly the feedback from visual cortex, are spatially specific [261]. Moreover, the recent studies of Reinagel *et al* [309] make it difficult to assign any role to bursts predicated on an impoverished information content *per se*. These considerations are consistent with the speculation [352] that the transition from burst mode to tonic mode may be the neural correlate of focal attention [292].

Spike train statistics. The spontaneous discharge of LGN relay neurons is more irregular than that of their retinal inputs. Spontaneous discharges are approximately renewal processes, with an interspike interval distribution approaching Poisson [122]. But as is the case for retinal ganglion cells, the statistics of spike trains elicited by visual stimuli cannot be described as a Poisson process, or even a modulated renewal process [302]. Two tendencies compete to add a small serial correlation to the spike discharge: the retinal input carries a small negative serial correlation, while the presence of burst and tonic firing modes tends to induce a small positive serial correlation. In addition to serial correlation [122], there are two other kinds of deviations from a renewal process. One deviation is that the initial portion of the response to a transient stimulus has greater regularity than the sustained portion, even when rate is taken into account. Its interspike interval distribution is approximated by a gamma process of order five, while the sustained portion of the response is approximately Poisson [122]. This greater regularity of the phasic portion of the response is not dependent on the mode (i.e. burst versus tonic) of the relay neuron.

The second kind of deviation from the behaviour expected from a modulated renewal process (and also not accounted for by a leaky integrate-and-fire model [302]) is the presence of multiple peaks in the interspike interval histogram [118]. The response elicited by the onset of a transient visual stimulus often consists of a burst, followed by a pause, and then tonic activity [118]. During tonic firing, relay neurons fire only when the corresponding retinal afferent fires, but not every retinal afferent spike elicits a spike in the relay neuron [178, 243]. Because firing rates of retinal neurons under steady illumination are reasonably regular [398], this spike dropout can result in a multimodal interspike interval distribution, with regularly spaced peaks [117]. The intrageniculate contribution to the surround [74, 162, 175] is one source of inhibitory signals that can lead to spike dropout, and the strength of this inhibition is necessarily stronger for spatially extensive than for spatially localized stimuli. Thus, it has been proposed that, in burst mode, the interspike interval statistics may represent a temporal code for the spatial structure of the relay neurons [118].

The influence of cortical feedback. The lateral geniculate receives extensive feedback from visual cortex. In one study of the effects of eliminating this feedback via cortical cooling [245], it appeared to play the role of a nonspecific modulatory influence rather than as the source of temporal structure. More recent studies involving both cortical stimulation [438] and cooling [116] indicate that cortical feedback sharpens the temporal precision of retinogeniculate transmission.

The anatomical divergence of the cortical feedback pathway [261] could serve as the source of long-range synchronizations seen during stimulation with spatially extensive stimuli. Sillito and co-workers [355] used cross-correlation analysis to show that spikes from nearby relay neurons in LGN become synchronized, on a timescale of 25 ms or more, when they are jointly stimulated by a moving bar of the appropriate orientation, and that this synchronization was dependent on feedback from visual cortex. The standard interpretation of these relatively narrow cross-correlations is that they represent the presence of common synaptic inputs [4, 288]. Synchronization of relay neuron spike activity through common driving by cortical feedback could thus be the physiologic substrate of linking of visual features. However, the intrinsic dynamics of LGN relay neurons complicates the picture [53]. Slow covariations (on the order of a second) of membrane potential of neighbouring relay neurons, perhaps due to shared modulatory non-retinal inputs, would induce correlations of their firing modes [54, 55], and consequently induce firing-time correlations on a timescale comparable to that observed by Sillito *et al* [355]. Thus, although there is strong evidence that corticogeniculate feedback modulates transmission from the retina and influences the dynamics of the resulting spike trains, its role in feature extraction remains unclear.

5. Conclusions

Each stage of early visual processing is accompanied by the addition of new dynamical features (see table 1). Photoreceptors may be considered to be quasilinear filters for small inputs, but demonstrate large changes in gain and dynamics as mean light level increases. Rods and cones differ in operating range and dynamics, but within each photoreceptor class, dynamics are quite uniform. The horizontal cells add an additional level of adaptive filtering, but also a substantial degree of heterogeneity, including subtypes in which chromatically distinct inputs interact in a nonlinear fashion. Adaptive filtering continues at the bipolar cells, but here the adaptive filtering is triggered by only modest changes in the size of the input signal, perhaps because of the high intrinsic gain of the bipolar cell. Bipolar cells first demonstrate two

Table 1. A summary of the main dynamical features of neurons in the retina and lateral geniculate nucleus.

Photoreceptors
Two classes (rods and cones) with distinct ranges of sensitivity and dynamics
Quasilinear behaviour for small inputs
Adaptive changes in gain and dynamics across large changes in average light intensity
Horizontal cells
Quasilinear behaviour for small inputs
Adaptive changes in gain and dynamics across large changes in average light intensity
Subtypes with spectral opponency and nonlinear interactions between chromatically distinct inputs
Bipolar cells
Quasilinear combination of antagonistic receptive field regions with distinct dynamics
ON and OFF dichotomy, approximately push–pull but distinct dynamics
Adaptive changes in gain and dynamics across modest changes in input variance (contrast)
Amacrine cells
Increased transience
Subtypes with highly nonlinear (ON–OFF) behaviour even for small inputs
Subtypes with direction selectivity
Subtypes with spiking behaviour
Ganglion cells
Spikes as the sole mode of information transmission
Subtypes with highly nonlinear (ON–OFF) behaviour even for small inputs
Contrast gain control
Coupling of chromatic, spatial, and temporal aspects of responses
Phase-locking behaviour at high contrasts
Concerted firing patterns across cells
Lateral geniculate nucleus (relay cells)
Subtypes with highly nonlinear (ON–OFF) behaviour even for small inputs
Lagged and nonlagged subtypes
Spike deletion
‘Burst’ and ‘tonic’ modes of firing
Modulation by non-visual inputs
Modulation by cortical feedback

features characteristic of later stages of visual processing: centre–surround antagonism, and the ON–OFF dichotomy. Centre and surround signals typically have different dynamics, so this simple quasilinear combination of signals couples the spatial structure of the input into the temporal structure of the response. The two branches of the ON–OFF dichotomy are only approximately push–pull, owing to the distinct kinds of synaptic mechanisms required to generate both inhibitory (for the ON bipolar) and excitatory (for the OFF bipolar) responses to the same neurotransmitter signal. This foreshadows a greater asymmetry at the ganglion cell stage, due to the difference in firing rates of typical ON and OFF ganglion cells.

In the inner retina, the number of distinguishable neuronal subtypes grows dramatically. The amacrine cell class as a whole is characterized by transient response properties and both

serial and recurrent inhibition. Some amacrine cells demonstrate highly nonlinear (ON–OFF) behaviour even for localized, low-contrast inputs, and thus represent the basic architecture of the 'nonlinear subunit' structure seen more centrally. Amacrine cells also have intrinsic membrane nonlinearities that accentuate their transience.

Ganglion cells are universally spiking neurons, and represent the 'information bottleneck' at the retinal output. The ON–OFF dichotomy set up at the bipolar cell level continues, and, for both ON and OFF ganglion cells, subtypes that either manifest or do not manifest the ON–OFF nonlinearity are present—probably due to the presence or absence of a strong input from the appropriate class of nonlinear amacrine cells. Many ganglion cells manifest a new kind of adaptive filtering, the contrast gain control, that adjusts dynamics parametric in the variance (rather than the mean) of the input signal. Two new dynamical features of the ganglion cell response depend in an intrinsic manner on their spiking behaviour: high-precision phase locking at high contrasts, and concerted firing patterns across neighbouring cells, probably related to sharing inputs from a common interneuron.

The relay cells of the lateral geniculate manifest a new dichotomy, the lagged versus nonlagged distinction, probably laying the groundwork for motion analysis at more central stages. The intrinsic membrane properties of relay neurons add another dynamical feature: a distinctive mode of behaviour in which a burst of spikes can be triggered by a single retinal input, provided that the relay neuron has been hyperpolarized for a sufficiently long period of time. The relay nucleus is also the target of modulatory inputs from the brainstem, and for feedback projections from visual cortex, whose role (modulatory versus specific) is as yet unclear. While these effects on relay neuron dynamics can be described in terms of a quasilinear influence on firing rate, this is at best a first approximation: firing mode shifts and feedback influences are intrinsically nonlinear and have marked influences on the statistical structure of the spike train as well.

This tour of dynamics of precortical visual processing provides an important backdrop for the recent surge of interest in mechanisms of coding and information processing by neurons at more central levels [59]. Central neurons are capable of high-precision firing (on the order of 1 ms [226]). For temporally rich stimuli, this high-precision firing is informative [59], but for stimuli that do not have a strong intrinsic temporal structure, spike times are informative to a precision of no better than 10–30 ms [153, 414]. Thus, one key question is the extent to which the overall firing rate of a neuron (measured perhaps over fairly brief time periods and an ensemble of similar cells) provides a sufficient basis for understanding neural coding and computation [343] or, alternatively, whether the detailed statistics of individual neurons' firing patterns needs to be considered [414]. A related but broader question can be asked on the population level—does it suffice to consider average responses, or must one come to grips with the correlation structure, intrinsic oscillations, and non-stationarities [57, 257, 316]? Substantial challenges, both experimental and theoretical, hinder a direct assault on these questions in the mammalian brain. This makes it tempting to conclude that central processing can be adequately described by simple population-average rate measures and quasilinear dynamics. But the progressive layering of dynamical features from photoreceptor to thalamus suggests otherwise.

Acknowledgments

This work was supported by NIH grant EY9314. The author thanks Keith Purpura, Nicholas Schiff, Ferenc Mechler, and especially Daniel Reich for their many helpful comments, Mary Conte for assistance with preparation of the figures, and Tal Levin for proofreading the manuscript. The author also expresses appreciation to the many investigators who have provided preprints and reprints of their work.

References

[1] Abeles M 1982 *Local Cortical Circuits, An Electrophysiological Study* (Berlin: Springer)

[2] Abeles M and Gerstein G L 1988 Detecting spatiotemporal firing patterns among simultaneously recorded single neurons *J. Neurophysiol.* **60** 909–24

[3] Adelson E H and Bergen J 1985 Spatiotemporal energy models for the perception of motion *J. Opt. Soc. Am.* A **2** 284–99

[4] Aertsen A M H J, Gerstein G L, Habib H K and Palm G 1989 Dynamics of neuronal firing correlation: modulaton of 'effective connectivity' *J. Neurophysiol.* **61** 900–17

[5] Alonso J-M, Usrey W M and Reid R C 1996 Precisely correlated firing in cells of the lateral geniculate nucleus *Nature* **383** 815–19

[6] Amthor F R and Grzywacz N 1991 Nonlinearity of the inhibition underlying retinal direction selectivity *Vis. Neurosci.* **6** 197–206

[7] Amthor F R and Grzywacz N M 1993 Directional selectivity in vertebrate retinal ganglion cells *Rev. Oculomot Res.* **5** 79–100

[8] Ariel M and Daw N W 1982 Pharmacological analysis of directionally sensitive rabbit retinal ganglion cells *J. Physiol.* **324** 161–85

[9] Ariel M, Daw N W and Rader R K 1983 Rhythmicity in rabbit retinal ganglion cell responses *Vis. Res.* **23** 1485–93

[10] Ashmore J F and Copenhagen D R 1980 Different postsynaptic events in two types of retinal bipolar cells *Nature* **288** 84–6

[11] Atick J J and Redlich A N 1990 Towards a theory of early visual processing *Neural Comput.* **2** 308–20

[12] Atick J J, Li Z and Redlich A N 1992 Understanding retinal colour coding from first principles *Neural Comput.* **4** 559–72

[13] Attwell D, Borges S, Wu M and Wilson M 1987 Signal clipping by the rod output synapse *Nature* **328** 522–4

[14] Babloyantz A and Destexhe A 1986 Low-dimensional chaos in an instance of epilepsy *Proc. Natl Acad. Sci., USA* **83** 3513–7

[15] Bader C R, Bertrand D and Schwartz E A 1982 Voltage-activated and calcium-activated currents studied in solitary rod inner segments from the salamander retina *J. Physiol.* **331** 253–84

[16] Bair W, Koch C, Newsome W and Britten K 1994 Power spectrum analysis of bursting cells in area MT in the behaving monkey *J. Neurosci.* **14** 2870–92

[17] Bal T, von Krosigk M and McCormick D A 1995 Role of the ferret perigeniculate nucleus in the generation of synchronized oscillations *in vitro J. Physiol.* **483** 665–85

[18] Barlow H B 1961 Possible principles underlying the transformation of sensory messages *Sensory Communication* ed W A Rosenblith (Cambridge, MA: MIT)

[19] Baylor D A 1987 Photoreceptor signals and vision *Invest. Ophth. Vis. Sci.* **28** 34–49

[20] Baylor D A, Fuortes M G F and O'Bryan P M 1971 Lateral interaction between vertebrate photoreceptors *Vis. Res.* **11** 1195–6

[21] Baylor D A and Hodgkin A L 1974 Changes in time scale and sensitivity in turtle photoreceptors *J. Physiol.* **242** 729–58

[22] Baylor D A, Hodgkin A L and Lamb T D 1974 Reconstruction of the electrical responses of turtle cones to flashes and steps of light *J. Physiol.* **242** 759–91

[23] Baylor D A, Nunn B J and Schnapf J L 1987 Spectral sensitivity of cones of the monkey *Macaca fascicularis J. Physiol.* **390** 145–60

[24] Belgum J H and Copenhagen D R 1988 Synaptic transfer of rod signals to horizontal and bipolar cells in the retina of the toad (*bufo marinus*) *J. Physiol.* **396** 225–45

[25] Benardete E 1994 Functional dynamics of primate retinal ganglion cells *Thesis* The Rockefeller Univeristy, New York

[26] Benardete E A and Kaplan E 1997 The receptive field of the primate P retinal ganglion cell. I: Linear dynamics *Vis. Neurosci.* **14** 169–85

[27] Benardete E A and Kaplan E 1997 The receptive field of the primate P retinal ganglion cell. II: Nonlinear dynamics *Vis. Neurosci.* **14** 187–205

[28] Benardete E A and Kaplan E 1999 The dynamics of primate M retinal ganglion cells *Vis. Neurosci.* **16** 355–68

[29] Benardete E A, Kaplan E and Knight B W 1992 Contrast gain control in the primate retina: P cells are not X-like, some M cells are *Vis. Neurosci.* **8** 483–6

[30] Bennett P J and Banks M S 1987 Sensitivity loss in odd-symmetric mechanisms and phase anomalies in peripheral vision *Nature* **326** 873–6

[31] Berry M J and Meister M 1998 Refractoriness and neural precision *J. Neurosci.* **18** 2200–11

[32] Berry M J, Warland D K and Meister M 1997 The structure and precision of retinal spike trains *Proc. Natl*

Acad. Sci., USA **94** 5411–16
[33] Bialek W and Owen W G 1990 Temporal filtering in retinal bipolar cells. Elements of an optimal computation? *Biophys. J.* **58** 1227–33
[34] Bialek W, Rieke F, de Ruyter van Steveninck R R and Warland D 1991 Reading a neural code *Science* **252** 1854–7
[35] Bilotta J and Abramov I 1989 Spatial properties of goldfish ganglion cells *J. Gen. Physiol.* **93** 1147–69
[36] Bloomfield S A, Hamos J E and Sherman S M 1987 Passive cable properties and morphological correlates of neurones in the lateral geniculate nucleus of the cat *J. Physiol.* **383** 653–92
[37] Borges S and Wilson M 1987 Structure of the receptive fields of bipolar cells in the salamander retina *J. Neurophysiol.* **58** 1275–91
[38] Bowen R W 1995 Isolation and interaction of ON and OFF pathways in human vision: pattern–polarity effects on contrast discrimination *Vis. Res.* **35** 2479–90
[39] Bowen R W, Pokorny J and Smith V C 1989 Sawtooth contrast sensitivity: decrements have the edge *Vis. Res.* **29** 1501–9
[40] Bowen R W, Pokorny J, Smith V C and Fowler M A 1992 Sawtooth contrast sensitivity: effects of mean illuminance and low temporal frequencies *Vis. Res.* **32** 1239–47
[41] Boycott B B and Dowling J E 1969 Organization of the primate retina: light microscopy *Phil. Trans. R. Soc.* B **255** 109–94
[42] Boycott B B and Hopkins J M 1991 Cone bipolar cells and cone synapses in the primate retina *Vis. Neurosci.* **7** 49–60
[43] Boycott B B and Wässle H 1974 The morphological types of ganglion cells of the domestic cat's retina *J. Physiol.* **240** 397–419
[44] Boycott B B and Wässle H 1991 Morphological classification of bipolar cells in the macaque monkey retina *Eur. J. Neurosci.* **3** 1069–88
[45] Boycott B B and Wässle H 1999 Parallel processing in the mammalian retina *Invest. Ophth. Vis. Sci.* **40** 1313–27
[46] Boynton R M 1979 *Human Colour Vision* (New York: Holt, Rinehart and Winston)
[47] Brandstatter J H, Greferath U, Euler T and Wässle H 1995 Co-stratification of $GABA_A$ receptors with the directionally selective circuitry of the rat retina *Vis. Neurosci.* **12** 345–58
[48] Brillinger D R 1981 *Time Series: Data Analysis and Theory (Expanded Edition)* (New York: McGraw-Hill)
[49] Brindley G S, Du Croz J J and Rushton W A H 1966 The flicker fusion frequency of the blue-sensitive mechanism of colour vision *J. Physiol.* **183** 497–500
[50] Brivanlou I H, Warland D K and Meister M 1998 Mechanisms of concerted firing among retinal ganglion cells *Neuron* **20** 527–39
[51] Brodie S E, Knight B W and Ratliff F 1978 The response of the Limulus retina to moving stimuli: a prediction by Fourier synthesis *J. Gen. Physiol.* **72** 129–66
[52] Brodie S E, Knight B W and Ratliff F 1978 The spatiotemporal transfer function of the Limulus lateral eye *J. Gen. Physiol.* **72** 167–202
[53] Brody C D 1998 Slow covariations in neuronal resting potentials can lead to artefactually fast cross-correlations in their spike trains *J. Neurophysiol.* **80** 3345–51
[54] Brody C D 1999 Disambiguating different covariation types *Neural Comput.* **11** 1527–35
[55] Brody C D 1999 Correlations without synchrony *Neural Comput.* **11** 1537–51
[56] Bullier J and Nowak L C 1995 Parallel versus serial processing: new vistas on the distributed organization of the visual system *Curr. Opin. Neurobiol.* **5** 497–503
[57] Bullock T H 1997 Signals and signs in the nervous system: the dynamic anatomy of electrical activity is probably information-rich *Proc. Natl Acad. Sci., USA* **94** 1–6
[58] Bullock T H, Achimowicz J Z, Duckrow R B, Spencer S S and Iragui-Madoz V J 1997 Bicoherence of intracranial EEG in sleep, wakefulness and seizures *Electroencephalogr. Clin. Neurophysiol.* **103** 661–78
[59] Buracas G T and Albright T D 1999 Gauging sensory representations in the brain *Trends Neurosci.* **22** 303–9
[60] Burkhardt D A and Hassin G 1983 Quantitative relations between colour-opponent response of horizontal cells and action spectra of cones *J. Neurophysiol.* **49** 961–75
[61] Calkins D J, Schein S J, Tsukamoto Y, Masarachia P and Sterling P 1992 Parallel pathways to midget ganglion cells in macaque fovea *Invest. Ophth. Vis. Sci.* **33** 1173
[62] Calkins D J, Schein S J, Tsukamoto Y and Sterling P 1994 M and L cones in macaque fovea connect to midget ganglion cells by different numbers of excitatory synapses *Nature* **371** 70–2
[63] Calkins D J, Tsukamoto Y and Sterling P 1998 Microcircuitry and mosaic of a blue–yellow ganglion cell in the primate retina *J. Neurosci.* **18** 3373–85
[64] Campbell F W and Robson J G 1968 Application of Fourier analysis to the visibility of gratings *J. Physiol.* **197** 551–66

[65] Cariani P 1995 As if time really mattered: temporal strategies for neural coding of sensory information *Commun. Cognition (AI: Special Issue on Self-Reference in Biological and Cognitive Systems)* **12** 157–219
[66] Carlton A G 1969 On the bias of information estimates *Psychol. Bull.* **71** 108–9
[67] Chan R Y and Naka K-I 1980 Spatial organizations of catfish retinal neurons. II. Circular stimulus *J. Neurophysiol.* **43** 832–50
[68] Chappell R L, Naka K-I and Sakuranaga M 1985 Dynamics of turtle horizontal cell response *J. Gen. Physiol.* **86** 423–53
[69] Chee-Orts M-N and Optican L M 1993 Cluster method for analysis of transmitted information in multivariate neuronal data *Biol. Cybern.* **69** 29–35
[70] Cheng H, Chino Y M, Smith E L 3rd, Hamamoto J and Yoshida K 1995 Transfer characteristics of lateral geniculate nucleus X neurons in the cat: effects of spatial frequency and contrast *J. Neurophysiol.* **74** 2548–57
[71] Chun M H and Wässle H 1989 GABA-like immunoreactivity in the cat retina: electron microscopy *J. Comput. Neurol.* **279** 55–67
[72] Churchland P S and Sejnowski T J 1988 Pespectives on cognitive neuroscience *Science* **242** 741–5
[73] Cleland B G, Dubin M W and Levick W R 1971 Sustained and transient neurones in the retina and lateral geniculate nucleus *J. Physiol.* **217** 473–96
[74] Cleland B G and Lee B B 1985 A comparison of visual responses of cat lateral geniculate nucleus neurones with those of ganglion cells afferent to them *J. Physiol.* **369** 249–68
[75] Copenhagen D R, Ashmore J F and Schnapf J K 1983 Kinetics of synaptic transmission from photoreceptors to horizontal and bipolar cells in turtle retina *Vis. Res.* **23** 363–9
[76] Cowey A and Stoerig P 1989 Projection patterns of surviving neurons in the dorsal lateral geniculate nucleus following discrete lesions of striate cortex: implications for residual vision *Exp. Brain Res.* **75** 631–8
[77] Croner L J, Purpura K and Kaplan E 1993 Response variability in retinal ganglion cells of primates *Proc. Natl Acad. Sci., USA* **90** 8128–30
[78] Croner L J and Albright T D 1999 Segmentation by colour influences responses of motion-sensitive neurons in the cortical middle temporal visual area *J. Neurosci.* **19** 3935–51
[79] Dacey D M 1996 Circuitry for colour coding in the primate retina *Proc. Natl Acad. Sci., USA* **93** 582–8
[80] Dacey D M and Lee B B 1994 The 'blue-on' opponent pathway in primate retina originates from a distinct bistratified ganglion cell type *Nature* **367** 731–5
[81] Dacey D M and Lee B B 1995 Physiological identification of cone inputs to HI and HII horizontal cells in macaque retina *Invest. Ophth. Vis. Sci.* **36** 3
[82] Daly S J and Normann R A 1985 Temporal information processing in cones: effects of light adaptation on temporal summation and modulation *Vis. Res.* **25** 1197–1206
[83] Dan Y, Atick J J and Reid R C 1996 Efficient coding of natural scenes in the lateral geniculate nucleus: experimental test of a computational theory *J. Neurosci.* **16** 3351–62
[84] Dan Y, Alonso J-M, Usrey W M and Reid R C 1998 Coding of visual information by precisely correlated spikes in the lateral geniculate nucleus *Nature Neurosci.* **1** 501–7
[85] Daw N, Jensen R J and Brunken W J 1990 Rod pathways in mammalian retinae *Trends Neurosci.* **13** 110–5
[86] Dayhoff J E and Gerstein G L 1983 Favoured patterns in spike trains. I. Detection *J. Neurophysiol.* **49** 1334–46
[87] Dayhoff J E and Gerstein G L 1983 Favoured patterns in spike trains. II. Application *J. Neurophysiol.* **49** 1347–63
[88] Dean A F 1981 The variability of discharge of simple cells in the cat striate cortex *Exp. Brain Res.* **44** 437–40
[89] Derrington A M, Krauskopf J and Lennie P 1984 Chromatic mechanisms in lateral geniculate nucleus of macaque *J. Physiol.* **357** 241–65
[90] Ding Y and Casagrande V A 1997 The distribution and morphology of LGN K pathway axons within the layers and CO blobs of owl monkey V1 *Vis. Neurosci.* **14** 691–704
[91] Detwiler P B, Hodgkin A L and McNaughton P A 1980 Temporal and spatial characteristics of the voltage response of rods in the retina of the snapping turtle *J. Physiol.* **300** 213–50
[92] Dong D W and Atick J J 1995 Temporal decorrelation: a theory of lagged and nonlagged responses in the lateral geniculate nucleus *Network* **6** 159–68
[93] Dowling J E 1970 Organization of vertebrate retinas *Invest. Ophth. Vis. Sci.* **9** 655–80
[94] Dowling J E and Boycott B B 1966 Organization of the primate retina: electron microscopy *Proc. R. Soc.* B **166** 80–111
[95] Dow B M, Snyder A Z, Vautin R G and Bauer R 1981 Magnification factor and receptive field size in foveal striate cortex of the monkey *Exp. Brain Res.* **44** 213–28
[96] Eckert M P and Buchsbaum G 1993 Efficient coding of natural time varying images in the early visual system *Phil. Trans. R. Soc.* B **339** 385–95

[97] Eckhorn R 1994 Oscillatory and non-oscillatory synchronizations in the visual cortex and their possible roles in associations of visual features *Prog. Brain Res.* **102** 405–26
[98] Eckhorn R, Bauer R, Jordan W, Brosch M, Kruse W, Munk M and Reitboeck H 1988 Coherent oscillations: a mechanism of feature linking in the visual cortex? Multiple electrode and correlation analyses in the cat *Biol. Cybern.* **60** 121–30
[99] Emerson R C, Bergen J R and Adelson E H 1992 Directionally selective complex cells and the computation of motion energy in cat visual cortex *Vis. Res.* **32** 203–18
[100] Enroth-Cugell C and Robson J G 1966 The contrast sensitivity of retinal ganglion cells of the cat *J. Physiol.* **187** 517–52
[101] Enroth-Cugell C, Robson J, Schweitzer-Tong D E and Watson A B 1983 Spatiotemporal interactions in cat retinal ganglion cells showing linear spatial summation *J. Physiol.* **341** 279–308
[102] Enroth-Cugell C and Pinto L 1970 Algebraic summation of centre and surround input to retinal ganglion cells of the cat *Nature* **226** 458–9
[103] Famiglietti E V Jr and Kolb H 1976 Structural basis for on- and off-centre responses in retinal ganglion cells *Science* **194** 193–5
[104] Farell B 1999 Colour and luminance in the perception of 1- and 2-dimensoinal motion *Vis. Res.* **39** 2633–47
[105] Felleman D J and Van Essen D C 1991 Distributed hierarchical processing in the primate cerebral cortex *Cerebral Cortex* **1** 1–47
[106] Fitzgerald K M, Cibis G W, Giambrone S A and Harris D J 1994 Retinal signal transmission in Duchenne muscular dystrophy: evidence for dysfunction in the photoreceptor/depolarizing bipolar cell pathway *J. Clin. Invest.* **93** 2425–30
[107] FitzHugh R 1957 The statistical detection of threhold signals in the retina *J. Gen. Physiol.* **40** 925–48
[108] Foerster M H, van de Grind W A and Grüsser O-J 1977 Frequency transfer properties of three distinct types of cat horizontal cells *Exp. Brain Res.* **29** 347–66
[109] Foerster M H, van de Grind W A and Grüsser O-J 1977 The response of cat horizontal cells to flicker stimuli of different area, intensity and frequency *Exp. Brain Res.* **29** 367–85
[110] Fohlmeister J F, Coleman P A and Miller R F 1990 Modelling the repetitive firing of retinal ganglion cells *Brain Res.* **510** 343–5
[111] Fohlmeister J F and Miller R F 1997 Impulse encoding mechanisms of ganglion cells in the tiger salamander retina *J. Neurophysiol.* **78** 1935–47
[112] Fohlmeister J F and Miller R F 1997 Mechanisms by which cell geometry controls repetitive impulse firing in retinal ganglion cells *J. Neurophysiol.* **78** 1948–64
[113] Freed M A, Pflug R, Kolb H and Nelson R 1996 ON–OFF amacrine cells in cat retina *J. Comput. Neurol.* **364** 556–66
[114] Frishman L J, Freeman A W, Troy J B, Schweitzer-Tong D E and Enroth-Cugell C 1987 Spatiotemporal frequency responses of cat retinal ganglion cells *J. Physiol.* **341** 279–308
[115] Frumkes T E, Miller R F, Slaughter M and Dacheux R F 1981 Physiological and pharmacological basis of GABA and glycine action on neurons of mudpuppy retina. III. Amacrine-mediated inhibitory influences on ganglion cell receptive-field organization: a model *J. Neurophysiol.* **45** 783–803
[116] Funke K, Nelle E, Li B and Wörgötter F 1996 Corticofugal feedback improves the timing of retino-geniculate signal transmission *Neuroreport* **7** 2130–4
[117] Funke K and Wörgötter F 1995 Temporal structure in the light response of relay cells in the dorsal lateral geniculate nucleus of the cat *J. Physiol.* **485** 715–37
[118] Funke K and Wörgötter F 1997 On the significance of temporally structured activity in the dorsal lateral geniculate nucleus (LGN) *Prog. Neurobiol.* **53** 67–119
[119] Gallego A 1971 Horizontal and amacrine cells in the mammal's retina *Vis. Res.* **3** 33–50
[120] Gawne T J 1999 Temporal coding as a means of information transfer in the primate visual system *Crit. Rev. Neurobiol.* **13** 83–101
[121] Gawne T J, Kjaer T W and Richmond B J 1996 Latency: another potential code for feature binding in striate cortex *J. Neurophysiol.* **76** 1356–60
[122] Gazères N, Borg-Graham L J and Frégnac Y 1998 A phenomenological model of visually evoked spike trains in cat geniculate nonlagged X-cells *Vis. Neurosci.* **15** 1157–74
[123] Gegenfurtner K R and Hawken M J 1996 Interaction of motion and colour in the visual pathways *Trends Neurosci.* **19** 394–401
[124] Gershon E D, Wiener M C, Latham P E and Richmond B J 1998 Coding strategies in monkey V1 and inferior temporal cortices *J. Neurophysiol.* **79** 1135–44
[125] Gerstein G L and Mandelbrot B 1964 Random walk models for the spike activity of a single neuron *Biophys. J.* **4** 41

[126] Gerstein G L and Perkel D H 1969 Simultaneously recorded trains of action potentials: analysis and functional interpretation *Science* **164** 828–30
[127] Gerstein G L and Perkel D H 1972 Mutual temporal relationships among neuronal spike trains. Statistical techniques for display and analysis *Biophys. J.* **12** 453–73
[128] Gestri G 1978 Dynamics of a model for the variability of the interspike intervals in a retinal neuron *Biol. Cybern.* **31** 97–8
[129] Gielen C C A M, Ginsbergen J A M v and Vendrik A J 1981 Characterization of spatial and temporal properties of monkey LGN Y cells *Biol. Cybern.* **40** 157–70
[130] Gielen C C A M, Ginsbergen J A M v and Vendrik A J 1982 Reconstruction of cone-system contributions to responses of colour-opponent neurons in monkey lateral geniculate *Biol. Cybern.* **44** 211–21
[131] Golomb D, Hertz J, Panzeri S, Treves A and Richmond B 1997 How well can we estimate the information carried in neuronal responses from limited samples? *Neural Comput.* **9** 649–65
[132] Golomb D, Kleinfeld D, Reid R C, Shapley R M and Shraiman B I 1994 On temporal codes and the spatiotemporal response of neurons in the lateral geniculate nucleus *J. Neurophysiol.* **72** 2990–3003
[133] Gray C M and McCormick D A 1996 Chattering cells: superficial pyramidal neurons contributing to the generation of synchronous oscillations in the visual cortex *Science* **274** 109–13
[134] Green D M and Swets J A 1966 *Signal Detection Theory and Psychophysics* (New York: Wiley)
[135] van de Grind W A and Grüsser O-J 1981 Frequency transfer properties of cat retina horizontal cells *Vis. Res.* **21** 1565–72
[136] Grünert U 1997 Anatomical evidence for rod input to the parvocellular pathway in the visual system of the primate *Eur. J. Neurosci.* **9** 617–21
[137] Grünert U and Martin P R 1991 Rod bipolar cells in the macaque monkey retina: Immunoreactivity and connectivity *J. Neurosci.* **11** 2742–58
[138] Grünert U and Wässle H 1990 GABA-like immunoreactivity in the Macaque monkey retina: A light and electron microscopic study *J. Comput. Neurol.* **297** 509–24
[139] Grünert U and Wässle H 1996 Glycine receptors in the rod pathway of the macaque monkey retina *Vis. Neurosci.* **13** 101–15
[140] Grzywacz N M and Amthor F R 1993 Facilitation in ON–OFF directionally selective ganglion cells of the rabbit retina *J. Neurophysiol.* **69** 2188–99
[141] Grzywacz N M, Amthor F R and Merwine D K 1994 Directional hyperacuity in ganglion cells of the rabbit retina *Vis. Neurosci.* **11** 1019–25
[142] Grzywacz N M and Koch C 1987 Functional properties of models for direction selectivity in the retina *Synapse* **1** 417–34
[143] Guido W, Lu S-M, Vaughn J W, Godwin D W and Sherman S M 1995 Receiver operating characteristic (ROC) analysis of neurons in the cat's lateral geniculate nucleus during tonic and burst response mode *Vis. Neurosci.* **12** 723–41
[144] Guido W and Sherman S M 1998 Response latencies of cells in the cat's lateral geniculate nucleus are less variable during burst than tonic firing *Vis. Neurosci.* **15** 231–7
[145] Han Y, Zhang J and Slaughter M M 1997 Partition of transient and sustained inhibitory glycinergic input to retinal ganglion cells *J. Neurosci.* **17** 3392–400
[146] Hare W A and Owen W G 1990 Spatial organization of the bipolar cell's receptive field in the retina of the tiger salamander *J. Physiol.* **421** 223–45
[147] Hartveit E and Heggelund P 1992 The effect of contrast on the visual response of lagged and nonlagged cells in the cat lateral geniculate nucleus *Vis. Neurosci.* **9** 515–25
[148] Hartveit E and Heggelund P 1995 Brainstem modulation of signal transduction through the cat dorsal lateral geniculate nucleus *Exp. Brain Res.* **103** 372–84
[149] Hartline H K 1938 The response of single optic nerve fibres of the vertebrate eye to the illumination of the retina *Am. J. Physiol.* **121** 400–15
[150] Hartline H K and Graham C H 1932 Nerve impulses from single receptors in the eye *J. Cell. Comput. Physiol.* **1** 277–95
[151] He S and Masland R H 1997 Retinal direction selectivity after targeted laser ablation of starburst amacrine cells *Nature* **389** 378–82
[152] Heeger D J and Simoncelli E P 1992 Model of visual motion sensing *Spatial Vision in Humans and Robots* ed L Harris and M Jenkins (New York: Cambridge University Press)
[153] Heller J, Hertz J A, Kjaer T W and Richmond B J 1995 Information flow and temporal coding in primate pattern vision *J. Comput. Neurosci.* **2** 175–93
[154] Heinrich S P and Bach M 1997 Stimulus-induced modulations of 30 and 40 Hz domains in the EEG *Invest. Ophth. Vis. Sci.* **38** 994

[155] Hendry S H and Yoshioka T 1994 A neurochemically distinct third channel in the macaque dorsal lateral geniculate nucleus *Science* **264** 575–7
[156] Hertz J 1997 Reading the information in the outcome of neural computation *Building Blocks for Intelligent Systems* ed D Amit *et al* (Rome: Enciclopedia Italiana) at press
[157] Hilgetag C C, O'Neill M A and Young M P 1996 Indeterminate organization of the visual system *Science* **271** 776–7
[158] Hochstein S and Shapley R M 1976 Quantitative analysis of retinal ganglion cell classifications *J. Physiol.* **262** 237–64
[159] Hochstein S and Shapley R M 1976 Linear and nonlinear spatial subunits in Y cat retinal ganglion cells *J. Physiol.* **262** 265–84
[160] Holdefer R N and Norton T T 1995 Laminar organization of receptive field properties in the dorsal lateral geniculate nucleus of the tree shrew (*Tupaiaglis belangeri*) *J. Comput. Neurol.* **358** 401–13
[161] Hosokawa Y and Naka K-I 1985 Spontaneous membrane fluctuation in catfish type-N cells *Vis. Res.* **25** 539–42
[162] Hubel D H and Wiesel T N 1961 Integrative action in the cat's lateral geniculate body *J. Physiol.* **155** 385–98
[163] Humphrey A L and Saul A B 1992 Action of brain stem reticular afferents on lagged and nonlagged cells in the cat lateral geniculate nucleus *J. Neurophysiol.* **68** 673–91
[164] Humphrey A L, Sur M, Uhlrich D J and Sherman S M 1985 Termination patterns of individual X- and Y-cell axons in the visual cortex of the cat: projections to area 18, to the 17/18 border region, and to both areas 17 and 18 *J. Comput. Neurol.* **233** 190–212
[165] Humphrey A L and Weller R E 1988 Functionally distinct groups of X-cells in the lateral geniculate nucleus of the cat *J. Comput. Neurol.* **268** 429–47
[166] Humphrey A L and Weller R E 1988 Structural correlates of functionally distinct X-cells in the lateral geniculate nucleus of the cat *J. Comparative Neurol.* **268** 448–68
[167] Irvin G E, Casagrande V A and Norton T T 1993 Center/surround relationships of magnocellular, parvocellular and koniocellular relay cells in primate lateral geniculate nucleus *Vis. Neurosci.* **10** 363–73
[168] Jahnsen H and Llinás R 1984 Electrophysiological properties of guinea-pig thalamic neurons: an in vitro study *J. Physiol.* **349** 205–26
[169] Jahnsen H and Llinás R 1984 Ionic basis for the electroresponsiveness and oscillatory properties of guinea-pig thalamic neurons *in vitro J. Physiol.* **349** 227–47
[170] Jakiela H 1978 The effect of retinal image motion on the responsiveness of retinal ganglion cells in the cat *PhD Dissertation* Northwestern University, Evanston, IL
[171] Jones E G 1985 *The Thalamus* (New York: Plenum) p 935
[172] Kaneko A 1970 Physiological and morphological identification of horizontal, bipolar and amacrine cells in the goldfish retina *J. Physiol.* **207** 623–33
[173] Kaneko A 1971 Physiological studies of single retinal cells and their morphological identification *Vis. Res.* **3** 17–26
[174] Kaplan E, Lee B B and Shapley R M 1990 New views of primate retinal function *Progress in Retinal Research* vol 9, ed N Osborne and J Chader (Oxford: Pergamon) pp 273–336
[175] Kaplan E, Marcus S and So Y T 1979 Effects of dark adaptation on spatial and temporal properties of receptive fields in cat lateral geniculate nucleus *J. Physiol.* **294** 561–80
[176] Kaplan E, Purpura K and Shapley R M 1987 Contrast affects the transmission of visual information through the mammalian lateral geniculate nucleus *J. Physiol.* **391** 267–88
[177] Kaplan E and Shapley R M 1982 X and Y cells in the lateral geniculate nucleus of macaque monkeys *J. Physiol.* **330** 125–43
[178] Kaplan E and Shapley R M 1984 The origin of the S (slow) potential in the mammalian lateral geniculate nucleus *Exp. Brain Res.* **55** 111–6
[179] Kaplan E and Shapley R M 1986 The primate retina contains two types of ganglion cells, with high and low contrast sensitivity *Proc. Natl Acad. Sci., USA* **83** 2755–7
[180] Keener J P, Hoppensteadt F C and Rinzel J 1981 Integrate-and-fire models of nerve membrane response to oscillatory input *SIAM J. Appl. Math.* **41** 503–17
[181] Kelso J A S and Fuchs A 1995 Self-organizing dynamics of the human brain: critical instabilities and Šilnikov chaos *Chaos* **5** 64–9
[182] Kelly D H 1961 Visual responses to time-dependent stimuli. I. Amplitude sensitivity measurements *J. Opt. Soc. Am.* **51** 422–9
[183] Kelly D H 1971 Theory of flicker and transient responses. I. Uniform fields *J. Opt. Soc. Am.* **61** 537–46
[184] Kelly D H 1975 Luminous and chromatic flickering patterns have opposite effects *Science* **188** 371–2
[185] Kim U and McCormick D A 1998 The functional influence of burst and tonic firing mode on synaptic interactions in the thalamus *J. Neurosci.* **18** 9500–16

[186] Kjaer T W, Hertz J A and Richmond B J 1994 Decoding cortical neuronal signals: network models, information estimation and spatial tuning *J. Comput. Neurosci.* **1** 109–39
[187] Knight B W 1972 Dynamics of encoding in a population of neurons *J. Gen. Physiol.* **59** 734–66
[188] Knight B W 1972 The relationship between the firing rate of a single neuron and the level of activity in a population of neurons *J. Gen. Physiol.* **59** 767–78
[189] Knight B W, Brodie S E and Sirovich L 1979 Treatment of nerve impulse data for comparison with theory *Proc. Natl Acad. Sci., USA* **76** 6026–9
[190] Kolb H 1994 The architecture of functional neural circuits in the vertebrate retina *Invest. Ophth. Vis. Sci.* **35** 2385–403
[191] Kolb H 1970 Organization of the outer plexiform layer of the primate retina: electron microscopy of Golgi-impregnated cells *Phil. Trans. R. Soc.* B **258** 261–83
[192] Kolb H, Ahnelt P, Fisher S K, Linberg K A and Christian K 1989 Chromatic connectivity of the three horizontal cell types in the human retina *Invest. Ophth. Vis. Sci.* **30** 348
[193] Kolb H, Boycott B H and Dowling J E 1969 A second type of midget bipolar cell in the primate retina *Phil. Trans. R. Soc.* B **255** 177–84
[194] Kolb H and Dekorver L 1991 Midget ganglion cells of the parafovea of the human retina: a study by electron microscopy and serial section reconstructions *J. Comput. Neurol.* **303** 617–36
[195] Kolb H, Linberg K A and Fisher S K 1992 Neurons of the human retina: a Golgi study *J. Comput. Neurol.* **318** 147–87
[196] Kontsevich L L 1995 The nature of the inputs to cortical motion detectors *Vis. Res.* **35** 2785–93
[197] Korenberg M J, Sakai H M and Naka K-I 1989 Dissection of the neuron network in the catfish inner retina. III. Interpretation of spike kernels *J. Neurophysiol.* **61** 1110–20
[198] Kouyama N and Marshak D W 1992 Bipolar cells specific for blue cones in the macaque retina *J. Neurosci.* **12** 1233–52
[199] Krauskopf J 1980 Discrimination and detection of changes in luminance *Vis. Res.* **20** 671–7
[200] Krausz H and Naka K-I 1980 Spatiotemporal testing and modelling of catfish retinal neurons *Biophys. J.* **29** 13–36
[201] Lankheet M J M, Lennie P and Krauskopf J 1998 Distinctive characteristics of subclasses of red–green P-cells in the LGN of macaque *Vis. Neurosci.* **15** 37–46
[202] Lankheet M J M, Lennie P and Krauskopf J 1998 Temporal-chromatic interactions in LGN P-cells *Vis. Neurosci.* **15** 47–54
[203] Lankheet M J M, Przybyszewski A W and van de Grind W A 1993 The lateral spread of light adaptation in cat horizontal cell responses *Vis. Res.* **33** 1173–84
[204] Lasansky A 1992 Properties of depolarizing bipolar cell responses to central illumination in salamander slices *Brain Res.* **576** 181–96
[205] Lasater E M 1988 Membrane currents of retinal bipolar cells in culture *J. Neurophysiol.* **60** 1460–80
[206] Lee B B 1996 Receptive field structure in the primate retina *Vis. Res.* **36** 631–44
[207] Lee B B, Martin P R and Valberg A 1989 Sensitivity of macaque retinal ganglion cells to chromatic and luminance flicker *J. Physiol.* **414** 223–43
[208] Lee B B, Martin P R and Valberg A 1989 Nonlinear summation of M- and L-cone inputs to phasic retinal ganglion cells of the macaque *J. Neurosci.* **9** 1433–42
[209] Lee B B, Silveira L C, Yamada E and Kremers J 1996 Parallel pathways in the retina of Old and New World primates *Rev. Bras. Biol.* **56** 323–38
[210] Lee B B and Yeh T 1998 Receptive fields of primate retinal ganglion cells studied with a novel technique *Vis. Neurosci.* **15** 161–75
[211] Legendy C R and Salcman M 1985 Bursts and recurrences of bursts in the spike trains of spontaneously active striate cortex neurons *J. Neurophysiol.* **53** 926–39
[212] Lennie P, Haake P W and Williams D R 1991 The design of chromatically opponent receptive fields *Computational Models of Vis. Processing* ed M S Landy and J A Movshon (Cambridge, MA: MIT) pp 71–82
[213] Lestienne R 1996 Determination of the precision of spike timing in the visual cortex of anaesthetised cats *Biol. Cybern.* **74** 55–61
[214] LeVay S and Gilbert C D 1976 Laminar patterns of geniculocortical projection in the cat *Brain Res.* **113** 1–19
[215] LeVay S and McConnell S K 1982 ON and OFF layers in the lateral geniculate nucleus of the mink *Nature* **300** 350–1
[216] Levi D M, Klein S A and Aitsebaomo A P 1985 Vernier acuity, crowding and cortical magnification *Vis. Res.* **25** 963–77
[217] Levine M W 1991 The distribution of the intervals between neural impulses in the maintained discharges of retinal ganglion cells *Biol. Cybern.* **65** 459–67

[218] Levine M W 1992 Modelling the variability of firing rate of retinal ganglion cells *Math. Biosci.* **112** 225–42
[219] Levine M W and Troy J B 1986 The variability of the maintained discharge of cat dorsal lateral geniculate cells *J. Physiol.* **375** 339–59
[220] Lisman J E 1997 Bursts as a unit of neural information: making unreliable synapses reliable *Trends Neurosci.* **20** 38–43
[221] Livingstone M S and Hubel D H 1987 Psychophysical evidence for separate channels for the perception of form, colour, movement and depth *J. Neurosci.* **7** 3416–68
[222] Lovegrove W J, Garzia R P and Nicholson S B 1990 Experimental evidence for a transient system deficit in specific reading disability *J. Am. Optom. Assoc.* **61** 137–46
[223] Lund J S 1988 Anatomical organization of macaque monkey striate visual cortex *Ann. Rev. Neurosci.* **11** 253–88
[224] Maass W 1998 A simple model for neural computation with firing rates and firing correlations *Network: Comput. Neural Syst.* **9** 381–97
[225] MacKay D and McCulloch W S 1952 The limiting information capacity of a neuronal link *Bull. Math. Biophys.* **14** 127–35
[226] Mainen Z and Sejnowski T J 1995 Reliability of spike timing in neocortical neurons *Science* **268** 1503–6
[227] Malach R 1992 Dendritic sampling across processing streams in monkey striate cortex *J. Comparative Neurology* **315** 303–12
[228] Mangel S C 1991 Analysis of horizontal cell contribution to the receptive field surround of ganglion cells in the rabbit retina *J. Physiol.* **442** 211–34
[229] Mao B, MacLeish P R and Victor J D 1996 Voltage-dependent potassium current is sufficient for the changes in gain and dynamics of isolated retinal bipolar cells of the tiger salamander *Invest. Ophth. Vis. Sci.* **37** 1054 (abstract)
[230] Mao B, MacLeish P R and Victor J D 1998 The intrinsic dynamics of retinal bipolar cells isolated from tiger salamander *Vis. Neurosci.* **15** 425–38
[231] Marchiafava P L and Torre V 1978 The responses of amacrine cells to light and intracellularly applied currents *J. Physiol.* **276** 83–102
[232] Mariani A P 1984 Bioplar cells in monkey retina selective for the cones likely to be blue-sensitive *Nature* **308** 184–6
[233] Mariani A P 1990 Amacrine cells of the rhesus monkey retina *J. Comput. Neurol.* **301** 382–400
[234] Marmarelis P Z and Marmarelis V Z 1978 *Analysis of Physiological Systems: The White-Noise Approach* (New York: Plenum)
[235] Marmarelis P Z and Naka K-I 1972 Spatial distribution of potential in a flat cell: application to the horizontal cell layers *Biophys. J.* **12** 1515–32
[236] Marmarelis P Z and Naka K-I 1973 Nonlinear analysis and synthesis of receptive field responses in the catfish retina II. One-input white noise analysis *J. Neurophysiol.* **36** 619–33
[237] Martin P R, White A J, Goodchild A K, Wilder H D and Sefton A E 1997 Evidence that blue-on cells are part of the third geniculocortical pathway in primates *Eur. J. Neurosci.* **9** 1536–41
[238] Masland R H 1988 Amacrine cells *Trends Neurosci.* **11** 405–10
[239] Masland R H and Tauchi M 1986 The cholinergic amacrine cell *Trends Neurosci.* **9** 218–23
[240] Mast J and Victor J D 1991 Fluctuations of steady-state VEP's: interaction of driven evoked potentials and the EEG *Electroencephalogr. Clin. Neurophysiol.* **78** 389–401
[241] Mastronarde D N 1983 Interactions between ganglion cells in cat retina *J. Neurophysiol.* **49** 350–65
[242] Mastronarde D N 1987 Two classes of single-input X-cells in cat lateral geniculate nucleus. I. Receptive-field properties and classification of cells *J. Neurophysiol.* **57** 357–80
[243] Mastronarde D N 1987 Two classes of single-input X-cells in cat lateral geniculate nucleus. II. Retinal inputs and the generation of receptive-field properties *J. Neurophysiol.* **57** 381–413
[244] Mastronarde D N, Humphrey A L and Saul A B 1991 Lagged Y cells in the cat lateral geniculate nucleus *Vis. Neurosci.* **7** 191–200
[245] McClurkin J W, Optican L M and Richmond B J 1994 Cortical feedback increases visual information transmitted by monkey parvocellular lateral geniculate neurons *Vis. Neurosci.* **11** 601–17
[246] McClurkin J W, Optican L M, Richmond BJ and Gawne T J 1991 Concurrent processing and complexity of temporally coded messages in visual perception *Science* **253** 675–7
[247] McCormick D A 1989 Cholinergic and noradrenergic modulation of thalamocortical processing *Trends Neurosci.* **12** 215–21
[248] McCormick D A and Huguenard J R 1992 A model of the electrophysiological properties of thalamocortical relay neurons *J. Neurophysiol.* **68** 1384–400
[249] McIlwain J T 1964 Receptive fields of optic tract axons and lateral geniculate cells: peripheral extent and barbiturate sensitivity *J. Neurophysiol.* **27** 1154–73

[250] Meister M 1996 Multineuronal codes in retinal signalling *Proc. Natl Acad. Sci., USA* **93** 609–14
[251] Meister M and Berry M J 1998 The neural code of the retina *Neuron* submitted
[252] Meister M, Lagnado L and Baylor D A 1995 Concerted signalling by retinal ganglion cells *Science* **270** 1207–10
[253] Menger N, Pow D V and Wässle H 1998 Glycinergic amacrine cells of the rat retina *J. Comparative Neurol.* **401** 34–46
[254] Middlebrooks J C, Clock A E, Xu L and Green D M 1994 A panoramic code for sound location by cortical neurons *Science* **264** 842–4
[255] Miller G A 1955 Note on the bias on information estimates *Information Theory in Psychology; Problems and Methods* **II-B** 95–100
[256] Mills S L and Massey S C 1995 Differential properties of two gap junctional pathways made by AII amacrine cells *Nature* **377** 734–7
[257] Miltner W H R, Braun C, Arnold M, Witte H and Taub E 1999 Coherence of gamma-band EEG activity as a basis for associative learning *Nature* **397** 434–6
[258] Molenaar J, van de Grind W A and Eckhorn R 1983 Dynamic properties of cat horizontal cell light responses *Vis. Res.* **23** 257–66
[259] Mukherjee P 1994 The dynamics of neurons in the cat lateral geniculate nucleus: a model system for computational neuroscience *Thesis* The Rockefeller University, New York
[260] Mukherjee P and Kaplan E 1995 Dynamics of neurons in the cat lateral geniculate nucleus: *in vivo* electrophysiology and computational modelling *J. Neurophysiol.* **74** 1222–43
[261] Murphy P C and Sillito A M 1996 Functional morphology of the feedback pathway from area 17 of the cat visual cortex to the lateral geniculate nucleus *J. Neurosci.* **16** 1180–92
[262] Murray I J, Parry N R A, Carden D and Kulikowski J J 1987 Human visual evoked potentials to chromatic and achromatic gratings *Clin. Vis. Sci.* **1** 231–44
[263] Murthy A, Humphrey A L, Saul A B and Feidler J C 1998 Laminar differences in the spatiotemporal structure of simple cell receptive fields in cat area 17 *Vis. Neurosci.* **15** 239–56
[264] Naka K-I, Marmarelis P Z and Chan R Y 1975 Morphological and functional identifications of catfish retinal neurons. III. Functional identification *J. Neurophysiol.* **38** 92–131
[265] Naka K-I and Rushton W A H 1966 S-potentials from colour units in the retina of fish (Cyprinidae) *J. Physiol.* **195** 536–55
[266] Naka K-I, Sakai H M and Ishii N 1988 Generation and transformation of second-order nonlinearity in catfish retina *Ann. Biomed. Engng* **16** 53–64
[267] Nakatani K and Yau K-W 1988 Calcium and light adaptation in retinal rods and cones *Nature* **334** 69–71
[268] Nakayama K 1985 Biological image motion processing: a review *Vis. Res.* **25** 625–60
[269] Nealey T A and Maunsell J H R 1994 Magnocellular and parvocellular contributions to the responses of neurons in macaque striate cortex *J. Neurosci.* **14** 2069–79
[270] Nelson R 1977 Cat cones have rod input: a comprison of response properties of cones and horizontal cell bodies in the retina of the cat *J. Comput. Neurol.* **172** 109–36
[271] Nelson R 1982 AII amacrine cells quicken time course of rod signals in the cat retina *J. Neurophysiol.* **47** 928–47
[272] Nelson R, Famiglietti E V Jr and Kolb H 1978 Intracellular staining reveals different levels of stratification for on- and off-centre ganglion cells in cat retina *J. Neurophysiol.* **41** 472–83
[273] Nelson R and Kolb H 1985 A17: A broad-field amacrine cell in the rod system of the cat retina *J. Neurophysiol.* **54** 592–614
[274] Nelson R, Kolb H, Famiglietti E V and Gouras P 1976 Neural responses in the rod and cone systems of the cat retina: Intra-cellular records and procion stains *Invest. Ophth. Vis. Sci.* **15** 946–53
[275] Neuenschwander S, Castelo-Branco M and Singer W 1999 Synchronous oscillations in the cat retina *Vis. Res.* **39** 2485–97
[276] Newsome W T, Britten K H and Movshon J A 1989 Neuronal correlates of a perceptual decision *Nature* **341** 52–4
[277] Normann R A and Perlman I 1979 The effects of background illumination on the photoresponses of red and green cones *J. Physiol.* **286** 491–507
[278] Normann R A and Werblin F S 1974 Control of retinal sensitivity: I. Light and dark adaptation of vertebrate rods and cones *J. Gen. Physiol.* **63** 37–61
[279] Norton T T and Casagrande V A 1982 Laminar organization of receptive-field properties in lateral geniculate nucleus of bush baby (*Galago crassicaudatus*) *J. Neurophysiol.* **47** 715–41
[280] Ohzawa I, Sclar G and Freeman R D 1985 Contrast gain control in the cat's visual system *J. Neurophysiol.* **54** 651–67
[281] Optican L M, Gawne T J, Richmond B J and Joseph P J 1991 Unbiased measures of transmitted information

and channel capacity from multivariate neuronal data *Biol. Cybern.* **65** 305–10
[282] Optican L M and Richmond B J 1987 Temporal encoding of two-dimensional patterns by single units in primate inferior temporal cortex. III. Information theoretic analysis *J. Neurophysiol.* **57** 162–78
[283] Overbeck C J 1978 *Am. J. Phys.* **46** 323
[284] Pan Z H and Slaughter M M 1991 Control of retinal information coding by $GABA_B$ receptors *J. Neurosci.* **11** 1810–21
[285] Panzeri S and Treves A 1996 Analytical estimates of limited sampling biases in different information measures *Network* **7** 87–107
[286] Passaglia C, Dodge F, Herzog E, Jackson S and Barlow R 1997 Deciphering a neural code for vision *Proc. Natl Acad. Sci., USA* **94** 12 649–54
[287] Perkel D H, Gerstein G L and Moore G P 1967 Neuronal spike trains and stochastic point processes. I. The single spike train *Biophys. J.* **7** 391–418
[288] Perkel D H, Gerstein G L and Moore G P 1967 Neuronal spike trains and stochastic point processes. II. Simultaneous spike trains *Biophys. J.* **7** 419–40
[289] Perlman I, Normann R A, Itzhaki A and Daly S J 1985 Chromatic and spatial information processing by red cones and L-type horizontal cells in the turtle retina *Vis. Res.* **25** 543–9
[290] Peskin C S, Tranchina D and Hull D M 1984 How to see in the dark: photon noise in vision and nuclear medicine *Ann. NY Acad. Sci.* **435** 48–72
[291] Polyak S L 1941 *The Retina* (Chicago, IL: Chicago University Press)
[292] Posner M I and Petersen S E 1990 The attention system of the human brain *Ann. Rev. Neurosci.* **13** 25–42
[293] Purpura K, Kaplan E and Shapley R M 1988 Background light and contrast gain of primate P and M retinal ganglion cells *Proc. Natl Acad. Sci., USA* **85** 4534–7
[294] Purpura K P and Schiff N D 1997 The thalamic intralaminar nuclei: a role in visual awareness *Neuroscientist* **3** 314–21
[295] Rabin J, Switkes E, Crognale M, Schneck M E and Adams A J 1994 Visual evoked potentials in three-dimensional colour space: correlates of spatio-chromatic processing *Vis. Res.* **34** 2657–71
[296] Rakic P 1977 Genesis of the dorsal lateral geniculate nucleus in the monkey *J. Comput. Neurol.* **176** 23–52
[297] Rapp P E, Zimmerman I D, Vining E P, Cohen N, Albano A M and Jiménez-Montaño M A 1994 The algorithmic complexity of neural spike trains increases during focal seizures *J. Neurosci.* **14** 4731–9
[298] Ratliff F, Knight B W and Milkman N 1970 Superposition of excitatory and inhibitory influences in the retina of Limulus: effect of delayed inhibition *Proc. Natl Acad. Sci., USA* **67** 1558–64
[299] Regan D 1973 Evoked potentials specific to spatial patterns of luminance and colour *Vis. Res.* **13** 1933–41
[300] Regan D and He P 1996 Magnetic and electrical brain responses to chromatic contrast in human *Vis. Res.* **36** 1–18
[301] Reich D S, Victor J D, Knight B W, Ozaki T and Kaplan E 1997 Response variability and timing precision of neuronal spike trains *in vivo J. Neurophysiol.* **77** 2836–41
[302] Reich D S, Victor J D and Knight B W 1998 The power ratio and the interval map: spiking models and extracellular data *J. Neurosci.* **18** 10 090–104
[303] Reichardt W 1961 Autocorrelation, a principle for the evaluation of sensory information by the central nervous system *Sensory Communication* ed W A Rosenblith (New York: Wiley) pp 303–17
[304] Reid R C and Alonso J M 1996 The processing and encoding of information in the visual cortex *Curr. Opin. Neurobiol.* **6** 475–80
[305] Reid R C, Alonso J M and Hendry S H C 1997 S-cone input is relayed to visual cortex from two koniocellular layers of macaque LGN *Soc. Neurosci. Abstracts* **23** 13
[306] Reid R C and Shapley R M 1992 Spatial structure of cone inputs to receptive fields in primate lateral geniculate nucleus *Nature* **356** 716–8
[307] Reid R C, Soodak R E and Shapley R M 1987 Linear mechanisms of directional selectivity in simple cells of cat striate cortex *Proc. Natl Acad. Sci., USA* **84** 8740–4
[308] Reid R C, Soodak R E and Shapley R M 1991 Directional selectivity and spatiotemporal structure of receptive fields of simple cells in cat striate cortex *J. Neurophysiol.* **66** 505–29
[309] Reinagel P, Godwin D, Sherman S M and Koch C 1999 Encoding of visual information by LGN bursts *J. Neurophysiol.* **81** 2558–69
[310] Rentschler I and Treutwein B 1985 Loss of spatial phase relationships in extrafoveal vision *Nature* **313** 308–10
[311] Richmond B J and Optican L M 1992 Structure and interpretation of neuronal codes in the visual system *Neural Networks for Perception* vol 1, ed H Wechsler (New York: Academic) pp 105–20
[312] Rieke F, Warland D, de Ruyter van Steveninck R R and Bialek W 1997 *Spikes: Exploring the Neural Code* (Cambridge, MA: MIT) p 394
[313] Riehle A, Grün S, Diesmann M and Aertsen A M H J 1997 Spike synchronization and rate modulation

differentially involved in motor cortical function *Science* **278** 1950–3
[314] Robson J G and Troy J B 1987 Nature of the maintained discharge of Q, X and Y retinal ganglion cells of the cat *J. Opt. Soc. Am.* A **4** 2301–7
[315] Rodieck R W and Brening R K 1983 Retinal ganglion cells: Properties, types, genera, pathways and cross-species comparisons *Brain Behav. Evol.* **23** 121–64
[316] Rodriguez E, George N, Lachaux J-P, Marinerie M, Renault B and Varela F 1999 Perception's long shadow: long-distance synchronization of human brain activity *Nature* **397** 430–3
[317] Roelfsema P R, Konig P, Engel A K, Sireteanu R and Singer W 1994 Reduced synchronization in the visual cortex of cats with strabismic amblyopia *Eur. J. Neurosci.* **6** 1645–55
[318] Rohaly A M and Buchsbaum G 1988 Inference of global spatiochromatic mechanisms from contrast sensitivity functions *J. Opt. Soc. Am.* A **5** 572–6
[319] Rowe M H and Cox J F 1993 Spatial receptive-field structure of cat retinal W cells *Vis. Neurosci.* **10** 765–79
[320] de Ruyter van Steveninck R R and Laughlin S B 1996 The rate of information transfer at graded-potential synapses *Nature* **379** 642–5
[321] de Ruyter van Steveninck R R, Lewen G D, Strong S P, Koberle R and Bialek W 1997 Reproducibility and variability in neural spike trains *Science* **275** 1805–8
[322] Sakai H M and Naka K-I 1987 *Neuron Network in Catfish Retina: 1968–1987 (Progress in Retinal Research vol 7)* ed N Osborne and G Chader (Oxford: Pergamon) pp 149–208
[323] Sakai H M and Naka K-I 1990 Dissection of the neuron network in the catfish inner retina. V. Interactions between NA and NB amacrine cells *J. Neurophysiol.* **63** 120–30
[324] Sakai H M, Machuca H and Naka K-I 1997 Processing of colour- and noncolour-coded signals in the gourami retina I: Horizontal cells *J. Neurophysiol.* **78** 2002–17
[325] Sakuranaga M and Naka K-I 1985 Signal transmission in the catfish retina. I. Transmission in the outer retina *J. Neurophysiol.* **53** 373–89
[326] Sakuranaga M and Naka K-I 1985 Signal transmission in the catfish retina. II. Transmission to type-N cell *J. Neurophysiol.* **53** 390–410
[327] Sakuranaga M and Naka K-I 1985 Signal transmission in the catfish retina. III. Transmission to type-C cell *J. Neurophysiol.* **53** 411–28
[328] Sankeralli M J and Mullen K T 1997 Postreceptoral chromatic detection mechanisms revealed by noise masking in three-dimensional cone contrast space *J. Opt. Soc. Am.* A **14** 2633–46
[329] Saul A B and Humphrey A L 1990 Spatial and temporal response properties of lagged and nonlagged cells in cat lateral geniculate nucleus *J. Neurophysiol.* **64** 206–24
[330] Saul A B and Humphrey A L 1992 Temporal-frequency tuning of direction selectivity in cat visual cortex *Vis. Neurosci.* **8** 365–72
[331] Schiff N D, Purpura K P and Victor J D 1999 Gating of local network signals appears as stimulus-dependent activity envelopes in striate cortex *J. Neurophysiol.* accepted for publication
[332] Schnapf J L, Nunn B J, Meister M and Baylor D A 1990 Visual transduction in cones of the monkey *Macaca fascicularis J. Physiol.* **390** 145–60
[333] Schnapf J L, Kraft T W and Baylor D A 1987 Spectral sensitivity of human cone photoreceptors *Nature* **325** 439–41
[334] Schiller P H 1992 The ON and OFF channels of the visual system *Trends Neurosci.* **15** 86–92
[335] Schiller P H, Logothetis N K and Charles E R 1990 Functions of the colour-opponent and broad-band channels of the visual system *Nature* **343** 68–70
[336] Schiller P H and Logothetis N K 1990 The colour-opponent and broad-band channels of the primate visual system *Trends Neurosci.* **13** 392–8
[337] Schiller P H, Sandell J H and Maunsell J H R 1986 Functions of the ON and OFF channels of the visual system *Nature* **322** 824–5
[338] Sclar G 1987 Expression of 'retinal' contrast gain control by neurons of the cat's lateral geniculate nucleus *Exp. Brain Res.* **66** 589–96
[339] Schmolesky M T, Wang Y, Hanes D P, Thompson K G, Leutgeb S, Schall J D and Leventhal A G 1998 Signal timing across the macaque visual system *J. Neurophysiol.* **79** 3272–8
[340] Sejnowski T 1997 The year of the dendrite *Science* **275** 178–9
[341] Sen K, Jorge-Rivera J C, Marder E and Abbott L F 1996 Decoding synapses *J. Neurosci.* **16** 6307–18
[342] Shadlen M N, Britten K H, Newsome W T and Movshon J A 1996 A computational analysis of the relationship between neuronal and behavioural responses to visual motion *J. Neurosci.* **16** 1486–510
[343] Shadlen M N and Newsome W T 1998 The variable discharge of cortical neurons: implications for connectivity, computation and information coding *J. Neurosci.* **18** 3870–96
[344] Shannon C E and Weaver W 1949 *The Mathematical Theory of Communication* (Urbana, IL:

University of Illinois Press)
[345] Shapley R M 1971 Fluctuations of the impulse rate in Limulus eccentric cells *J. Gen. Physiol.* **57** 539–56
[346] Shapley R and Enroth-Cugell C 1984 Visual adaptation and retinal gain controls *Progress in Retinal Research* vol 3, ed N Osborne and G Chader (Oxford: Pergamon) pp 263–346
[347] Shapley R M and Gordon J 1978 The eel retina. Ganglion cell classes and spatial mechanisms *J. Gen. Physiol.* **71** 139–55
[348] Shapley R and Perry V H 1986 Cat and monkey retinal ganglion cells and their functional roles *Trends Neurosci.* **9** 229–35
[349] Shapley R and Victor J D 1978 The effect of contrast on the transfer properties of cat retinal ganglion cells *J. Physiol.* **285** 275–98
[350] Shapley R and Victor J D 1979 Nonlinear spatial summation and the contrast gain control of cat retinal ganglion cells *J. Physiol.* **290** 141–61
[351] Shapley R and Victor J D 1981 How the contrast gain control modifies the frequency response of cat retinal ganglion cells *J. Physiol.* **318** 161–79
[352] Sherman S M 1996 Dual response modes in lateral geniculate neurons: mechanisms and functions *Vis. Neurosci.* **13** 205–13
[353] Shiells R and Falk G 1995 Signal transduction in retinal bipolar cells *Prog. Retinal Eye Res.* **14** 223–47
[354] Shipp S 1995 Visual processing. The odd couple *Curr. Biol.* **5** 116–9
[355] Sillito A M, Jones H E, Gerstein G L and West D C 1994 Feature-linked synchronization of thalamic relay cell firing induced by feedback from the visual cortex *Nature* **369** 479–82
[356] Singer W 1977 Control of thalamic transmission by corticofugal and ascending reticular pathways in the visual system *Physiol. Rev.* **57** 386–420
[357] Singer W and Gray C M 1995 Visual feature integration and the temporal correlation hypothesis *Ann. Rev. Neurosci.* **18** 555–86
[358] Sirovich L and Knight B W 1986 Characteristic patterns of an inhomogeneous imaging system with an application to vision *J. Opt. Soc. Am.* A **3** 358–64
[359] Sirovich L, Knight B W and Omurtag A 1999 Dynamics of neuronal populations: the equilibrium solution *SIAM J. Appl. Math.* accepted for publication
[360] Smith R G and Vardi N 1995 Simulation of the AII amacrine cell of mammalian retina: functional consequences of electrical coupling and regenerative membrane properties *Vis. Neurosci.* **12** 851–60
[361] Smith V C, Lee B B, Pokorny J, Martin P R and Valberg A 1992 Responses of macaque ganglion cells to the relative phase of heterochromatically modulated lights *J. Physiol.* **458** 191–221
[362] Smith V C and Pokorny J 1975 Spectral sensitivity of the foveal cone photopigments between 400 and 500 nm *Vis. Res.* **15** 161–71
[363] Snider R K, Kabara J F, Roig B R and Bonds A B 1998 Burst firing and modulation of functional connectivity in cat striate cortex *J. Neurophysiol.* **80** 730–44
[364] So Y T and Shapley R 1979 Spatial properties of X and Y cells in the lateral geniculate nucleus of the cat and conduction velocities of their inputs *Exp. Brain Res.* **36** 533–50
[365] So Y T and Shapley R 1981 Spatial tuning of cells in and around lateral geniculate nucleus of the cat: X and Y relay cells and perigeniculate interneurons *J. Neurophysiol.* **45** 107–20
[366] Solomon S G, White A J R, Grünert U and Martin P R 1998 Temporal contrast sensitivity of koniocellular pathway cells in the primate visual system *Soc. Neurosci. Abstracts* **24** 140
[367] Sompolinsky H and Shapley R 1997 New perspectives on the mechanisms for orientation selectivity *Curr. Opin. Neurobiol.* **7** 514–22
[368] Soodak R, Shapley R M and Kaplan E 1987 Linear mechanism of orientation tuning in the retina and lateral geniculate nucleus of the cat *J. Neurophysiol.* **58** 267–75
[369] Spekreijse H and Oosting J 1970 A method for analysing and synthesizing nonlinear systems *Kybernetik* **7** 23–31
[370] Srinivasan M V, Laughlin S B and Dubs A 1982 Predictive coding: a fresh view of inhibition in the retina *Proc. R. Soc.* B **216** 427–59
[371] Stafford D K and Dacey D M 1997 Physiology of the A1 amacrine: a spiking, axon-bearing interneuron of the macaque monkey retina *Vis. Neurosci.* **14** 507–22
[372] Stanford L R, Friedlander M J and Sherman S M 1981 Morphology of physiologically identified W-cells in the C laminae of the cat's lateral geniculate nucleus *J. Neurosci.* **1** 578–84
[373] Stein R H 1969 The information capacity of nerve cells using a frequency code *Biophys. J.* **7** 797–826
[374] Steinberg R H 1969 Rod and cone contributions to S-potentials from the cat retina *Vis. Res.* **9** 1319–29
[375] Steriade M and Llinás R 1988 The functional states of the thalamus and the associated neuronal interplay *Physiol. Rev.* **68** 649–742

[376] Sterling P 1983 Microcircuitry of the cat retina *Ann. Rev. Neurosci.* **6** 149–85
[377] Stockman A, MacLeod D I A and Lebrun S J 1993 Faster than the eye can see: blue cones respond to rapid flicker *J. Opt. Soc. Am.* A **10** 1396–402
[378] Stone C and Pinto L H 1993 Response properties of ganglion cells in the isolated mouse retina *Vis. Neurosci.* **10** 31–9
[379] Stone J and Fukuda Y 1974 Properties of cat retinal ganglion cells: a comparison of W cells with X and Y cells *J. Neurophysiol.* **37** 722–48
[380] Stone S L 1994 White noise analysis of a chromatic type horizontal cell in the Xenopus retina *J. Gen. Physiol.* **103** 991–1017
[381] Stryker M P and Zahs K R 1983 On and off sublaminae in the lateral geniculate nucleus of the ferret *J. Neurosci.* **3** 1943–51
[382] Tallon C, Bertrand O, Bouchet P and Pernier J 1995 Gamma-range activity evoked by coherent visual stimuli in humans *Eur. J. Neurosci.* **7** 1285–91
[383] Tallon-Baudry C, Bertrand O, Delpuech C and Pernier J 1996 Stimulus specificity of phase-locked and non-phase-locked 40 Hz visual responses in humans *J. Neurosci.* **16** 4240–9
[384] Theiler J and Rapp P E 1996 Reexamination of the evidence for low-dimensional, nonlinear structure in the human electroencephalogram *Electroencephalogr. Clin. Neurophysiol.* **98** 213–22
[385] Theunissen F and Miller J P 1995 Temporal encoding in nervous systems: a rigorous definition *J. Comput. Neurosci.* **2** 149–62
[386] Thibos L N and Werblin F S 1978 The properties of surround antagonism elicited by spinning windmill patterns in the mudpuppy retina *J. Physiol.* **278** 101–16
[387] Thomson A M 1997 More than just frequency detectors? *Science* **275** 179–80
[388] Tian N and Slaughter M M 1995 Functional properties of a metabotropic glutamate receptor at dendritic synapses of on-bipolar cells in the amphibian retina *Vis. Neurosci.* **12** 755–65
[389] Tolhurst D J, Movshon J A and Dean A F 1983 The statistical reliability of signals in single neurons in cat and monkey visual cortex *Vis. Res.* **8** 775–85
[390] Torre V and Poggio T 1978 A synaptic mechanism possibly underlying directdional selectivity to motion *Proc. R. Soc.* B **202** 409–16
[391] Toyoda J-I 1974 Frequency characteristics of retinal neurons in the carp *J. Gen. Physiol.* **63** 214–34
[392] Toyoda J-I, Hashimoto H and Ohtsu K 1973 Bipolar-amacrine transmission in the carp retina *Vis. Res.* **13** 295–307
[393] Tranchina D, Gordon J, Shapley R and Toyoda J-I 1981 Linear information processing in the retina: a study of horizontal cell responses *Proc. Natl Acad. Sci., USA* **78** 6540–2
[394] Tranchina D, Gordon J and Shapley R 1983 Spatial and temporal properties of luminosity horizontal cells in the turtle retina *J. Gen. Physiol.* **82** 573–98
[395] Tranchina D, Gordon J and Shapley R 1984 Retinal light adaptation—evidence for a feedback mechanism *Nature* **310** 314–16
[396] Treves A and Panzeri S 1995 The upward bias in measures of information derived from limited data samples *Neural Comput.* **7** 399–407
[397] Troy J B 1983 Spatio-temporal interaction in neurones of the cat's dorsal lateral geniculate nucleus *J. Physiol.* **344** 419–32
[398] Troy J B and Robson J G 1992 Steady discharges of X and Y retinal ganglion cells of cat under photopic illuminance *Vis. Neurosci.* **9** 535–53
[399] Tuttle J R and Scott L C 1979 X-like and Y-like ganglion cells in the *Necturus* retina *Invest. Ophth. Vis. Sci.* **18** 524–7
[400] Tyler C W, Chan H and Liu L 1992 Different spatial tunings for ON and OFF pathway stimulation *Ophth. Physiol. Opt.* **12** 233–40
[401] Uhlrich D J, Cucchiaro J B, Humphrey A L and Sherman S M 1991 Morphology and axonal projection patterns of individual neurons in the cat perigeniculate nucleus *J. Neurophysiol.* **65** 1528–41
[402] Ungerleider L G and Mishkin M 1982 Two cortical visual systems *Analysis of Visual Behaviour* ed D J Ingle *et al* (Cambridge, MA: MIT) pp 549–86
[403] Usrey W M, Reppas J B and Reid R C 1997 Paired-pulse interactions between retina and thalamus *Neurosci. Abstracts* **23** 170
[404] Usrey W M and Reid R C 1999 Synchronous activity in the visual system *Ann. Rev. Physiol.* **61** 435–56
[405] van Santen J P H and Sperling G 1984 Temporal covariance model of human motion perception *J. Opt. Soc. Am.* A **1** 451–73
[406] Vardi N and Smith R G 1996 The AII amacrine network: coupling can increase correlated activity *Vis. Res.* **36** 3743–57

[407] Vardi N, Morigiwa K, Wang T L, Shi Y J and Sterling P 1998 Neurochemistry of the mammalian cone 'synaptic complex' *Vis. Res.* **38** 1359–69
[408] Victor J D 1979 Nonlinear systems analysis: comparison of white noise and sum of sinusoids in a biological system *Proc. Natl Acad. Sci., USA* **76** 996–8
[409] Victor J D 1987 The dynamics of the cat retinal X cell centre *J. Physiol.* **386** 219–46
[410] Victor J D 1988 The dynamics of the cat retinal Y cell subunit *J. Physiol.* **405** 289–320
[411] Victor J D and Conte M M 1988 Dynamics and summation within the cat retinal X-cell surround *Invest. Ophth. Vis. Sci.* **29** 294
[412] Victor J D and Knight B 1979 Nonlinear analysis with an arbitrary stimulus ensemble *Q. Appl. Math.* **37** 113–36
[413] Victor J D and Purpura K 1994 A new approach to the analysis of spike discharges: cost-based metrics *Soc. Neurosci. Abstracts* **20** 315
[414] Victor J D and Purpura K 1996 Nature and precision of temporal coding in visual cortex: a metric-space analysis *J. Neurophysiol.* **76** 1310–26
[415] Victor J D and Purpura K 1997 Metric-space analysis of spike trains: theory, algorithms and application *Network* **8** 127–64
[416] Victor J D and Purpura K P 1998 Spatial phase and the temporal structure of the response to gratings in V1 *J. Neurophysiol.* **80** 554–71
[417] Victor J D and Shapley R 1979 Receptive field mechanisms of cat X and Y retinal ganglion cells *J. Gen. Physiol.* **74** 275–98
[418] Victor J D and Shapley R 1979 The nonlinear pathway of Y ganglion cells in the cat retina *J. Gen. Physiol.* **74** 671–89
[419] Victor J D and Shapley R 1980 A method of nonlinear analysis in the frequency domain *Biophys. J.* **29** 459–84
[420] Viviani P 1990 Eye movements in visual search: cognitive, perceptual and motor aspects *Eye Movements and their Role in Visual and Cognitive Processes* ed E Kowler (Amsterdam: Elsevier) pp 353–93
[421] von der Marlsburg C and Bienenstock E 1986 A neural network for the retrieval of superimposed connectin patterns *Disordered Systems and Biological Organization* ed F Fogelman *et al* (Berlin: Springer)
[422] Wandell B 1995 *Foundations of Vision* (Sunderland, MA: Sinauer Associates)
[423] Warland D K, Reinagel P and Meister M 1997 Decoding visual information from a population of retinal ganglion cells *J. Neurophysiol.* **78** 2336–50
[424] Wässle H 1997 Diversity of the directional selective circuitry of the mammalian retina *Boden Conf. (Thredbo, Australia)*
[425] Wässle H and Boycott B B 1991 Functional architecture of the mammalian retina *Physiol. Rev.* **71** 447–80
[426] Wässle H, Boycott B B and Röhrenbeck J 1989 Horizontal cells in the monkey retina: cone connections and dendritic network *Eur. J. Neurosci.* **1** 421–35
[427] Wässle H, Grünert U, Martin P and Boycott B B 1994 Immunocytochemical characterization and spatial distribution of midget bipolar cells in the macaque monkey retina *Vis. Res.* **34** 561–79
[428] Wässle H, Grünert U, Chun M H and Boycott B B 1995 The rod pathway of the macaque monkey retina: identification of AII-amacrine cells with antibodies against calretinin *J. Comput. Neurol.* **361** 537–51
[429] Wässle H, Yamashita M, Greferath U, Grünert U and Müller F 1991 The rod bipolar cell of the mammalian retina *Vis. Neurosci.* **7** 99–112
[430] Werblin F S 1971 Adaptation in a vertebrate retina: intracellular recording in Necturus *J. Neurophysiol.* **34** 228–41
[431] Werblin F S 1972 Lateral interactions at inner plexiform layers of vertebrate retina: antagonistic responses to change *Science* **175** 1008–10
[432] Werblin F S and Copenhagen D R 1974 Control of retinal sensitivity. III. Lateral interactions at the inner plexiform layer *J. Gen. Physiol.* **63** 88–110
[433] Werblin F S and Dowling J E 1969 Organization of the retina of the mudpuppy, *Necturus maculosus*. II. Intracellular recording *J. Neurophysiol.* **32** 339–55
[434] Wiener M C and Richmond B J 1998 Using response models to study coding strategies in monkey visual cortex *BioSystems* **48** 279–96
[435] Wilson H R and Cowan J D 1973 A mathematical theory of the functional dynamics of cortical and thalamic nervous tissue *Kybernetik* **13** 55–80
[436] Winslow R L, Miller R F and Ogden T E 1989 Functional role of spines in the retinal horizontal cell network *Proc. Natl Acad. Sci., USA* **86** 387–91
[437] Wolfe J and Palmer L A 1998 Temporal diversity in the lateral geniculate nucleus of cat *Vis. Neurosci.* **15** 653–75
[438] Wörgötter F, Nelle E, Li B and Funke K 1998 The influence of corticofugal feedback on the temporal structure of visual responses of cat thalamic relay cells *J. Physiol.* **509** 797–815

[439] Wörgötter F, Suder K, Zhao Y, Kerscher N, Eysel U T and Funke K 1998 State-dependent receptive field restructuring in the visual cortex *Nature* **396** 165–8
[440] Wu S M and Yang X-L 1992 Modulation of synaptic gain by light *Proc. Natl Acad. Sci., USA* **89** 11 755–8
[441] Wyszecki G and Stiles W S 1967 *Colour Science: Concepts and Methods, Quantitative Data and Formulae* (New York: Wiley)
[442] Yang X L, Tauchi M and Kaneko A 1982 Quantitative analysis of photoreceptor inputs to external horizontal cells in the goldfish retina *Japan. J. Physiol.* **32** 399–420
[443] Yeh T, Lee B B and Kremers J 1995 Temporal response of ganglion cells of the macaque retina to cone-specific modulation *J. Opt. Soc. Am.* A **12** 456–64
[444] Yeh T, Lee B B and Kremers J 1996 The time course of adaptation in macaque retinal ganglion cells *Vis. Res.* **36** 913–31
[445] Yoshioka T, Levitt J B and Lund J S 1994 Independence and merger of thalamocortical channels within macaque monkey primary visual cortex: anatomy of interlaminar projections *Vis. Neurosci.* **11** 467–89
[446] Young M P 1992 Objective analysis of the topological organization of the primate cortical visual system *Nature* **358** 152–5
[447] Zemon V, Gordon J and Welch J 1988 Asymmetries in ON and OFF visual pathways of humans revealed using contrast-evoked cortical potentials *Vis. Neurosci.* **1** 145–50
[448] Zhang J, Jung C-S and Slaughter M M 1997 Serial inhibitory synapses in retina *Vis. Neurosci.* **14** 553–63